JAERI-M
8737

EXPERIMENTAL DATA OF ROSA-III INTEGRAL TEST RUN706 (STANDARD TEST WITHOUT ECCS ACTUATION)

March 1980

Mitsuhiro SUZUKI, Kanji TASAKA
Hiromichi ADACHI, Motoaki OKAZAKI
Kunihisa SODA, Makoto SOBAJIMA
Yasuo KOIZUMI, Yoshinari ANODA
Hideo MURATA and Masayoshi SHIBA

日本原子力研究所
Japan Atomic Energy Research Institute

Experimental Data of ROSA-III Integral Test RUN706 (Standard Test without ECCS Actuation)

Mitsuhiro SUZUKI, Kanji TASAKA
Hiromichi ADACHI, Motoaki OKAZAKI
Kunihisa SODA, Makoto SOBAJIMA
Yasuo KOIZUMI, Yoshinari ANODA
Hideo MURATA, Masayoshi SHIBA

Division of Reactor Safety,
Tokai Research Establishment, JAERI
(Received January 31, 1980)

RUN 706 in the ROSA-III program, which obtains information of the thermo-hydraulic phenomena of the coolant in a loss-of-coolant accident (LOCA) using a simulated test facility for assessment of the system computer code, simulates a 200% double-ended break at the inlet of a recirculation pump. Purpose of the test was to observe thermo-hydraulic behavior in the core under LOCA conditions in core heating without ECCS actuation.

The primary initial conditions are steam dome pressure 7.17MPa, steam dome temperature 561K (saturation), lower plenum subcooling 12K, initial power 3.405MW and core inlet flow 36.2 kg/s. Recirculation pump power supply, main steam discharge flow and feed water flow were suspended instantaneously upon the break. Following are the experimental results.

(1) Jet pump suction uncovering and lower plenum flashing occurred 8.5s and 17s, respectively, after the break.
(2) Lower plenum flashing improved core cooling in the lower half of the heater rods.
(3) Electric power supply to the heater rods was cut off 156s after the break to protect the rods.
(4) Separate mixture levels were observed in the core and the lower plenum during blowdown.

Key words: BWR, LOCA, ROSA-III Program, Simulation Test, ECCS, Double-ended break, Blowdown, Lower Plenum Flashing, Thermo-Hydraulic Behavior.

ROSA - Ⅲ実験データレポート：RUN 706
（ECCS不作動下の標準試験）

日本原子力研究所東海研究所安全工学部

鈴木光弘・田坂完二・安達公道
岡崎元昭・早田邦久・傍島　真
小泉安郎・安濃田良成・村田秀男
斯波正誼

（1980 年 1 月 31 日受理）

ROSA - Ⅲ計画は，実験装置を用いた冷却材喪失実験で，冷却材の熱流体的現象を研究するものであり，Run 706 はその中で再循環ポンプ吸込側配管の200 %両端破断を模擬した実験である。この実験の目的の1つは，系全体を扱う計算コードの評価を行うための実験データを提供することであり，他の1つは，ECCS を作動させない場合の，発熱下の炉心における熱流体挙動を調べることにある。

主要な実験条件は，蒸気ドーム圧力は 7.17 MPa，同温度は 561 K（飽和），下部プレナムのサブクール度 12K，初期出力 3.405 MW，および炉心入口流量 36.2 kg/sec である。また，破断直後に，再循環ポンプ電源を遮断し，通常蒸気流出と通常給水を停止するよう設定した。

主な実験結果は次の通りである。

(1) ジェットポンプ吸込側露出は約 8.5 秒に，下部プレナム・フラッシングは約 17 秒に生じた。
(2) 下部プレナムフラッシングにより，燃料棒の下半分に冷却効果があった。
(3) 燃料棒加熱用電源は，燃料棒保護のため，破断後 156 秒で遮断された。
(4) 炉心と下部ペレナムに独立に水位が形成された。

Contents

目　　次

List of Tables and Figures

ABBREVIATIONS

Systems

ROSA	Rig of Safety Assessment
BWR	Boiling Water Reactor
LBWR	Large Boiling Water Reactor
ECCS	Emergency Core Cooling System
HPCS	High Pressure Core Spray
LPCS	Low Pressure Core Spray
LPCI	Low Pressure Coolant Injection
ADS	Automatic Depressurization System

Vessels

PV	Pressure Vessel
PWT	Pure Water Tank
FWT	Feed Water Tank
AT	Air Tank
CWT	Cooling Water Tank
HPCST	High Pressure Core Spray Tank
LPCST	Low Pressure Core Spray Tank
LPCIT	Low Pressure Coolant Injection Tank
POOL	Pool

Pumps

JP	Jet Pump
MRP	Main Recirculation Pump
HPWP	High Pressure Water Pump
WSP	Water Supply Pump
FWP	Feed Water Pump
HPCSP	High Pressure Core Spray Pump
LPCSP	Low Pressure Core Spray Pump
LPCIP	Low Pressure Core Injection Pump

Piping

V	Valve
AV	Air actuation Valve
CV	Control Valve
CHV	Check Valve
QSV	Quick Shut-off Valve
OR	Orifice
RD	Rupture Disk
RCN	Rapid Condenser
(2)B	(2) inches pipe of Schedule 80
DL(+100)	Elevation (+100 mm) from the bottom of PV

Measurements

P	Pressure
D	Differential Pressure
F	Flow Rate
T	Temperature
TS	Temperature of Solid
TF	Temperature of Fuel
L	Liquid Level
LB	Liquid Level in Channel Box
LL	Liquid Level in the Lower Plenum
S	Signal
W	Power
N	Rotation Speed
DF	Density of Fluid
M	Momentum Flux

Units

K	Kelvin
kg	Kilogram
ℓ	Liter
m	Meter
mm	Milimeter
MPa	Megapascal
rpm	Revolution per Minute
s	Second
W	Watt

Miscallaneous

ESF	Engineered Safety Features
LOCA	Loss-of-Coolant Accident
LOCE	Loss-of-Coolant Experiment
MLHR	Maximum Linear Heat Rate

1. INTRODUCTION

The ROSA (Rig of Safety Assessment)-III Program is one of several water reactor research test programs conducted by JAERI (Japan Atomic Energy Research Institute).

The ROSA-III facility is a volumetrically scaled (1/424) boiling water reactor (BWR)[1] system with electrically heated core designed to to study the response of the engineered safety features (ESF) in commercial BWR systems during the postulated loss-of-coolant accident (LOCA). With recognition of the differences in commercial BWR designs and inherent distortions in reduced scale systems, the design objective for the ROSA-III facility was to produce the significant thermal-hydraulic phenomena that would occur in commercial BWR systems in the same sequence and with approximately the same time frames and magnitudes. The objectives of the ROSA-III experimental program are:

(1) To provide data required to evaluate the adequacy and improve the analytical methods currently used to predict the LOCA response of large BWRs. The performance of the ESFs, with particular emphasis on emergency core cooling systems (ECCS), and the quantitative margins of safety inherent in performance of the ESF are of primary interest.

(2) To identify and investigate any unexpected event(s) or threshold(s) in the response of either the plant or the ESF and develop analytical techniques that adequately describe and account for such unexpected behavior.

The information acquired from loss-of-coolant experiments (LOCE) is thus used for evaluation and development of LOCA analytical methods and assessment for the quantitative margins of safety of ESFs in response to a LOCA.

RUN 706 in the ROSA-III program was performed on March 12, 1979, to investigate thermo-hydraulic behavior in the core under the conditions with core heating and without ECCS actuation. The major experimental conditions are as follows.

(1) 200 % double-ended break test at the inlet of recirculation pump in the blowdown loop simulating the design basis accident (DBA) of a BWR.

(2) Heat generation in the core after break simulates the decay heat power, delayed-neutron fission power and stored heat release from

the fuel rods.

(3) No ECCS actuation and termination of steady state fluid flow such as core flow, steam discharge flow and feed water flow soon after the break.

RUN 706 was conducted from the initial conditions of 3.405 MW steady state power, 7.17 MPa steam dome pressure (saturation) and 4.61 m water level in the pressure vessel. The subcooling in the lower plenum, core inlet flow rate and the core outlet quality are 12 K, 36.2 kg/s and 0.025, respectively. The steady state power for the core (3.405 MW) corresponds to 38 % of the steady state power of a BWR.

The purpose of this report is to present the data from RUN 706 in an uninterpreted but readily usable form for use by the nuclear community in advance of detailed analysis and interpretation. Section 2 briefly describes the ROSA-III configuration; Section 3 discusses the ROSA-III instrumentation system and the methods of obtaining certain measurements; and Section 4 summarizes RUN 706 initial conditions and test procedures. Section 5 presents the data with supporting information for data interpretation. Section 6 describes concluding remarks.

Pre- and post-test analyses(2)∿(9) for large break tests, the experimental data presentation of RUN 701(10) and the measuring system and data processing method(11) of the ROSA-III program are published already.

2. ROSA-III TEST FACILITY

The ROSA-III facility is a volumetrically scaled (1/424) boiling water reactor (BWR) system with electrically heated core designed to study the response of the engineered safety features (ESF) in commercial BWR systems during the postulated loss-of-coolant accident (LOCA).

The test assembly consists of four major subsystems which have been instrumented such that desirable system parameters can be measured and recorded during a LOCE. The subsystems include: (a) the pressure vessel with core, (b) the steam line and the feedwater line, (c) the coolant recirculation system, and (d) the ECCS. System instrumentation is discussed in Section III. The ROSA-III major components and the pressure vessel internal structure are shown schematically in Figure 2.1 and 2.2, respectively. The ROSA-III piping system is shown in Figure 2.3, and the major characteristics of the ROSA-III facility are compared with the fuel rods.

(3) No ECCS actuation and termination of steady state fluid flow such as core flow, steam discharge flow and feed water flow soon after the break.

RUN 706 was conducted from the initial conditions of 3.405 MW steady state power, 7.17 MPa steam dome pressure (saturation) and 4.61 m water level in the pressure vessel. The subcooling in the lower plenum, core inlet flow rate and the core outlet quality are 12 K, 36.2 kg/s and 0.025, respectively. The steady state power for the core (3.405 MW) corresponds to 38 % of the steady state power of a BWR.

The purpose of this report is to present the data from RUN 706 in an uninterpreted but readily usable form for use by the nuclear community in advance of detailed analysis and interpretation. Section 2 briefly describes the ROSA-III configuration; Section 3 discusses the ROSA-III instrumentation system and the methods of obtaining certain measurements; and Section 4 summarizes RUN 706 initial conditions and test procedures. Section 5 presents the data with supporting information for data interpretation. Section 6 describes concluding remarks.

Pre- and post-test analyses (2)∿(9) for large break tests, the experimental data presentation of RUN 701 (10) and the measuring system and data processing method (11) of the ROSA-III program are published already.

2. ROSA-III TEST FACILITY

The ROSA-III facility is a volumetrically scaled (1/424) boiling water reactor (BWR) system with electrically heated core designed to study the response of the engineered safety features (ESF) in commercial BWR systems during the postulated loss-of-coolant accident (LOCA).

The test assembly consists of four major subsystems which have been instrumented such that desirable system parameters can be measured and recorded during a LOCE. The subsystems include: (a) the pressure vessel with core, (b) the steam line and the feedwater line, (c) the coolant recirculation system, and (d) the ECCS. System instrumentation is discussed in Section III. The ROSA-III major components and the pressure vessel internal structure are shown schematically in Figure 2.1 and 2.2, respectively. The ROSA-III piping system is shown in Figure 2.3, and the major characteristics of the ROSA-III facility are compared with those of a LBWR in Table 2-1.

The pressure vessel simulates the pressure vessel of a BWR. It has a simulated core, a lower plenum, an upper plenum, an annular downcomer, a steam separator, a simulated steam dryer plate, and a steam dome. The core is composed of four half-length simulated fuel assemblies and a control rod simulator. Each fuel assembly contains 63 fuel rods which are spaced and supported in a square (8 × 8) array by lower and upper tie plates. The simulated fuel rod is heated electrically with chopped-cosine axial power distribution. The effective heated length is 1880 mm, one half of the active length of a BWR fuel rod. The orifice plate assembly at core inlet simulates the flow resistance of the nuclear core. Simulated fuel rod is named by one alphabet and two numerals. Alphabet shows the fuel channel, the first and the second numerals show column and row in 8 × 8 fuel rod array, respectively, for the fuel channel C. Fuel rods in other channels are named after rotating about the center of control rod simulator to the channel C. For example, C27 shows fuel rod in the second column and seventh row of fuel rod array in the fuel channel C. A17 shows fuel rod in the eighth column and second row of fuel rod array in the fuel channel A.

The steam line and the feedwater line simulate those of a BWR. Steam is discharged into the atmosphere through the steam line connected to the steam dome. The steam line has three branches. The first branch has a control valve to control the steady-state steam dome pressure before blowdown. The second branch simulates the automatic depressurization system (ADS). The third branch has an orifice to simulate the flow resistance of a steam turbine-generator. Immediately after the blowdown initiation, the steam line is charged from the first branch to the third one. The feedwater line is connected to the feedwater sparger located above the dowmcomer region. The ambient-temperature feedwater is supplied from the pure water tank (PWT) at steady state, and the feedwater tank (FWT) supplies preheated feedwater during the first two seconds in the blowdown.

The coolant recirculation system simulates the BWR recirculation loop. The system consists of two loops provided with a recirculation pump and two jet pumps in each loop. One is the intact loop which simulates the unbroken loop of a BWR and the other is the blowdown loop which simulates the broken loop of a BWR. The blowdown loop has two break simulators and a quick shutoff valve to simulate a double-ended shear break or a split break. Each break simulator is composed of an orifice which determines the break area, a rupture disk, and a spear to break the rupture disk. The break type, position, and area are experimental variables. The standard break condition is a 200 % double-ended shear break at the recirculation pump inlet side with the orifice diameter of 26.2 mm.

The ECCS of ROSA-III simulate those of a BWR, however, they were not actuated in RUN 706. The ECC systems include HPCS, LPCS, LPCI and ADS. The spray systems, the HPCS and the LPCS, spray the emergency cooling water on the top surface of the core. The LPCI system supplies the emergency cooling water into the core-shroud directly. Each ECCS is provided with a tank, a pump, a valve, and a control system to control the valve trip delay, valve opening speed, and the pump flow rate.

3. INSTRUMENTATION

The instrumentation system of the ROSA-III was designed to obtain thermo-hydraulic data in a BWR LOCA to contribute to assess the analytical code. The channel configuration of the instrumentation differs following the renewal of the simulated fuel assembly or remodeling of the loop system. The measurement list for the present run is shown in Table 3-1. Most of the measurements are recorded on the main data acquisition system (DATAC-2000B) with a half-inch width magnetic tape. The list number corresponds to the fuel assembly number. The instrumentation list 2 contains 375 measurements. Additional 25 informations listed in Table 3-2 were calculated from the original data by the data processing program, such as discharge mass flow rates, discharge qualities, maximum linear power (Ch.426 ∿ Ch.450). In RUN 706, most of the measurements were obtained successfully and shown in the report. Some of the measurements under development, however, were not given in the report. The obtained experimental data are shown in Table 3-3 and shown in Section 5.

Pressure measurements are done with semi-conductor transducers measuring the piezoelectric resistance. The detector is cooled by water for the protection from high temperature environment.

Differential pressure transducers with two direct current cables convert displacement of a diaphragm to electric charge and then to shear break or a split break. Each break simulator is composed of an orifice which determines the break area, a rupture disk, and a spear to break the rupture disk. The break type, position, and area are experimental variables. The standard break condition is a 200 % double-ended shear break at the recirculation pump inlet side with the orifice diameter of 26.2 mm.

The ECCS of ROSA-III simulate those of a BWR, however, they were not actuated in RUN 706. The ECC systems include HPCS, LPCS, LPCI and ADS. The spray systems, the HPCS and the LPCS, spray the emergency cooling water on the top surface of the core. The LPCI system supplies the emergency cooling water into the core-shroud directly. Each ECCS is provided with a tank, a pump, a valve, and a control system to control the valve trip delay, valve opening speed, and the pump flow rate.

3. INSTRUMENTATION

The instrumentation system of the ROSA-III was designed to obtain thermo-hydraulic data in a BWR LOCA to contribute to assess the analytical code. The channel configuration of the instrumentation differs following the renewal of the simulated fuel assembly or remodeling of the loop system. The measurement list for the present run is shown in Table 3-1. Most of the measurements are recorded on the main data acquisition system (DATAC-2000B) with a half-inch width magnetic tape. The list number corresponds to the fuel assembly number. The instrumentation list 2 contains 375 measurements. Additional 25 informations listed in Table 3-2 were calculated from the original data by the data processing program, such as discharge mass flow rates, discharge qualities, maximum linear power (Ch.426 ∿ Ch.450). In RUN 706, most of the measurements were obtained successfully and shown in the report. Some of the measurements under development, however, were not given in the report. The obtained experimental data are shown in Table 3-3 and shown in Section 5.

Pressure measurements are done with semi-conductor transducers measuring the piezoelectric resistance. The detector is cooled by water for the protection from high temperature environment.

Differential pressure transducers with two direct current cables convert displacement of a diaphragm to electric charge and then to proportional voltage. The pressure lead pipes are dual circular pipes for circulating cooling water to eliminate flashing of the fluid.

Flow rate is measured by orifice, venturi, turbine or electromagnetic flow meters depending on the fluid condition and the measurement location.

Electric power for simulated fuel rods is controlled by the predetermined function of time for the after power simulation and it is measured by fast response electric power meter.

Pump revolution speed is measured by counting the number of gear blades on the axis of a pump.

On-off signals such as valve position, pump revolution direction, rupture disk break and pump power supply are converted to voltage or current and recorded in respective channels in order to specify the exact time of the signal.

Temperatures of fluid, structure materials and fuel rods are measured with thermocouples of 1.6 mmϕ or 1.0 mmϕ.

Liquid levels are measured by means of needle type electrical conductivity probes developed in the ROSA-III program. The probes are attached on the walls of core barrel and channel boxes at several elevations and detect the existance of liquid water or steam at each level.

The void fraction of fluid is measured by a needle type electrical resistance probe or a correlation type electrical capacitance probe. The former detects passing bubble and the void fraction is obtained by integrating the void signal. The latter detects the average void distribution around the probe with the capacitance. The correlation between two sensors gives the velocity of the bubble.

Fluid density in the pipe is measured by means of a gamma ray densito-meter. Each gamma ray densitometer has two or three beams to estimate the flow regime. The gamma source is Cs-137 and the detector is NaI scintillator which is cooled by water.

Flow direction in the core is measured from the canti-lever contact signal. The canti-lever is moved to the direction of the fluid flow and generates a contact signal.

Two-phase flow rate measurement is done by means of the combination of two signals from drag disk, turbine and gamma ray densitometer in a pipe.

Some of measurement methods described above are still under development and further improvements are expected in accuracy and reliability.

The measurement location of each instrumentation in the measurement list are shown in the figures of flow diagram, loop instrumentation, in-vessel instrumentation, or in-core instrumentation (Figs. 3.1 - 3.14).

The data acquisition system utilizes two recording systems of major and minor importance. The data recorded on the magnetic tape of the main acquisition system are processed by the FACOM 230-75 computer at JAERI by off-line. After the evaluation of each data by comparing the initial and the final values with the standard values of the pressure for example, the data tape is re-processed using the correct conversion factors determined from consistency examination. Data processing program developed for the ROSA-III test can compare the measured data in a figure not only with other channels of the same test but also with the data of other runs or with calculated results by LOCA analysis code such as RELAP or ALARM.

4. TEST CONDITIONS AND TEST PROCEDURES

Test conditions of RUN 706, which simulated a 200 % double-ended break at the inlet of recirculation pump, are summarized in Table 4-1.

Prior to the blowdown, instrumentations were checked out. It took about 320 minutes to arrive at the set-up conditions of the test from the initiation of system heat-up and additional 40 minutes to attain a steady initial conditions; pressure in the steam dome of 7.17 MPa (saturated condition), its steam temperature of 561 K and water level in the downcomer of 4.61 m.

The steady state thermal output of heater rods in the core was 3.405 MW with flat radial and chopped cosine power distributions. The core inlet mass flow rate was 36.2 kg/s. The subcooling at the inlet of core was 12 K and the core outlet quality was calculated to be 2.5 % from the heat balance. Flow rate of each recirculating loop was nearly the same. Steam flow rate and feed water flow rate in steady state were 1.24 kg/s and 1.29 kg/s, respectively. The steady state power 3.405 MW corresponds to 38 % of the BWR steady state power (3800 MW × $\frac{1}{424}$) and the maximum linear heat rate (MLHR) was 10.2 kW/m. The transient power of each power supply was kept constant before 11s after break and simulated the heat transfer rate in a BWR core after 11s which is composed of the decay heat power, delayed-neutron fission power and the

The measurement location of each instrumentation in the measurement list are shown in the figures of flow diagram, loop instrumentation, in-vessel instrumentation, or in-core instrumentation (Figs. 3.1 - 3.14).

The data acquisition system utilizes two recording systems of major and minor importance. The data recorded on the magnetic tape of the main acquisition system are processed by the FACOM 230-75 computer at JAERI by off-line. After the evaluation of each data by comparing the initial and the final values with the standard values of the pressure for example, the data tape is re-processed using the correct conversion factors determined from consistency examination. Data processing program developed for the ROSA-III test can compare the measured data in a figure not only with other channels of the same test but also with the data of other runs or with calculated results by LOCA analysis code such as RELAP or ALARM.

4. TEST CONDITIONS AND TEST PROCEDURES

Test conditions of RUN 706, which simulated a 200 % double-ended break at the inlet of recirculation pump, are summarized in Table 4-1.

Prior to the blowdown, instrumentations were checked out. It took about 320 minutes to arrive at the set-up conditions of the test from the initiation of system heat-up and additional 40 minutes to attain a steady initial conditions; pressure in the steam dome of 7.17 MPa (saturated condition), its steam temperature of 561 K and water level in the downcomer of 4.61 m.

The steady state thermal output of heater rods in the core was 3.405 MW with flat radial and chopped cosine power distributions. The core inlet mass flow rate was 36.2 kg/s. The subcooling at the inlet of core was 12 K and the core outlet quality was calculated to be 2.5 % from the heat balance. Flow rate of each recirculating loop was nearly the same. Steam flow rate and feed water flow rate in steady state were 1.24 kg/s and 1.29 kg/s, respectively. The steady state power 3.405 MW corresponds to 38 % of the BWR steady state power (3800 MW $\times \frac{1}{424}$) and the maximum linear heat rate (MLHR) was 10.2 kW/m. The transient power of each power supply was kept constant before 11s after break and simulated the heat transfer rate in a BWR core after 11s which is composed of the decay heat power, delayed-neutron fission power and the stored heat release from the fuel rods (Figs. 5.3, 5.4).

The steam line and the feed water line are independent and each line has both a steady state line and a transient line as shown in Fig. 3.1. Each line has a flow meter. It takes about 0.1s for steady state lines to close and also for transient lines to open. The transient lines, however, were not opened after break in RUN 706.

In RUN 706 ECCS were not actuated except for the ADS line which was unexpectedly actuated from 35s to 69s (Fig. 5.14).

After establishing the specified test conditions, RUN 706 was initiated following the break by the mode No.2 (Fig. 4.1). Each delay time in the break sequences (T1 ∿ T17) was set as shown in Table 4-1. Two break units operated normally and the double-ended break blowdown initiated expectedly. Two recirculating pumps (MRP-1, MRP-2) began to coast down immediately after the break, the steady-state steam discharge flow was terminated within 3 seconds (Fig. 5.14) and the steady-state feed water flow was terminated within 15 seconds after break (Fig. 5.17).

5. DATA PRESENTATION

The integral test RUN 706 was performed as planned and the transient fluid behaviors were recorded in main data recording system (DATAC-2000B) for 520 seconds after break. The data from ch.170 to 299 were recorded up to 448s because of the termination of power supply to the data recording system at the time. Interpretation of the experimental data, however, are not affected by the limited recording time. The supplemental data recording system was not used in RUN 706. Most of the data recorded in DATAC-2000B are shown in the report, except for the instrumentations under development, such as void, flow direction (Cf. Table 3-3).

The time sequence of major events is shown in Table 5-1. It was estimated from the pressure transients in the blowdown loop and pressure vessel that the jet pump and the recirculation pump suctions were uncovered at 8.5s and 10s, respectively. Abrupt pressure decrease occurred after 8.5s in the data (P-5, 6, 10 ∿ 12) indicates steam discharge through the jet pump drive nozzles to the break A. While the abrupt pressure decrease occurred simultaneously after 10s in the data (P-1 ∿ 4, 7 ∿ 9) indicates steam discharge through the recirculation inlet nozzle to break B where the steam flow rate is much longer than break A.

stored heat release from the fuel rods (Figs. 5.3, 5.4).

The steam line and the feed water line are independent and each line has both a steady state line and a transient line as shown in Fig. 3.1. Each line has a flow meter. It takes about 0.1s for steady state lines to close and also for transient lines to open. The transient lines, however, were not opened after break in RUN 706.

In RUN 706 ECCS were not actuated except for the ADS line which was unexpectedly actuated from 35s to 69s (Fig. 5.14).

After establishing the specified test conditions, RUN 706 was initiated following the break by the mode No.2 (Fig. 4.1). Each delay time in the break sequences (T1 ∿ T17) was set as shown in Table 4-1. Two break units operated normally and the double-ended break blowdown initiated expectedly. Two recirculating pumps (MRP-1, MRP-2) began to coast down immediately after the break, the steady-state steam discharge flow was terminated within 3 seconds (Fig. 5.14) and the steady-state feed water flow was terminated within 15 seconds after break (Fig. 5.17).

5. DATA PRESENTATION

The integral test RUN 706 was performed as planned and the transient fluid behaviors were recorded in main data recording system (DATAC-2000B) for 520 seconds after break. The data from ch.170 to 299 were recorded up to 448s because of the termination of power supply to the data recording system at the time. Interpretation of the experimental data, however, are not affected by the limited recording time. The supplemental data recording system was not used in RUN 706. Most of the data recorded in DATAC-2000B are shown in the report, except for the instrumentations under development, such as void, flow direction (Cf. Table 3-3).

The time sequence of major events is shown in Table 5-1. It was estimated from the pressure transients in the blowdown loop and pressure vessel that the jet pump and the recirculation pump suctions were uncovered at 8.5s and 10s, respectively. Abrupt pressure decrease occurred after 8.5s in the data (P-5, 6, 10 ∿ 12) indicates steam discharge through the jet pump drive nozzles to the break A. While the abrupt pressure decrease occurred simultaneously after 10s in the data (P-1 ∿ 4, 7 ∿ 9) indicates steam discharge through the recirculation inlet nozzle to break B where the steam flow rate is much longer than break A.

Lower plenum flashing initiated from 17s after break causing temporal rewetting of heater rods below midplane of the core (Pos. 4 ∿ 6) and slowing down the pressure decrease rate. The lower plenum flashing, however, were not effective for cooling the heater rods in the upper part of the core (Pos. 1 ∿ 3). These facts indicate that the mixture level went up between Pos. 3 and Pos. 4 of heater rods from 20 to 30s after break (cf. Fig. 5.1 and 5.2).

Power supply to simulated fuel rods were terminated at 156 seconds after break due to the trip signal (fuel rod temperature at 973 K) to protect the fuel assembly. Then, most of the fuel rod temperatures began to decrease even in the steam atmosphere.

The test data are presented from Fig. 5.1 through 5.67. They are divided into 3 groups; system data, flow data and temperature data.

Fig. 5.1 shows the transient of mixture level in the core and lower plenum and Fig. 5.2 shows exposure and rewetting behavior of fuel rods and tie rods (unheated rods). The mixture level was formed in the lower plenum before the mixture level in the core reached bottom of the core. Fig. 5.3 and 5.4 show the power and the maximum linear power density supplied to simulated fuel rods by the three power supplies 550 kW, 1800 kW and 2100 kW.

Fig. 5.5 through 5.8 show pressure transients in the ROSA-III system. Fig. 5.9 through 5.13 show the differential pressures. Fig. 5.14 through 5.18 show the flow rates.

Fig. 5.19 shows revolution velocities of two recirculation pumps. The revolution of MRP-2 after 3s is reversed. Fig. 5.20 and 5.21 show performance signals.

Fig. 5.22 through 5.26 show the system temperatures. Fig. 5.27 and 5.28 show the condensed water temperature and discharge fluid quality for each break unit. Fig. 5.29 shows the fluid temperature at the steam line.

Fig. 5.30 through 5.33 show the metal temperatures in the system. Fig. 5.34 shows the surface temperatures of the fuel rod A11. There is little difference in fuel surface temperatures among different fuel rods. Fig. 5.35 through 5.45 show the surface temperature of other fuel rods and the temperature responses of non-instrumented fuel rods are expected similar with these data.

Fig.5.46 through 5.49 show the tie rod temperatures. Fig. 5.50 through 5.59 show the fluid temperatures at the inlets and outlets of

channel boxes, at inner surfaces of channel boxes, in the lower plenum, and above and below the upper tie-plate. Fig. 5.60 through 5.67 show the the signals of liquid level probes in the core and the lower plenum.

6. CONCLUDING REMARKS

The integral test RUN 706 in ROSA-III program was conducted as it had been expected and experimental data were obtained concerning the loss-of-coolant phenomena in the facility. Most of the instrumentations worked well and the experimental data obtained are useful for assessing the computor code for BWR LOCA/ECCS analyses.

Acknowledgement

The authors are grateful to H. Itoh, H. Osaki, and T. Chiba of Safety Facility Engineering Service Section, and to H. Asahi, T. Odaira, S. Sekiguchi, M. Tokoi, and J. Tamura of Nuclear Engineering Corporation who conducted the experiment.

channel boxes, at inner surfaces of channel boxes, in the lower plenum, and above and below the upper tie-plate. Fig. 5.60 through 5.67 show the the signals of liquid level probes in the core and the lower plenum.

6. CONCLUDING REMARKS

The integral test RUN 706 in ROSA-III program was conducted as it had been expected and experimental data were obtained concerning the loss-of-coolant phenomena in the facility. Most of the instrumentations worked well and the experimental data obtained are useful for assessing the computor code for BWR LOCA/ECCS analyses.

Acknowledgement

The authors are grateful to H. Itoh, H. Osaki, and T. Chiba of Safety Facility Engineering Service Section, and to H. Asahi, T. Odaira, S. Sekiguchi, M. Tokoi, and J. Tamura of Nuclear Engineering Corporation who conducted the experiment.

channel boxes, at inner surfaces of channel boxes, in the lower plenum, and above and below the upper tie-plate. Fig. 5.60 through 5.67 show the the signals of liquid level probes in the core and the lower plenum.

6. CONCLUDING REMARKS

The integral test RUN 706 in ROSA-III program was conducted as it had been expected and experimental data were obtained concerning the loss-of-coolant phenomena in the facility. Most of the instrumentations worked well and the experimental data obtained are useful for assessing the computor code for BWR LOCA/ECCS analyses.

Acknowledgement

The authors are grateful to H. Itoh, H. Osaki, and T. Chiba of Safety Facility Engineering Service Section, and to H. Asahi, T. Odaira, S. Sekiguchi, M. Tokoi, and J. Tamura of Nuclear Engineering Corporation who conducted the experiment.

References

(1) "General Electric Standard Safety Analysis Report, BWR/6" DOCKET-STN-50477, GE Co.

(2) K. Tasaka, et. al., "Study on the Similarity between ROSA-III Experiment and BWR LOCA - Pre-analysis of ROSA-III - ", JAERI-M 6703 (1976), in Japanese.

(3) H. Kitaguchi, et. al., "Preliminary Analysis of ROSA-III Experiment (II), - Recirculation Line Break -", JAERI-M 7488 (1978), in Japanese.

(4) H. Kitaguchi, et. al., "Preliminary Analysis of ROSA-III Experiment (III)", JAERI-M 7791 (1978), in Japanese.

(5) H. Kitaguchi, et. al., "LOCA Analysis of BWR/6 for the ROSA-III Test", JAERI-M 8185 (1979), in Japanese.

(6) K. Soda, "Prediction of ROSA-III Experiment-RUN 701", JAERI-M 7712 (1978)

(7) Y. Koizumi, et. al., "Prediction of ROSA-III Experiment RUN 702", JAERI-M 7970 (1978), in Japanese.

(8) Y. Koizumi, et. al., "Prediction of ROSA-III Experiment RUN 703", JAERI-M 8300 (1979), in Japanese.

(9) O. Kikuchi, et. al., "Test Results and Post-Test Analysis of ROSA-III RUN 703", JAERI-M 8588 (1979), in Japanese.

(10) M. Sobajima, et. al., "Experiment Data of ROSA-III Test RUN 701 - Decay Heat Simulation Test with ECCS Actuation -", JAERI-M 8604 (1979).

(11) M. Sobajima, et. al., "Instrumentation and Data Processing" JAERI-M 8499 (1979), in Japanese.

Table 2-1 Primary Characteristics of BWR-6 and ROSA-III

	BWR-6	ROSA-III	BWR/ROSA
No. of Recirc. Loops	2	2	1
No. of Jet Pumps	24	4	6
No. of Separators	251	1	251
No. of Fuel Assemblies	848	4	212
Active Fuel Length (m)	3.76	1.88	2
Total Coolant Volume (m^3)	623	1.37	455
Power (MW)	3800	4.24	896
Pressure (MPa)	7.23	7.23	1
Core Flow (kg/sec)	1.39×10^4	36.4	382
Recirculation Flow (l/sec)	2970	7.01	424
Feedwater Flow (kg/sec)	2060	4.86	424
Feedwater Temp (°K)	489	489	1

Table 3-1 ROSA-III Measurement List 2

CH No.	Item	Symb.	Location	Range & Output	Accuracy	CH. No.	Item	Symb.	Location	Range & Output	Accuracy
1	Press.	P- 1	Lower Plenum	0~100 kg/cm² 0~10 V	±1.08 % F.S.	51	Flow	F-20	JP-3 Discharge −	0~1000 ℓ/min 2~10 V	±0.92 % F.S.
2	〃	P- 2	Mixing Plenum	〃	〃	52	〃	F-21	JP-4 Discharge +	〃	〃
3	〃	P- 3	Steam Dome	〃	〃	53	〃	F-22	JP-4 Discharge −	〃	〃
4	〃	P- 4	Downcomer Bottom	〃	〃	54	Power	W- 1	550 KVA Power	0~550 KVA 0~10 V	±1.0% F.S.
5	〃	P- 5	JP-3 Drive	〃	〃	55	〃	W- 2	1800 KVA Power	0~1700 KVA 0~10 V	〃
6	〃	P- 6	JP-4 Drive	〃	〃	56	〃	W- 3	2100 KVA Power	0~2100 KVA 0~10 V	〃
7	〃	P- 7	JP-3 Suction	〃	〃	57	Rev.No.	N- 1	MRP-1	0~5000 rpm 0~10 V	±1.08 % F.S.
8	〃	P- 8	JP-4 Suction	〃	〃	58	〃	N- 2	MRP-2	〃	〃
9	〃	P- 9	MRP-1 Suction	〃	〃	59	Signal	S- 1	Break Signal A	0~5 V	−
10	〃	P-10	MRP-2 Suction	〃	〃	60	〃	S- 2	Break Signal B	〃	−
11	〃	P-11	MRP-2 Discharge	〃	〃	61	〃	S- 3	QSV Signal	close~open 0~5 V	−
12	〃	P-12	Above Break A	〃	〃	62	〃	S- 9	Transient Feed Water	〃	−
13	〃	P-13	Below Break A	〃	〃	63	〃	S-10	Main Steam Isolation Valve	〃	−
14	〃	P-14	Above Break B	〃	〃	64	〃	S-11	Steam Line Valve	〃	−
15	〃	P-15	Below Break B	〃	〃	65	Temp.	T- 1	Lower Plenum	0~400 °C 0~10 V	±0.94 % F.S.
16	〃	P-16	Steam Line	〃	〃	66	〃	T- 2	Mixing Plenum	〃	〃
17	Diff. P	D- 1	Lower Pl.-Mixing Pl.	-0.5~3.5 kg/cm² 2~10 V	±0.63 % F.S.	67	〃	T- 3	Steam Dome	〃	〃
18	〃	D- 2	Mixing Pl.-Steam Dome	-1.0~9.0 kg/cm² 2~10 V	〃	68	〃	T- 4	Upper Downcomer	〃	〃
19	〃	D- 3	Lower Plenum Head	0~1.5 kg/cm² 2~10 V	〃	69	〃	T- 5	Lower Downcomer	〃	〃
20	〃	D- 4	Dowencomer Head	0~1.0 kg/cm² 2~10 V	〃	70	〃	T- 6	JP-1 Driving Water	〃	〃
21	〃	D- 5	PV. Bottom-Top	-1.0~9.0 kg/cm² 2~10 V	〃	71	〃	T- 7	JP-2 Driving Water	〃	〃
22	〃	D- 6	JP-1 Discharge-Suction	-1.0~3.0 kg/cm² 2~10 V	〃	72	〃	T- 8	JP-3 Driving Water	〃	〃
23	〃	D- 7	JP-1 Drive-Suction	0~25 kg/cm² 2~10 V	〃	73	〃	T- 9	JP-4 Driving Water	〃	〃
24	〃	D- 8	JP-2 Discharge-Suction	-1.0~3.0 kg/cm² 2~10 V	〃	74	〃	T-10	JP-1 Discharge	〃	〃
25	〃	D- 9	JP-2 Drive-Suction	0~25 kg/cm 2~10 V	〃	75	〃	T-11	JP-2 Discharge	〃	〃
26	〃	D-10	JP-3 Discharge-Suction	-1.0~3.0 kg/cm² 2~10 V	〃	76	〃	T-12	JP-3 Discharge	〃	〃
27	〃	D-11	JP-3 Drive-Suction	-5.0~25 kg/cm² 2~10 V	〃	77	〃	T-13	JP-4 Discharge	〃	〃
28	〃	D-12	JP-4 Discharge-Suction	-1.0~3.0 kg/cm² 2~10 V	〃	78	〃	T-14	MRP-1 Suction	〃	〃
29	〃	D-13	JP-4 Drive-Suction	-5.0~25 kg/cm² 2~10 V	〃	79	〃	T-15	MRP-1 Discharge	〃	〃
30	〃	D-14	MRP-1 Discharge-Suction	-1.0~25 kg/cm² 2~10 V	〃	80	〃	T-16	MRP-2 Suction	〃	〃
31	〃	D-15	MRP-2 Discharge-Suction	-1.0~25 kg/cm² 2~10 V	〃	81	〃	T-17	MRP-2 Discharge	〃	〃
32	Flow	F- 1	Main Steam Line	0~15 kg/sec 2~10 V	±0.92 % F.S.	82	〃	T-18	Above Break A	〃	〃
33	〃	F- 2	ADS. Steam Line	0~1.2 kg/sec 2~10 V	〃	83	〃	T-19	Above Break B	〃	〃
34	〃	F- 3	Condensed Water A	0~250 kg/sec 2~10 V	±1.4% F.S.	84	〃	T-20	Condensed Water A	〃	〃
35	〃	F- 4	Cooling Water A	〃	〃	85	〃	T-21	Condensed Water B	〃	〃
36	〃	F- 5	Condensed Water B	〃	〃	86	〃	T-22	Discharged Steam Above V.	〃	〃
37	〃	F- 6	Cooling Water B	〃	〃	87	〃	T-23	Discharged Steam Below V.	〃	〃
38	〃	F- 7	HPCS (Mixing Plenum)	0~150 ℓ/min 2~10 V	±0.79 % F.S.	88	〃	TS-15	Dummy Block B Side 3	〃	〃
39	〃	F- 8	HPCS (Lower Plenum)	〃	〃	89	〃	TS-18	Dummy Block B Side 6	〃	〃
40	〃	F- 9	LPCS (Mixing Plenum)	〃	〃	90	〃	TS-21	Dummy Block O Side 9	〃	〃
41	〃	F-10	LPCS (Lower Plenum)	〃	〃	91	〃	TS-24	Dummy Block O Side 12	〃	〃
42	〃	F-11	LPCI (Mixing Plenum)	0~500 ℓ/min 2~10 V	〃	92	〃	TS-25	JP-1 Diffuser Wall	〃	〃
43	〃	F-12	LPCI (Lower Plenum)	〃	〃	93	〃	TS-26	JP-2 Diffuser Wall	〃	〃
44	〃	F-13	LPCI MRP-2 Suction	0~250 ℓ/min 2~10 V	〃	94	〃	TS-27	JP-3 Diffuser Wall	〃	〃
45	〃	F-14	LPCI MRP-1 Suction	〃	〃	95	〃	TS-28	JP-4 Diffuser Wall	〃	〃
46	〃	F-15	Transient Feed Water	0~600 ℓ/min 2~10 V	〃	96	〃	TS-29	PV. Wall Inside 1-1	〃	〃
47	〃	F-16	Steady Feed Water	0~250 ℓ/min 2~10 V	〃	97	〃	TS-30	PV. Inner Surface 1-2	〃	〃
48	〃	F-17	JP-1 Discharge	0~1000 ℓ/min 2~10 V	±0.68 % F.S.	98	〃	TS-31	PV. Inner Surface 1-3	〃	〃
49	〃	F-18	JP-2 Discharge	〃	〃	99	〃	TS-32	PV. Wall Inside 2	〃	〃
50	〃	F-19	JP-3 Discharge +	〃	±0.92 % F.S.	100	〃	TS-33	PV. Wall Inside 3	〃	〃

CH. No.	Item	Synb.	Location	Range & Output	Accuracy	CH. No.	Item	Symb	Location	Range & Output	Accuracy
101	Temp.	TS-34	PV. Wall Inside 4	0 ~ 400 °C 0 ~ 10 V	±0.94 %F.S.	151	Temp.	TF2-48	A-77 Fuel Rod Pos. 2	0 ~ 1220 °C 0 ~ 10 V	
102	〃	TS-35	Lower Plenum Inner Surface	〃	〃	152	〃	-49	〃 3	〃	
103	〃	TS-36	Lower Plenum Wall Inside	〃	〃	153	〃	-50	〃 4	〃	
104	〃	TF2-1	A-11 Fuel Rod Pos. 3	0 ~ 1200 °C 0 ~ 10 V		154	〃	-51	〃 5	〃	
105	〃	TF2-2	〃 4	〃		155	〃	-52	〃 6	〃	
106	〃	TF2-3	〃 5	〃		156	〃	-53	〃 7	〃	
107	〃	- 4	A-13 Fuel Rod Pos. 3	〃		157	〃	-54	B-15 Fuel Rod Pos. 1	〃	
108	〃	- 5	〃 4	〃		158	〃	-55	〃 2	〃	
109	〃	- 6	〃 5	〃		159	〃	-56	〃 3	〃	
110	〃	- 7	A-15 Fuel Rod Pos. 3	〃		160	〃	-57	〃 4	〃	
111	〃	- 8	〃 4	〃		161	〃	-58	〃 5	〃	
112	〃	- 9	〃 5	〃		162	〃	-59	〃 6	〃	
113	〃	-10	A-17 Fuel Rod Pos. 3	〃		163	〃	-60	〃 7	〃	
114	〃	-11	〃 4	〃		164	〃	-61	B-85 Fuel Rod Pos. 1	〃	
115	〃	-12	〃 5	〃		165	〃	-62	〃 2	〃	
116	〃	-13	A-31 Fuel Rod Pos. 3	〃		166	〃	-63	〃 3	〃	
117	〃	-14	〃 4	〃		167	〃	-64	〃 4	〃	
118	〃	-15	〃 5	〃		168	〃	-65	〃 5	〃	
119	〃	-16	A-33 Fuel Rod Pos. 1	〃		169	〃	-66	〃 6	〃	
120	〃	-17	〃 2	〃		170	〃	-67	〃 7	0 ~ 976 °C 0 ~ 10 V	
121	〃	-18	〃 3	〃		171	〃	-68	C-11 Fuel Rod Pos. 3	〃	
122	〃	-19	〃 4	〃		172	〃	-69	〃 4	〃	
123	〃	-20	〃 5	〃		173	〃	-70	〃 5	〃	
124	〃	-21	〃 6	〃		174	〃	-71	C-13 Fuel Rod Pos. 3	〃	
125	〃	-22	〃 7	〃		175	〃	-72	〃 4	〃	
126	〃	-23	A-35 Fuel Rod Pos. 3	〃		176	〃	-73	〃 5	〃	
127	〃	-24	〃 4	〃		177	〃	-74	C-15 Fuel Rod Pos. 3	〃	
128	〃	-25	〃 5	〃		178	〃	-75	〃 4	〃	
129	〃	-26	A-37 Fuel Rod Pos. 3	〃		179	〃	-76	〃 5	〃	
130	〃	-27	〃 4	〃		180	〃	-77	C-31 Fuel Rod Pos. 3	〃	
131	〃	-28	〃 5	〃		181	〃	-78	〃 4	〃	
132	〃	-29	A-51 Fuel Rod Pos. 3	〃		182	〃	-79	〃 5	〃	
133	〃	-30	〃 4	〃		183	〃	-80	C-33 Fuel Rod Pos. 1	〃	
134	〃	-31	〃 5	〃		184	〃	-81	〃 2	〃	
135	〃	-32	A-53 Fuel Rod Pos. 3	〃		185	〃	-82	〃 3	〃	
136	〃	-33	〃 4	〃		186	〃	-83	〃 4	〃	
137	〃	-34	〃 5	〃		187	〃	-84	〃 5	〃	
138	〃	-35	A-57 Fuel Rod Pos. 3	〃		188	〃	-85	〃 6	〃	
139	〃	-36	〃 4	0 ~ 1220 °C 0 ~ 10 V		189	〃	-86	〃 7	〃	
140	〃	-37	〃 5	〃		190	〃	-87	C-35 Fuel Rod Pos. 3	〃	
141	〃	-38	A-71 Fuel Rod Pos. 3	〃		191	〃	-88	〃 4	〃	
142	〃	-39	〃 4	〃		192	〃	-89	〃 5	〃	
143	〃	-40	〃 5	〃		193	〃	-90	C-51 Fuel Rod Pos. 3	〃	
144	〃	-41	A-73 Fuel Rod Pos. 3	〃		194	〃	-91	〃 4	〃	
145	〃	-42	〃 4	〃		195	〃	-92	〃 5	〃	
146	〃	-43	〃 5	〃		196	〃	-93	C-53 Fuel Rod Pos. 3	〃	
147	〃	-44	A-75 Fuel Rod Pos. 3	〃		197	〃	-94	〃 4	〃	
148	〃	-45	〃 4	〃		198	〃	-95	〃 5	〃	
149	〃	-46	〃 5	〃		199	〃	-96	C-77 Fuel Rod Pos. 1	〃	
150	〃	TF2-47	A-77 Fuel Rod Pos. 1	〃		200	〃	TF2-97	〃 2	〃	

CH. No.	Item	Syemb	Location	Range & Output	Accuracy	CH. No.	Item	Syemb	Location	Range & Output	Accuracy
201	Temp.	TF2-98	C-77 Fuel Rod Pos. 3	0 ~ 976 °C 0 ~ 10 V		251	Temp.	TC - 4	Channel Box B Inlet	0 ~ 976 °C 0 ~ 10 V	
202	"	- 99	" 4	"		252	"	- 5	" C Outlet	"	
203	"	-100	" 5	"		253	"	- 6	" C Inlet	"	
204	"	-101	" 6	"		254	"	- 7	" D Outlet	"	
205	"	-102	" 7	"		255	"	- 8	" D Inlet	"	
206	"	-103	D-27 Fuel Rod Pos. 1	"		256	"	TB - 1	C.B. Inner Surface Pos. A-1	"	
207	"	-104	" 2	"		257	"	- 2	" A-2	"	
208	"	-105	" 3	"		258	"	- 3	" A-3	"	
209	"	-106	" 4	"		259	"	- 4	" A-4	"	
210	"	-107	" 5	"		260	"	- 5	" A-5	"	
211	"	-108	" 6	"		261	"	- 6	" A-6	"	
212	"	-109	" 7	"		262	"	- 7	" A-7	"	
213	"	-110	D-88 Fuel Rod Pos. 1	"		263	"	- 8	C.B. Inner Surface Pos. A-8	"	
214	"	-111	" 2	"		264	"	- 9	" A-9	"	
215	"	-112	" 3	"		265	"	-10	" A-10	"	
216	"	-113	" 4	"		266	"	-11	" A-11	"	
217	"	-114	" 5	"		267	"	-12	" A-12	"	
218	"	-115	" 6	"		268	"	-13	" A-13	"	
219	"	-116	" 7	"		269	"	-14	" A-14	"	
220	"	-117	A-55 Tie Rod Pos. 1	"		270	"	TP - 1	Lower PL. 0° High	"	
221	"	-118	" 2	"		271	"	- 2	" Middle	"	
222	"	-119	" 3	"		272	"	- 3	" Low	"	
223	"	-120	" 4	"		273	"	- 4	Lower PL. 180° High	"	
224	"	-121	" 5	"		274	"	- 5	" Middle	"	
225	"	-122	" 6	"		275	"	- 6	" Low	"	
226	"	-123	" 7	"		276	"	- 7	Lower PL. Center Low	"	
227	"	-124	B-55 Tie Rod Pos. 1	"		277	"	- 8	" Bottom	"	
228	"	-125	" 2	"		278	"	- 9	Lower PL. Guide Tube	"	
229	"	-126	" 3	"		279	"	-10	Lower PL. Outer Bottom	"	
230	"	-127	" 4	"		280	"	TG2- 1	Upper Tieplate A Up. 1	"	
231	"	-128	" 5	"		281	"	- 2	" 2	"	
232	"	-129	" 6	"		282	"	- 3	" 3	"	
233	"	-130	" 7	"		283	"	- 4	" 4	"	
234	"	-131	C-55 Tie Rod Pos. 1	"		284	"	- 5	" 5	"	
235	"	-132	" 2	"		285	"	- 6	" 6	"	
236	"	-133	" 3	"		286	"	- 7	" 7	"	
237	"	-134	" 4	"		287	"	- 8	" 8	"	
238	"	-135	" 5	"		288	"	- 9	" 9	"	
239	"	-136	" 6	"		289	"	-10	" 10	"	
240	"	-137	" 7	"		290	"	-11	Upper Tieplate A Low. 11	"	
241	"	-138	D-55 Tie Rod Pos. 1	"		291	"	-12	" 12	"	
242	"	-139	" 2	"		292	"	-13	" 13	"	
243	"	-140	" 3	"		293	"	-14	" 14	"	
244	"	-144	" 4	"		294	"	-15	" 15	"	
245	"	-142	" 5	"		295	"	-16	" 16	"	
246	"	-143	" 6	"		296	"	-17	" 17	"	
247	"	-144	" 7	"		297	"	-18	" 18	"	
248	"	TC - 1	Channel Box A Outlet	"		298	"	-19	" 19	"	
249	"	- 2	" A Inlet	"		299	"	-20	" 20	"	±0.94 % F.S.
250	"	- 3	" B Outlet	"		300	Water Level	LB - 1	C.B. Water Level Pos. 1-1	ON - OFF 0 ~ 10 V	

CH. No.	Item	Symb	Location	Range & Output	Accuracy
301	Water Level	LB－2	C.B.Water Level Pos.1－2	on ~ off 0 ~ 10 V	
302	〃	－3	〃 1－3	〃	
303	〃	－4	〃 1－4	〃	
304	〃	－5	〃 1－5	〃	
305	〃	－6	〃 1－6	〃	
306	〃	－7	〃 1－7	〃	
307	〃	－8	C.B.Water Level Pos.2－1	〃	
308	〃	－9	〃 2－2	〃	
309	〃	－10	〃 2－3	〃	
310	〃	－11	〃 2－4	〃	
311	〃	－12	〃 2－5	〃	
312	〃	－13	〃 2－6	〃	
313	〃	－14	〃 2－7	〃	
314	〃	－15	C.B.Water Level Pos.3－1	〃	
315	〃	－16	〃 3－2	〃	
316	〃	－17	〃 3－3	〃	
317	〃	－18	〃 3－4	〃	
318	〃	－19	〃 3－5	〃	
319	〃	－20	〃 3－6	〃	
320	〃	－21	〃 3－7	〃	
321	〃	LL－1	Lower PL.Center High	〃	
322	〃	－2	〃 Middle 1	〃	
323	〃	－3	〃 Middle 2	〃	
324	〃	－4	〃 Low	〃	
325	〃	－5	Lower Pℓ. 0° Low	〃	
326	〃	－6	〃 Bottom	〃	
327	〃	－7	Lower Pℓ. 180° Low	〃	
328	〃	－8	〃 Bottom	〃	
329	Void	VE－1	Lower Pℓ. Void 0°	0 ~ 1.0 0 ~ 10 V	
330	〃	－2	〃 Center	〃	
331	〃	－3	〃 180°	〃	
332	〃	－4	Outlet of Channel A－1	〃	
333	〃	－5	〃 －2	〃	
334	〃	－6	〃 －3	〃	
335	〃	－7	Outlet of Channel B－1	〃	
336	〃	－8	〃 －2	〃	
337	〃	－9	〃 －3	〃	
338	〃	－10	Outlet of Channel C－1	〃	
339	〃	－11	〃 －2	〃	
340	〃	－12	〃 －3	〃	
341	〃	－13	Outlet of Channel D－1	〃	
342	〃	－14	〃 －2	〃	
343	〃	－15	〃 －3	〃	
344	〃	VP－1	Lower Pℓ. Void 1－1	〃	
345	〃	－2	〃 1－2	〃	
346	〃	－3	〃 2－1	〃	
347	〃	－4	〃 2－2	〃	
348	Flow	FE－1	Channel A Outlet	0 ~ 3.0 m/sec 0 ~ 10 V	
349	〃	－2	〃 B 〃	〃	
350	〃	－3	〃 C 〃	〃	

CH. No.	Item	Symb	Location	Range & Output	Accuracy
351	Flow	FE－4	Channel D Outlet	0 ~ 3.0 m/sec 0 ~ 10 V	
352	Direc.	FD－1	Channel A Outlet	Pos. ~ Neg. +10 V ~ －10 V	
353	〃	－2	〃 B 〃	〃	
354	〃	－3	〃 C 〃	〃	
355	〃	－4	〃 D 〃	〃	
356	Dens.	DF－1	J.P－1.2 Outlet Beam 1	0 ~ 1000 kg/m³ 0 ~ 10 V log	
357	〃	－2	〃 2	〃	
358	〃	－3	〃 3	〃	
359	〃	－4	JP－3.4 Outlet Beam 1	〃	
360	〃	－5	〃 2	〃	
361	〃	－6	〃 3	〃	
362	〃	－7	Break A Beam 1	〃	
363	〃	－8	Break A Beam 2	〃	
364	Mome.F	M－1	JP－1.2 Outlet	$0 \sim 1.5\times10^{5}$ kg/ms² 0 ~ 10 V	
365	〃	－2	JP－3.4 Outlet	〃	
366	〃	－3	Break A	〃	
367	Flow	F－23	JP－1.2 Outlet	0 ~ 30 ℓ/sec 0 ~ 10 V	
368	〃	－24	JP－3.4 〃	〃	
369	〃	－25	Break A	0 ~ 30 kg/sec 0 ~ 10 V	
370	Press.	P－17	JP－1.2 Outlet	0 ~ 100 kg/cm² 0 ~ 10 V	±1.08 %F.S.
371		－18	JP－3.4 〃	〃	〃
372		－19	Break A	〃	〃
373	Temp.	T－24	JP－1.2 Outlet	0 ~ 400 °C 0 ~ 10 V	±0.94 %F.S.
374	〃	－25	JP－3.4 〃	〃	〃
375	〃	－26	Break A	〃	〃

Table 3-2 List of Calculated Properties from the Data (2)

Ch.No.	Symbol	Description	unit	Measuring Location
426	LP-1	Linear Power (550)	kw/m	
427	-2	" " (1800)	"	
428	-3	" " (2100)	"	
429	MF-1	Mass Flow	kg/s	Break Unit A
430	-2	" "	"	" " B
431	-3	" "	"	JP-1,2 Outlet
432	-4	" "	"	JP-3,4 "
433	-5	" "	"	Break Unit A
434	-7	" "	"	JP-1,2 Outlet
435	-8	" "	"	JP-3,4 "
436	-9	" "	"	Break Unit A
437	X -1	Quality	-	Break Unit A
438	-2	"	"	" " B
439	-3	"	"	JP-1,2 Outlet
440	-4	"	"	JP-3,4 "
441	-5	"	"	Break Unit A
442	DF-10	Density	kg/m^3	JP-1,2 Outlet
443	-11	"	"	JP-3,4 "
444	-12	"	"	Break Unit A
445	-14	"	"	JP-1,2 Outlet
446	-15	"	"	JP-3,4 Outlet
447	-16	"	"	Break Unit A Average
448	FG-1	Void Fraction	-	JP-1,2 Outlet
449	-2	" "	"	JP-3,4 "
450	-3	" "	"	Break Unit A

Table 3-3 ROSA-III. Measurement References

CH. No.	Item	Symb.	LOC. Fig.No.	Data Fig.No.	Comments	CH. No.	Item	Symb.	LOC. Fig.No.	Data Fig.No.	Comments
1	Press.	P- 1	3.2	5.5		51	Flow	F-20	-	-	no data
2	"	P- 2	"	"		52	"	F-21	3.3	5.18	
3	"	P- 3	"	"		53	"	F-22	-	-	no data
4	"	P- 4	"	5.5		54	Power	W- 1		5.3	
5	"	P- 5	3.3	5.6		55	"	W- 2		"	
6	"	P- 6	"	"		56	"	W- 3		"	
7	"	P- 7	"	"		57	Rev.No.	N- 1	3.4	5.19	
8	"	P- 8	"	"		58	"	N- 2	3.3	"	
9	"	P- 9	3.4	5.7		59	Signal	S- 1	3.5	5.20	
10	"	P-10	3.3	"		60	"	S- 2	"	"	
11	"	P-11	"	"		61	"	S- 3	"	"	
12	"	P-12	"	5.8		62	"	S- 9	-	-	no data
13	"	P-13	"	"		63	"	S-10	3.6	5.21	
14	"	P-14	"	"		64	"	S-11	"		
15	"	P-15	"	"		65	Temp.	T- 1	3.8	5.22	
16	"	P-16	"	5.5		66	"	T- 2	3.2	"	
17	Diff.P	D- 1	3.2	5.9		67	"	T- 3	"	"	
18	"	D- 2	"	"		68	"	T- 4	"	"	
19	"	D- 3	-	-	no data	69	"	T- 5	3.8	"	
20	"	D- 4	"	5.10		70	"	T- 6	3.4	5.23	
21	"	D- 5	"	5.9		71	"	T- 7	"	"	
22	"	D- 6	3.4	5.11		72	"	T- 8	3.3	5.24	
23	"	D- 7	"	"		73	"	T- 9	"	"	
24	"	D- 8	"	"		74	"	T-10	3.4	5.23	
25	"	D- 9	"	"		75	"	T-11	"	"	
26	"	D-10	3.3	5.12		76	"	T-12	3.3	5.24	
27	"	D-11	"	"		77	"	T-13	"	"	
28	"	D-12	"	"		78	"	T-14	3.4	5.25	
29	"	D-13	"	"		79	"	T-15	"	"	
30	"	D-14	3.4	5.13		80	"	T-16	3.3	5.26	
31	"	D-15	3.3	"		81	"	T-17	"	"	
32	Flow	F- 1	-	-	no data	82	"	T-18	3.5	"	
33	"	F- 2	3.6	5.14		83	"	T-19	"	"	
34	"	F- 3	3.5	5.15		84	"	T-20	"	5.27	
35	"	F- 4	"	"		85	"	T-21	"	5.28	
36	"	F- 5	"	5.16		86	"	T-22	3.6	5.29	
37	"	F- 6	"	"		87	"	T-23	-	-	no data
38	"	F- 7	-	-	no data	88	"	TS-15	3.11	5.30	
39	"	F- 8	-	-	"	89	"	TS-18	"	"	
40	"	F- 9	-	-	"	90	"	TS-21	"	"	
41	"	F-10	-	-	"	91	"	TS-24	"	"	
42	"	F-11	-	-	"	92	"	TS-25	3.4	5.31	
43	"	F-12	-	-	"	93	"	TS-26	"	"	
44	"	F-13	-	-	"	94	"	TS-27	3.3	"	
45	"	F-14	-	-	"	95	"	TS-28	"	"	
46	"	F-15	-	-	"	96	"	TS-29	3.8	5.32	
47	"	F-16	3.7	5.17		97	"	TS-30	"	"	
48	"	F-17	3.4	"		98	"	TS-31	"	"	
49	"	F-18	"	"		99	"	TS-32	"	5.33	
50	"	F-19	3.3	5.18		100	"	TS-33	"	"	

CH. No.	Item	Symb.	LOC. Fig.No.	Data Fig.No.	Comments	CH. No.	Item	Symb.	LOC. Fig.No.	Data Fig.No.	Comments
101	Temp.	TS-34	3.8	5.33		151	Temp.	TF2-48	3.12	5.38	
102	"	TS-35	"	5.32		152	"	-49	"	"	
103	"	TS-36	"	"		153	"	-50	"	"	
104	"	TF2-1	3.12	5.34		154	"	-51	"	"	
105	"	TF2-2	"	"		155	"	-52	"	"	
106	"	TF2-3	"	"		156	"	-53	"	"	
107	"	- 4	"	5.34		157	"	-54	"	5.39	
108	"	- 5	"	"		158	"	-55	"	"	
109	"	- 6	"	"		159	"	-56	"	"	
110	"	- 7	"	5.34		160	"	-57	"	"	
111	"	- 8	"	"		161	"	-58	"	"	
112	"	- 9	"	"		162	"	-59	"	"	
113	"	-10	"	5.34		163	"	-60	"	"	
114	"	-11	"	"		164	"	-61	"	5.40	
115	"	-12	"	"		165	"	-62	"	"	
116	"	-13	"	5.35		166	"	-63	"	"	
117	"	-14	"	"		167	"	-64	"	"	
118	"	-15	"	"		168	"	-65	"	"	
119	"	-16	"	5.36		169	"	-66	"	"	
120	"	-17	"	"		170	"	-67	"	"	
121	"	-18	"	"		171	"	-68	"	5.41	
122	"	-19	"	"		172	"	-69	"	"	
123	"	-20	"	"		173	"	-70	"	"	
124	"	-21	"	"		174	"	-71	"	5.41	
125	"	-22	"	"		175	"	-72	"	"	
126	"	-23	"	5.34		176	"	-73	"	"	
127	"	-24	"	"		177	"	-74	"	5.41	
128	"	-25	"	"		178	"	-75	"	"	
129	"	-26	"	5.34		179	"	-76	"	"	
130	"	-27	"	"		180	"	-77	"	5.41	
131	"	-28	"	"		181	"	-78	"	"	
132	"	-29	"	5.34		182	"	-79	"	"	
133	"	-30	"	"		183	"	-80	"	5.42	
134	"	-31	"	"		184	"	-81	"	"	
135	"	-32	"	5.34		185	"	-82	"	"	
136	"	-33	"	"		186	"	-83	"	"	
137	"	-34	"	"		187	"	-84	"	"	
138	"	-35	"	5.34		188	"	-85	"	"	
139	"	-36	"	"		189	"	-86	"	"	
140	"	-37	"	"		190	"	-87	"	5.41	
141	"	-38	"	5.34		191	"	-88	"	"	
142	"	-39	"	"		192	"	-89	"	"	
143	"	-40	"	"		193	"	-90	"	5.41	
144	"	-41	"	5.37		194	"	-91	"	"	
145	"	-42	"	"		195	"	-92	"	"	
146	"	-43	"	"		196	"	-93	"	5.41	
147	"	-44	"	5.34		197	"	-94	"	"	
148	"	-45	"	"		198	"	-95	"	"	
149	"	-46	"	"		199	"	-96	"	5.43	
150	"	TF2-47	"	5.38		200	"	TF2-97	"	"	

CH. No.	Item	Symb.	LOC. Fig.No.	Data Fig.No.	Comments	CH. No.	Item	Symb.	LOC. Fig.No.	Data Fig.No.	Comments
201	Temp.	TF2-98	3.12	5.43		251	Temp.	TC- 4	3.12	5.51	
202	"	- 99	"	"		252	"	- 5	"	5.50	
203	"	-100	"	"		253	"	- 6	"	5.51	
204	"	-101	"	"		254	"	- 7	"	5.50	
205	"	-102	"	"		255	"	- 8	"	5.51	
206	"	-103	"	5.44		256	"	TB- 1	"	5.52	
207	"	-104	"	"		257	"	- 2	"	"	
208	"	-105	"	"		258	"	- 3	"	"	
209	"	-106	"	"		259	"	- 4	"	"	
210	"	-107	"	"		260	"	- 5	"	"	
211	"	-108	"	"		261	"	- 6	"	"	
212	"	-109	"	"		262	"	- 7	"	"	
213	"	-110	"	5.45		263	"	- 8	"	5.53	
214	"	-111	"	"		264	"	- 9	"	"	
215	"	-112	"	"		265	"	-10	"	"	
216	"	-113	"	"		266	"	-11	"	"	
217	"	-114	"	"		267	"	-12	"	"	
218	"	-115	"	"		268	"	-13	"	"	
219	"	-116	"	"		269	"	-14	"	"	
220	"	-117	"	5.46		270	"	TP- 1	3.10	5.54	
221	"	-118	"	"		271	"	- 2	"	"	
222	"	-119	"	"		272	"	- 3	"	"	
223	"	-120	"	"		273	"	- 4	"	"	
224	"	-121	"	"		274	"	- 5	"	"	
225	"	-122	"	"		275	"	- 6	"	"	
226	"	-123	"	"		276	"	- 7	"	5.55	
227	"	-124	"	5.47		277	"	- 8	"	"	
228	"	-125	"	"		278	"	- 9	"	"	
229	"	-126	"	"		279	"	-10	"	"	
230	"	-127	"	"		280	"	TG2- 1	3.12	5.56	
231	"	-128	"	"		281	"	- 2	"	"	
232	"	-129	"	"		282	"	- 3	"	"	
233	"	-130	"	"		283	"	- 4	"	"	
234	"	-131	"	5.48		284	"	- 5	"	"	
235	"	-132	"	"		285	"	- 6	"	5.57	
236	"	-133	"	"		286	"	- 7	"	"	
237	"	-134	"	"		287	"	- 8	"	"	
238	"	-135	"	"		288	"	- 9	"	"	
239	"	-136	"	"		289	"	-10	"	"	
240	"	-137	"	"		290	"	-11	"	5.58	
241	"	-138	"	5.49		291	"	-12	"	"	
242	"	-139	"	"		292	"	-13	"	"	
243	"	-140	"	"		293	"	-14	"	"	
244	"	-141	"	"		294	"	-15	"	"	
245	"	-142	"	"		295	"	-16	"	5.59	
246	"	-143	"	"		296	"	-17	"	"	
247	"	-144	"	"		297	"	-18	"	"	
248	"	TC- 1	"	5.50		298	"	-19	"	"	
249	"	- 2	"	5.51		299	"	-20	"	"	
250	"	- 3	"	5.50		300	Water Level	LB- 1	"	5.60	

CH. No.	Item	Symb.	LOC. Fig.No.	Data Fig.No.	Comments	CH. No.	Item	Symb.	LOC. Fig.No.	Data Fig.No.	Comments
301	Water Level	LB- 2	3.12	5.60		351	Flow	FE- 4	-	-	undefined
302	"	- 3	"	"		352	Direc.	FD- 1	-	-	"
303	"	- 4	"	"		353	"	- 2	-	-	"
304	"	- 5	"	5.61		354	"	- 3	-	-	"
305	"	- 6	"	"		355	"	- 4	-	-	"
306	"	- 7	"	"		356	Dens.	DF- 1	-	-	"
307	"	- 8	"	5.62		357	"	- 2	-	-	"
308	"	- 9	"	"		358	"	- 3	-	-	"
309	"	-10	"	"		359	"	- 4	-	-	"
310	"	-11	"	"		360	"	- 5	-	-	"
311	"	-12	"	5.63		361	"	- 6	-	-	"
312	"	-13	"	"		362	"	- 7	-	-	"
313	"	-14	"	"		363	"	- 8	-	-	"
314	"	-15	"	5.64		364	Mome.F	M - 1	-	-	"
315	"	-16	"	"		365	"	- 2	-	-	"
316	"	-17	"	"		366	"	- 3	-	-	"
317	"	-18	"	"		367	Flow	F -23	-	-	"
318	"	-19	"	5.65		368	"	-24	-	-	"
319	"	-20	"	"		369	"	-25	-	-	"
320	"	-21	"	"		370	Press.	P -17	-	-	"
321	"	LL- 1	"	5.66		371	"	-18	-	-	"
322	"	- 2	"	"		372	"	-19	-	-	"
323	"	- 3	"	"		373	Temp.	T -24	-	-	"
324	"	- 4	"	"		374	"	-25	-	-	"
325	"	- 5	"	5.67		375	"	-26	-	-	"
326	"	- 6	"	"		426	Power	LP- 1	-	5.83	
327	"	- 7	"	"		427	"	- 2	-	"	
328	"	- 8	"	"		428	"	- 3	-	"	
329	Void	VE- 1	-	-	undefined	429	Flow	MF- 1	-	5.13	
330	"	- 2	-	-	"	430	"	- 2	-	5.14	
331	"	- 3	-	-	"	431	"	- 3	-	-	no data
332	"	- 4	-	-	"	432	"	- 4	-	-	"
333	"	- 5	-	-	"	433	"	- 5	-	-	"
334	"	- 6	-	-	"	434	"	- 7	-	-	"
335	"	- 7	-	-	"	435	"	- 8	-	-	"
336	"	- 8	-	-	"	436	"	- 9	-	-	"
337	"	- 9	-	-	"	437	Quali.	X - 1	-	5.26	
338	"	-10	-	-	"	438	"	- 2	-	5.27	
339	"	-11	-	-	"	439	"	- 3	-	-	undefined
340	"	-12	-	-	"	440	"	- 4	-	-	"
341	"	-13	-	-	"	441	"	- 5	-	-	"
342	"	-14	-	-	"	442	Dens.	DF-10	-	-	no data
343	"	-15	-	-	"	443	"	-11	-	-	"
344	"	VP- 1	-	-	"	444	"	-12	-	-	"
345	"	- 2	-	-	"	445	"	-14	-	-	"
346	"	- 3	-	-	"	446	"	-15	-	-	"
347	"	- 4	-	-	"	447	"	-16	-	-	"
348	Flow	FE- 1	-	-	"	448	Void	FG- 1	-	-	"
349	"	- 2	-	-	"	449	"	- 2	-	-	"
350	"	- 3	-	-	"	450	"	- 3	-	-	"

Table 4-1 Test Conditions of the ROSA-III RUN 706

Parameter		Specified Value	Measured Value
Break Conditions			
Location		MRP-2 Suction	
Type		Double Ended	
Break Orifice Diameter	(mm)	26.2/26.2	
Initial System Conditions			
Steam Dome Pressure	(MPa)	7.15	7.17
Lower Plenum Temperature	(°K)	-	561
Lower Plenum Subcooling	(°K)	-	12
Core Inlet Flow Rate	(kg/s)	36.4	36.2
Broken Loop Flow Rate	(m^3/s)	2.41×10^{-2}	2.36×10^{-2}
Intact Loop Flow Rate	(m^3/s)	2.41×10^{-2}	2.42×10^{-2}
Core Outlet Quality	(-)	0.025	0.025
Power Level	(M W)	3.450	3.405
Maximum Linear Heat Power			
of Region 1 [39 rods]	(kw/m)	10.05	10.10
Region 2 [63 rods]	(kw/m)	10.51	9.55
Region 3 [150 rods]	(kw/m)	10.18	10.18
Power Curve		dp + dn + sh [a]	dp + dn + sh [b]
Water Level in PV	(m)	4.62	4.61
Feedwater Conditions			
Steady State Line			
Temperature	(°K)		Room Temp.
Flow Rate	(m^3/s)		1.29×10^{-3} (Ch.47)

a ; dp = decay power of fission products
dn = delayed neutron fission power
sh = stored heat release from heater rods

b ; cf. Fig. 5.3

Table 4.1 (Continued)

Parameter		Specified Value	Measured Value
Feedwater Conditions (Continued)			
Transient Line			
Temperature	(°K)		
Flow Rate	(m^3/s)		
Termination Time	(sec)		
Steam Discharge Conditions			
Steady State Line			
Flow Rate	(kg/s)		1.24
Transient Line			
Flow Rate	(kg/s)	-	
Orifice Diameter	(mm)	-	
Termination Time	(sec)	-	
ECCS Conditions			
HPCS			
Injection Location			
Initiation Time	(sec)		
at Pressure in PV	(MPa)		
Water Level in PV	(m)		
Coolant Temperature	(°K)		
Injection Flow Rate	(ℓ/min)		
LPCS			
Injection Location			
Initiation Time	(sec)		
at Pressure in PV	(MPa)		
Water Level in PV	(m)		
Coolant Temperature	(°K)		
Injection Flow Rate	(ℓ/min)		

Table 4-1 (Continued)

Parameter		Specified Value	Measured Value
ECCS Conditions (Continued)			
LPCI			
Injection Location			
Initiation Time	(sec)		
at Pressure in PV	(MPa)		
Coolant Temperature	(°K)		
Injection Flow Rate	(ℓ/min)		
ADS Conditions			
Valve Opening Time	(sec)		35
Valve Closed Time	(sec)		69
Flow Rate	(m^3/s)		
Orifice Diameter	(mm)		

Delay time set for RUN 706 (cf. Fig. 4.1)

T_1 = 0.	T_6 = 0.	T_{10} = -	T_{14} = -
T_2 = 2.	T_7 = 0.	T_{11} = -	T_{15} = -
T_3 = 0.	T_8 = 0.	T_{12} = -	T_{16} = -
T_4 = 0.	T_9 = -	T_{13} = 0.	T_{17} = -
T_5 = 0.			

Table 5-1 Time Sequence of Major Events in RUN 706

Time (s)	Events
-10 ∿	Initiation of Recording System
0	. Break Initiation . MRP-1 Coast-down (0 ∿ 7s) . MRP-2 " (0 ∿ 3s) . Closure of Steam Line (0 ∿ 3s) . Closure of Feed Water (0 ∿ 15s)
3 ∿	MRP-2 Rotated in Reverse Direction
8.5	Jet Pump Suction Uncovered
10	Recirculation Pump Suction Line Uncovered
8 ∿ 15	Initiation of Fuel Rods Exposure (Pos.1 ∿ 6)
17	Initiation of Lower Plenum Flashing
17 ∿ 28	Rewetting of Fuel Rods (Pos.4 ∿ 6)
27 ∿ 72	Second Fuel Rods Exposure (Pos.4 ∿ 7) (Pos.7 : 1st Exposure)
35 ∿ 69	Leak from ADS Line
156	Power Supply to Fuel Rods Terminated
680	Termination of Recording System

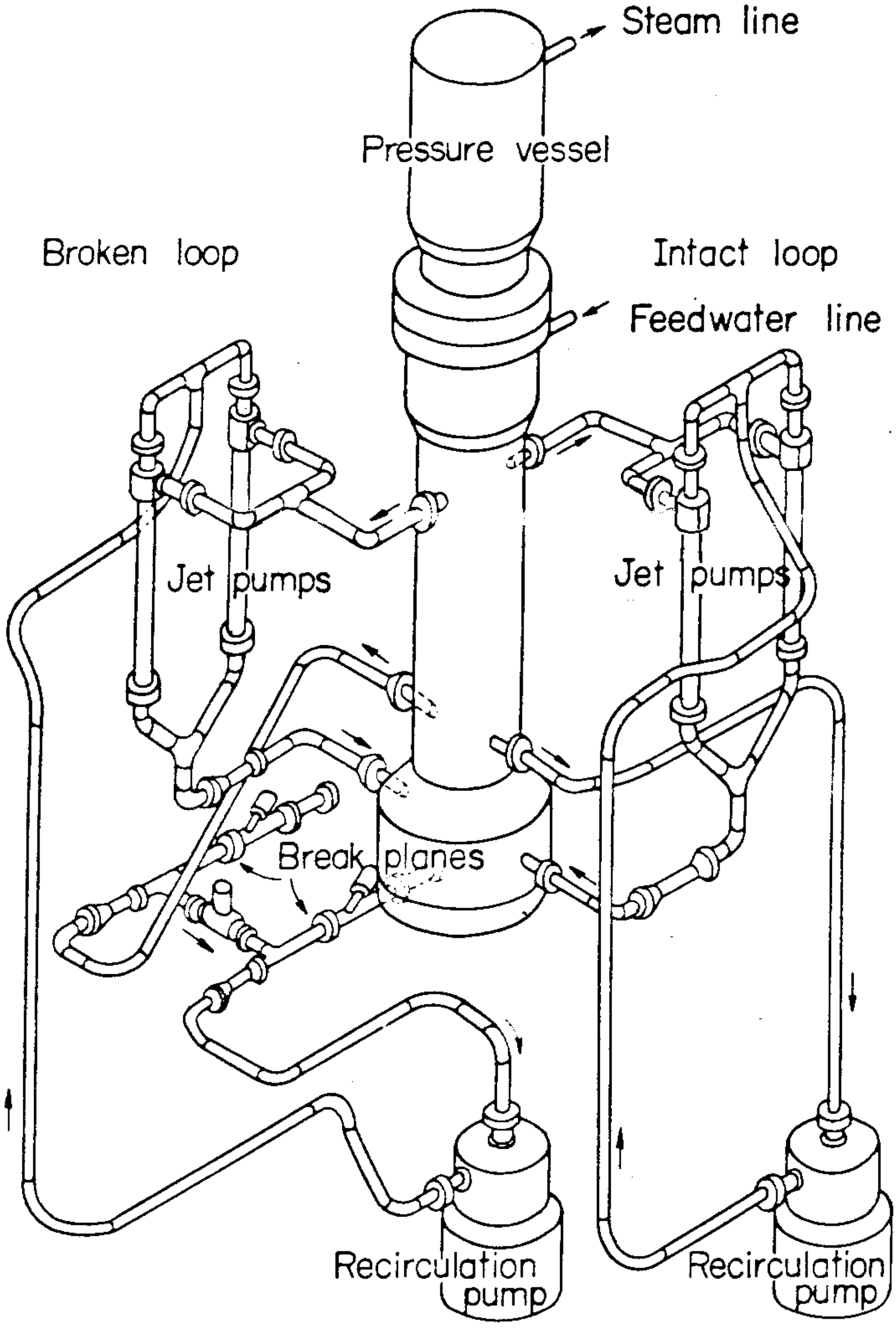

Fig.2.1 Schematic Diagram of ROSA-III Test Facility

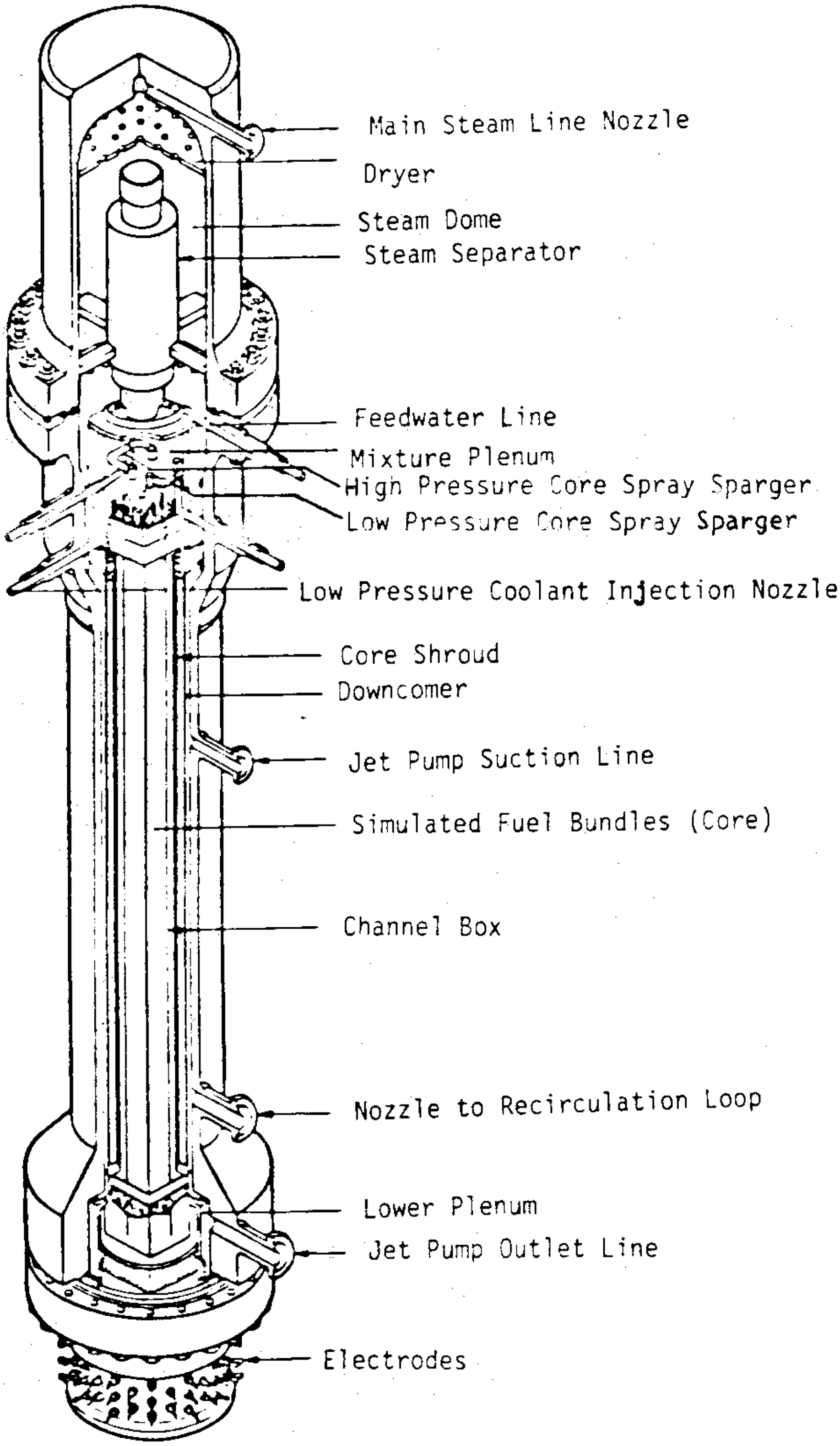

Fig. 2.2 Internal Structure of Pressure Vessel of ROSA-III

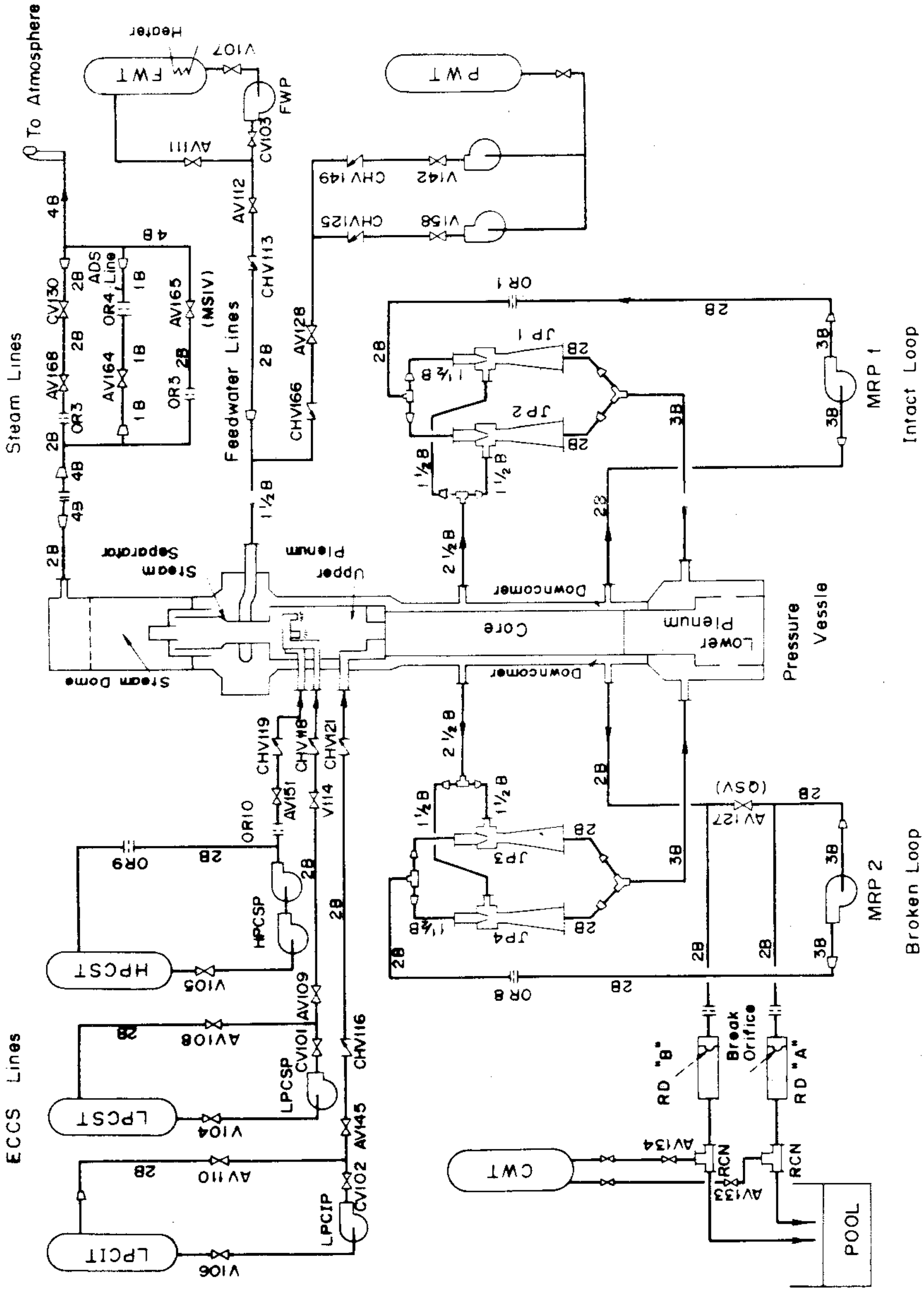

Fig.2.3 ROSA-III Piping Schematic

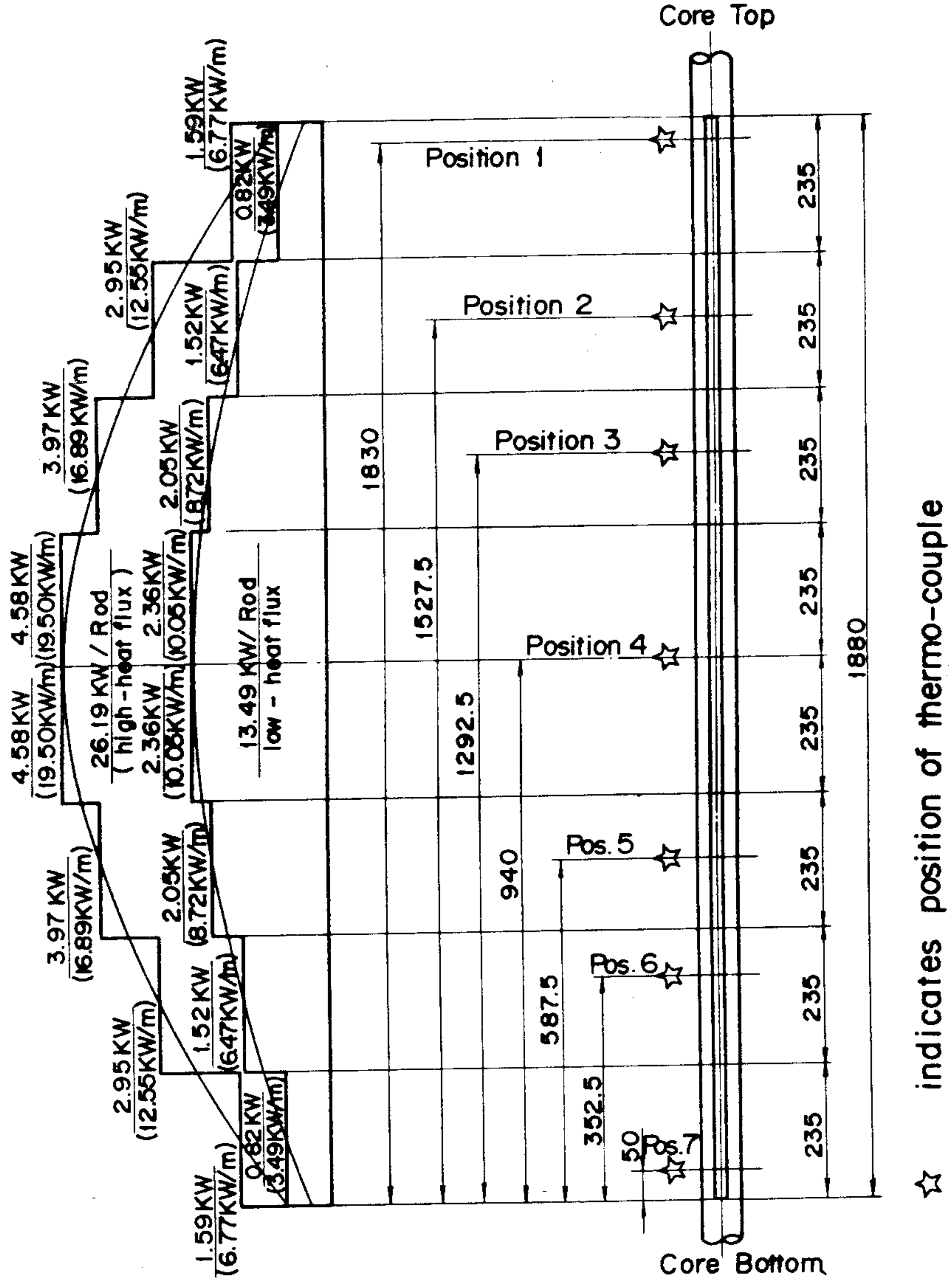

Fig.2.4 Axial Power Distribution of Simulated Fuel Rods (2)

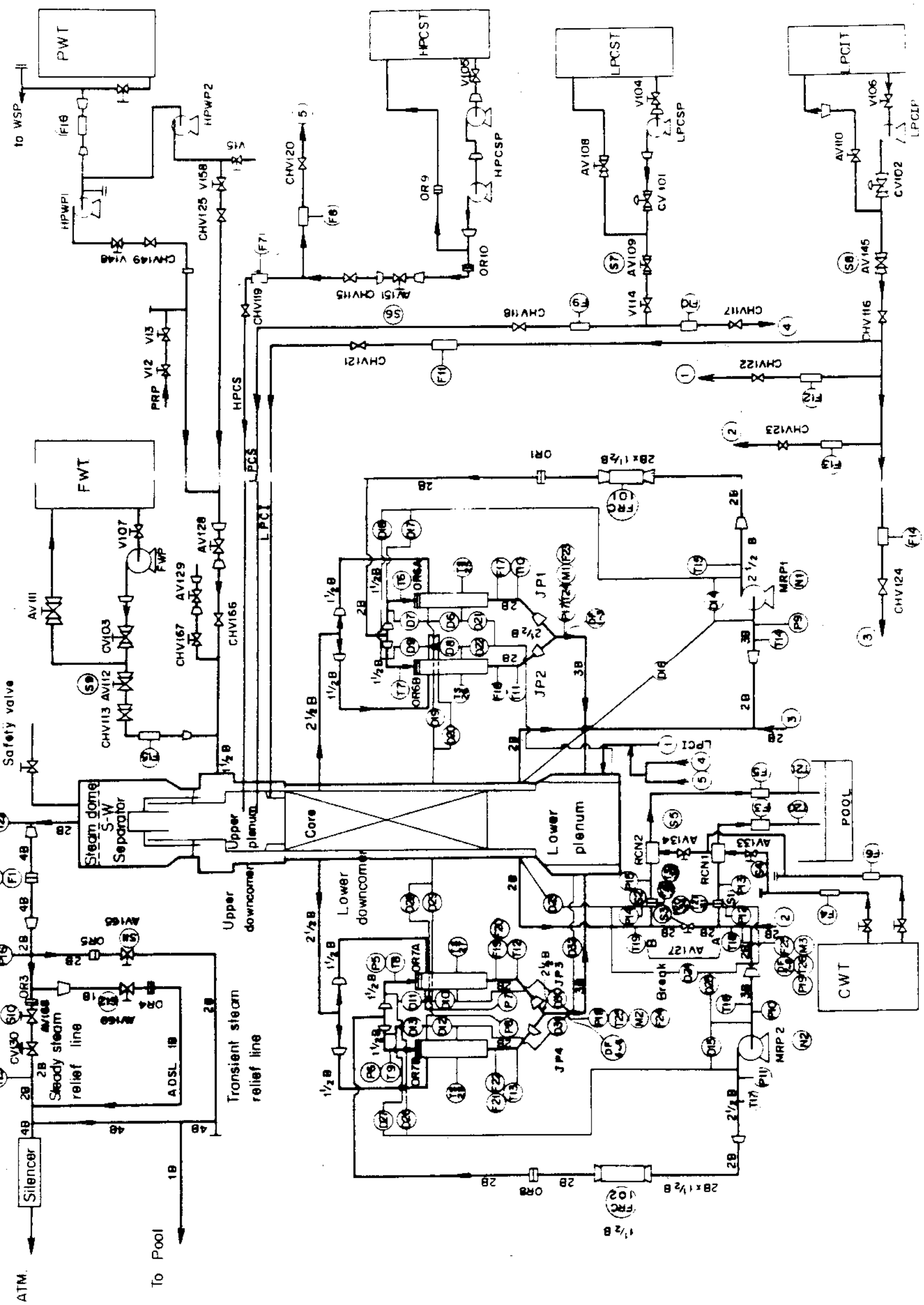

Fig. 3.1 Flow Diagram and Instrumentation Location of ROSA-III Facility

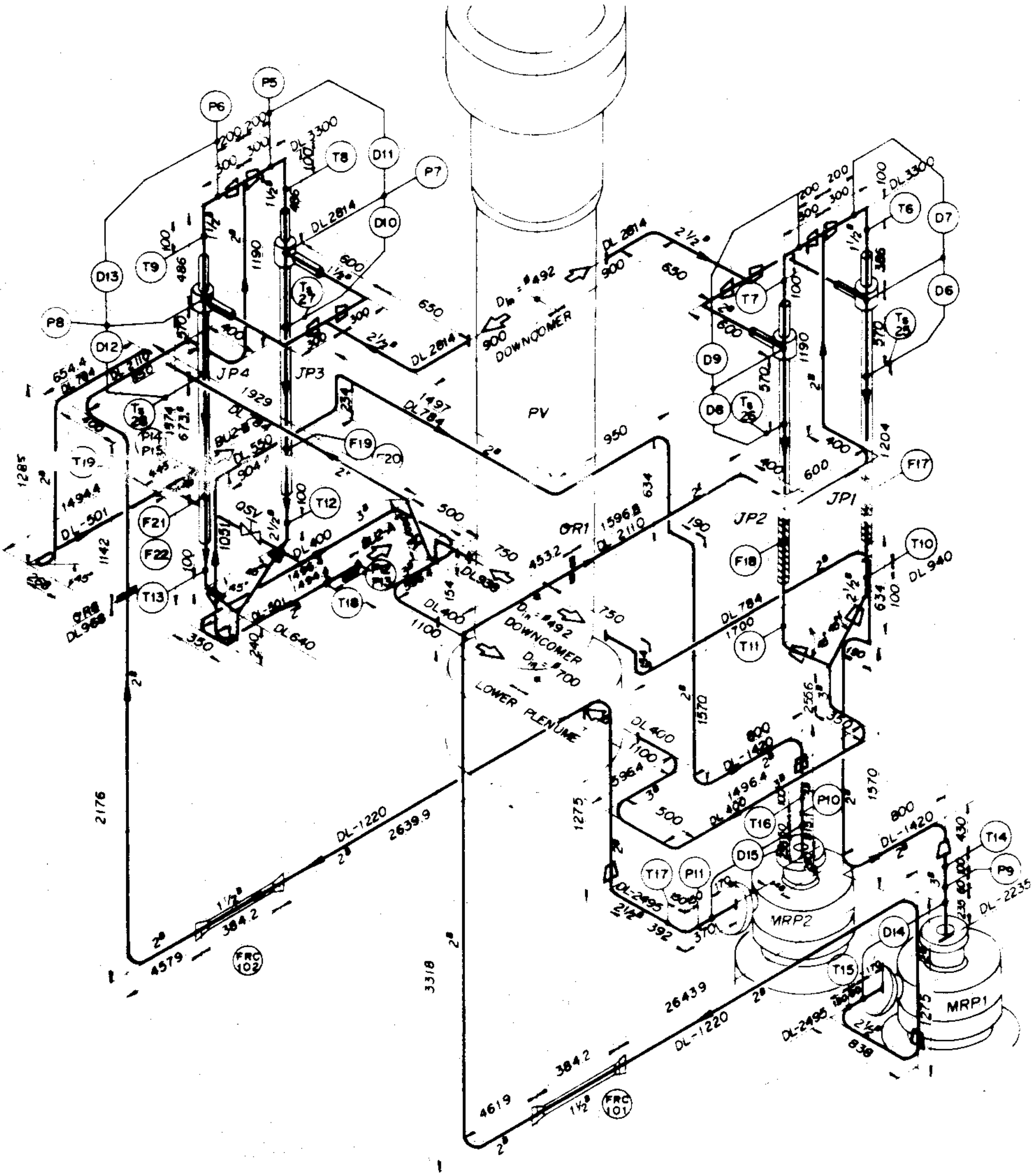

Fig.3.2 ROSA-III Recirculation Loops with Instrumentation

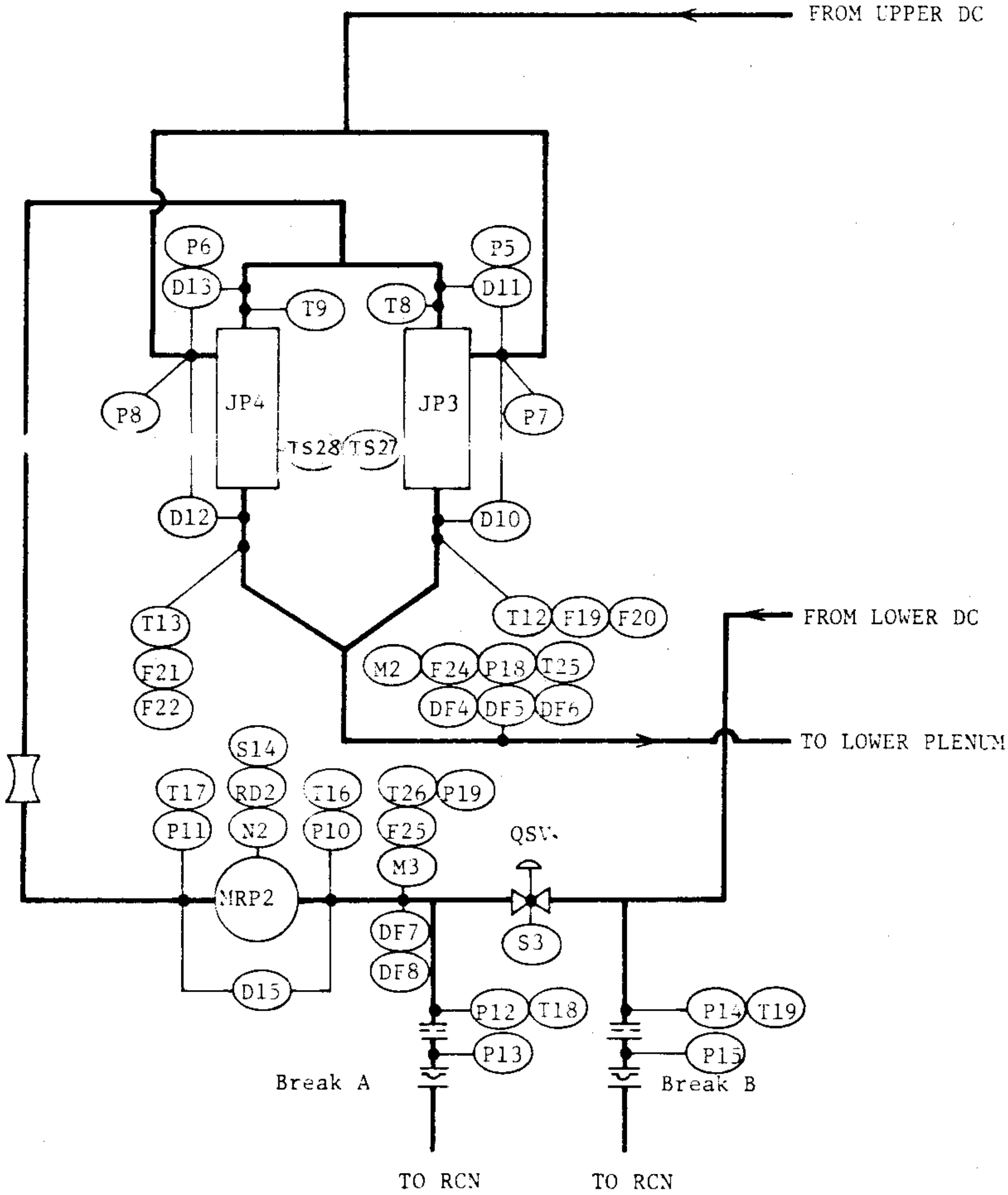

Fig. 3.3 Instrumentation in the Blowdown Loop

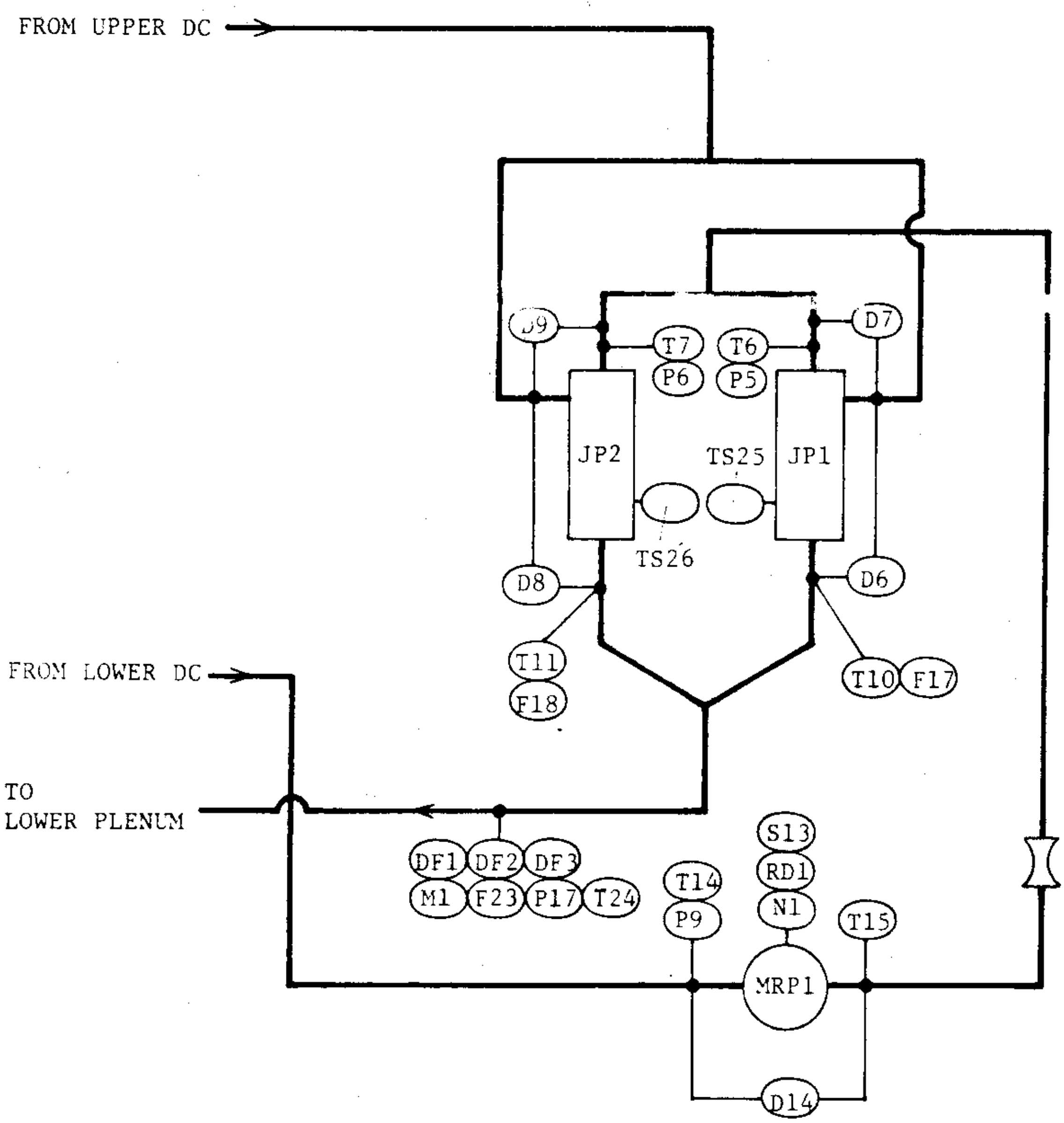

Fig.3.4 Instrumentation in the Intact Loop

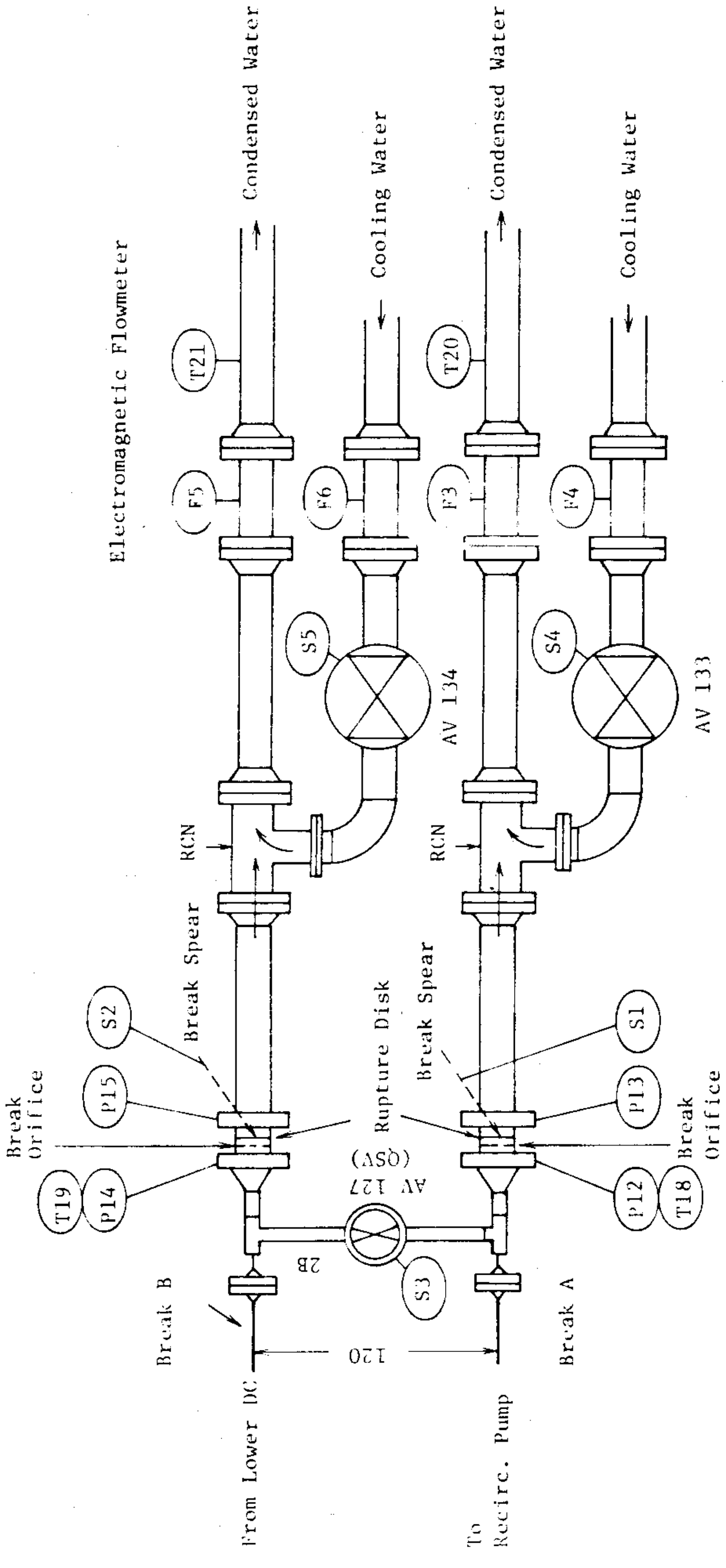

Fig.3.5 Instrumentation in the Break Unit

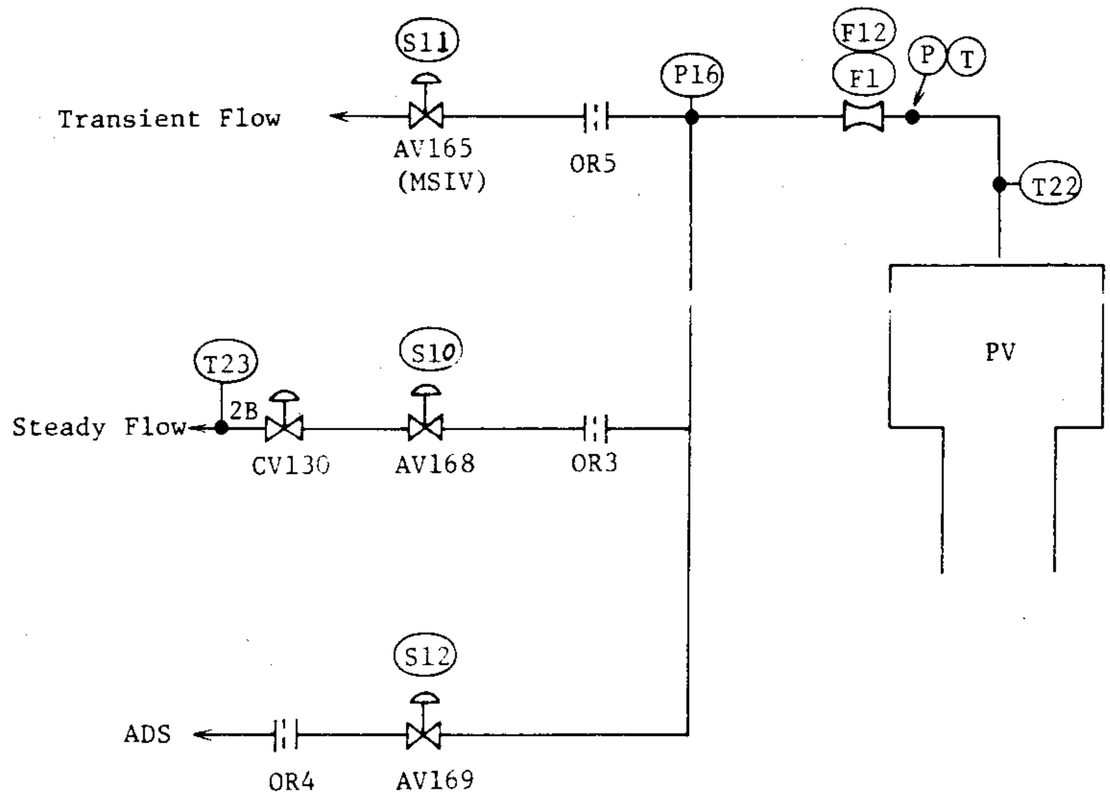

Fig.3.6 Instrumentation in the Steam Line

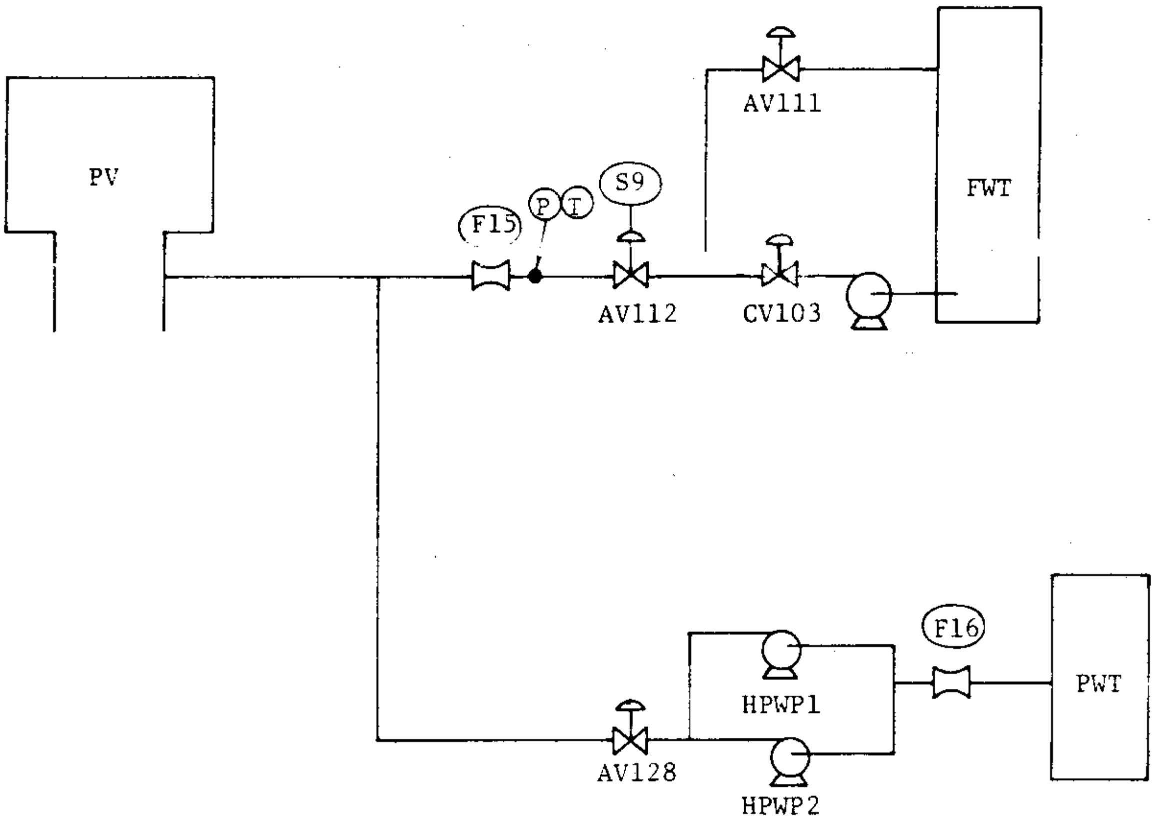

Fig.3.7 Instrumentation in the Feedwater Line

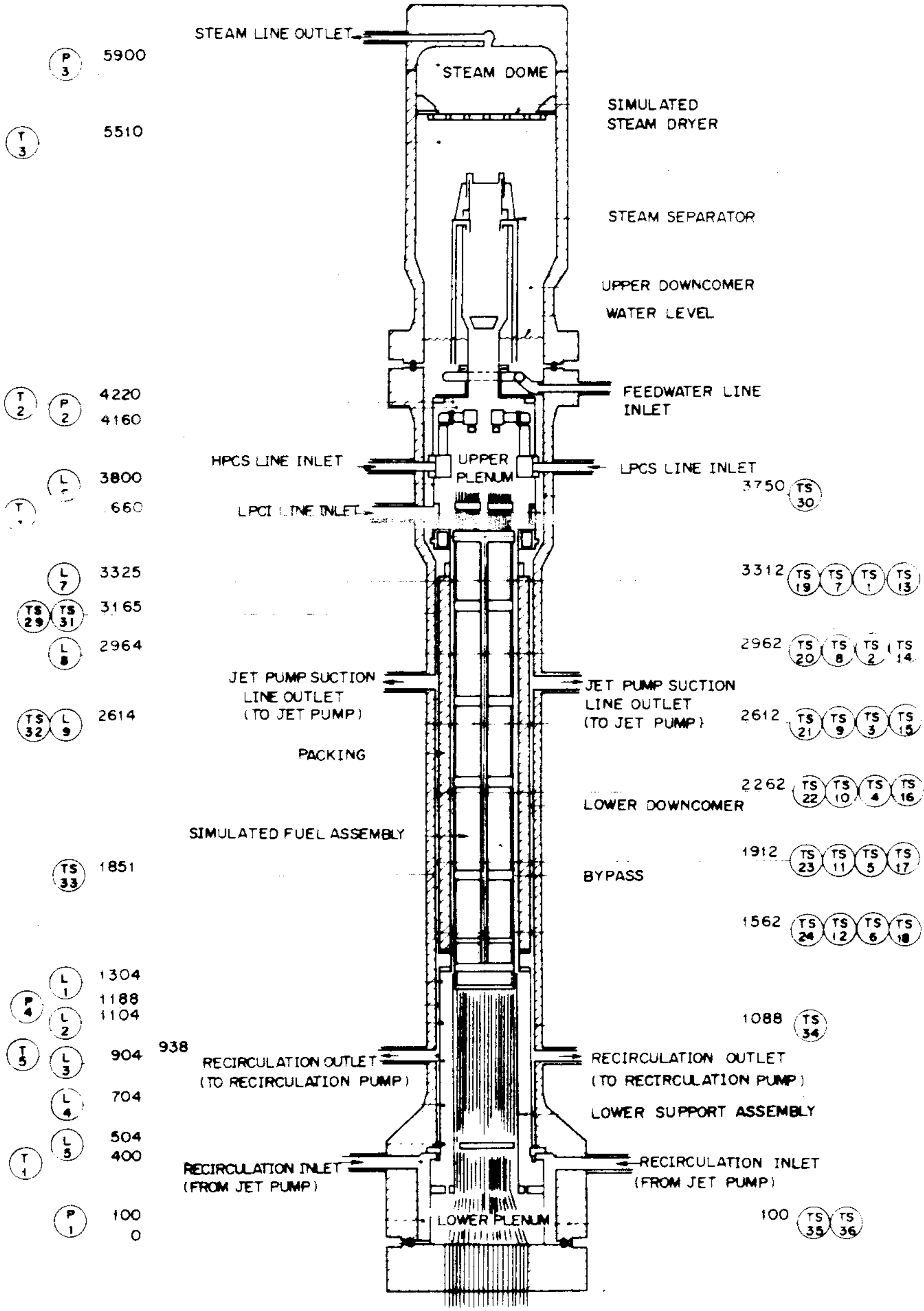

Fig.3.8 ROSA-III Pressure Vessel with Instrumentation

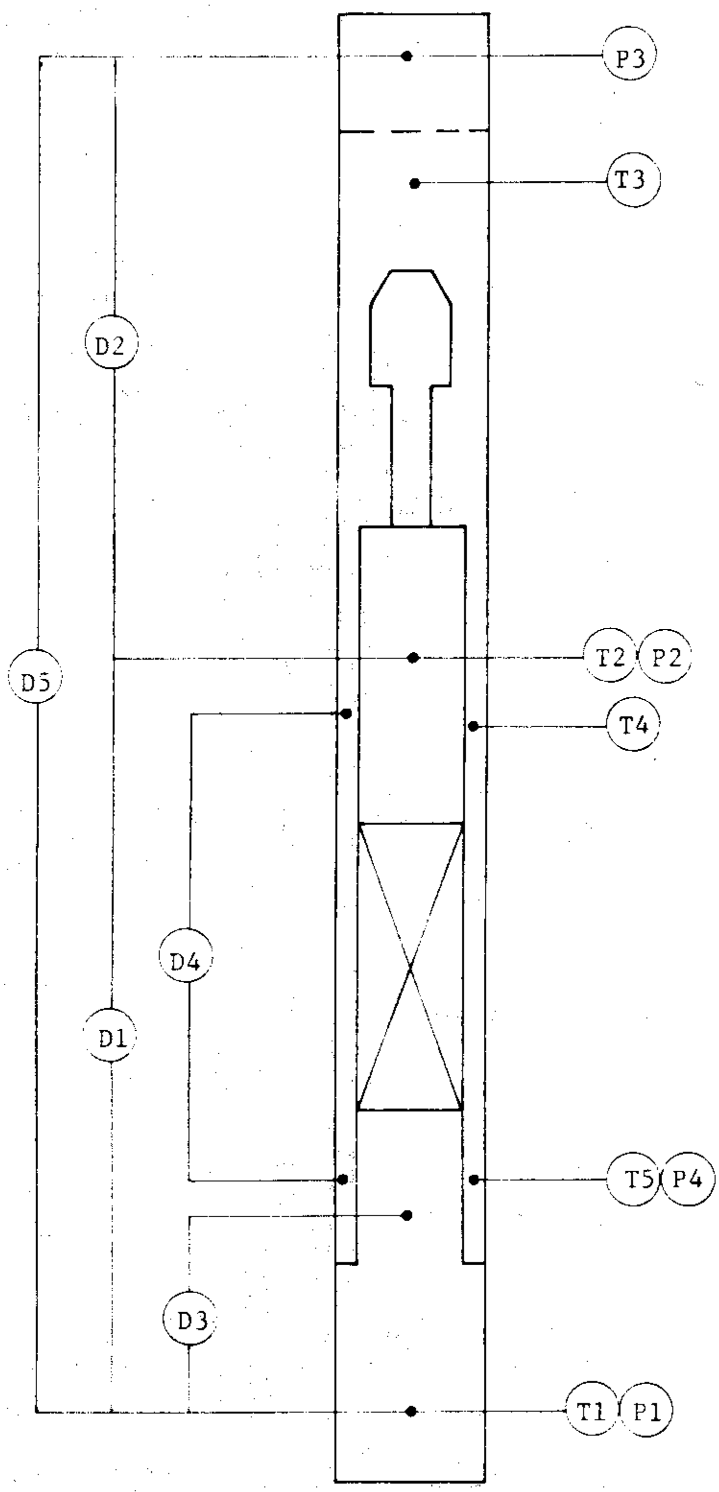

Fig.3.9   Instrumentation in the Pressure Vessel

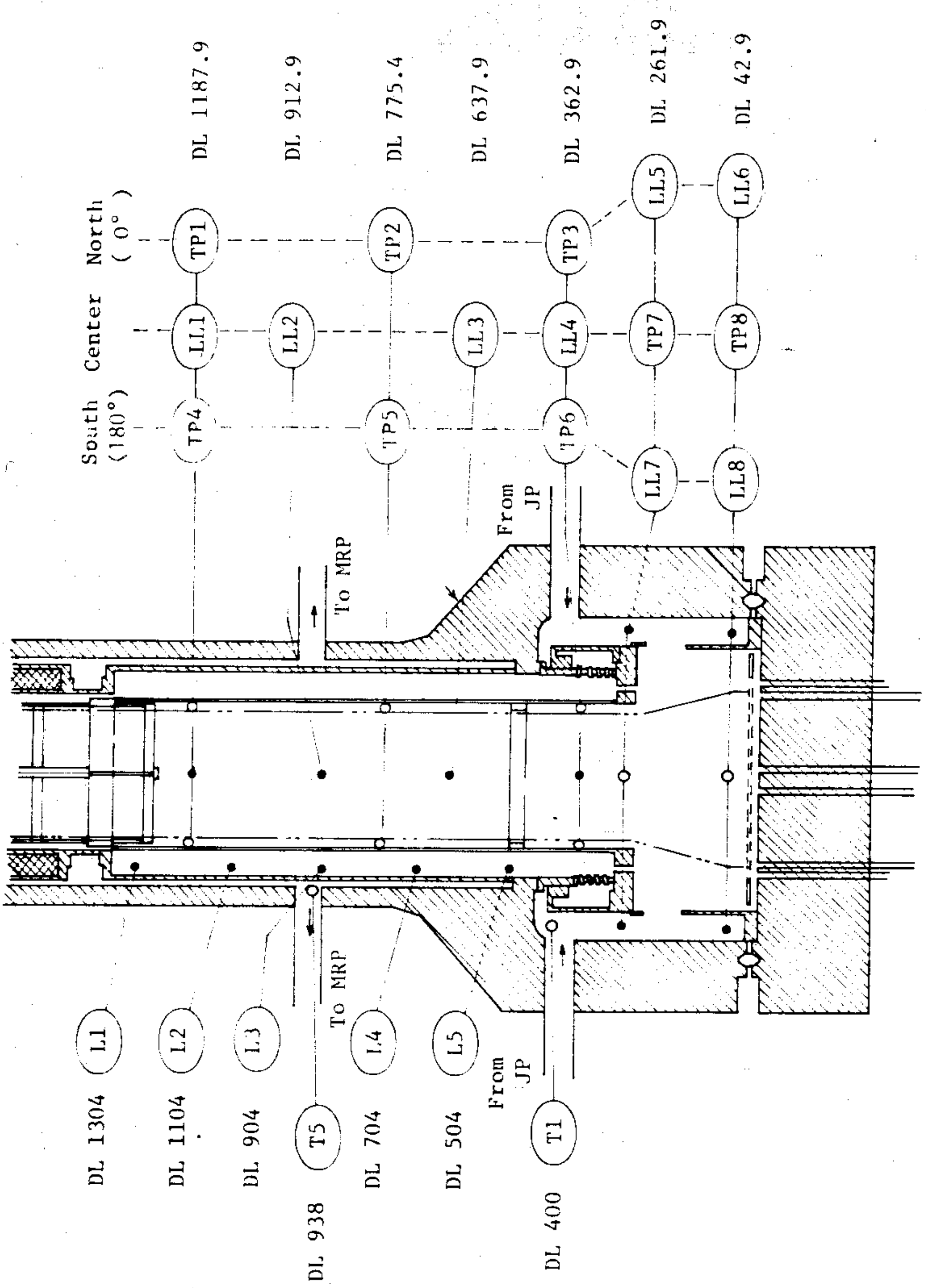

Fig.3.10 Instrumentation Location in Lower Plenum

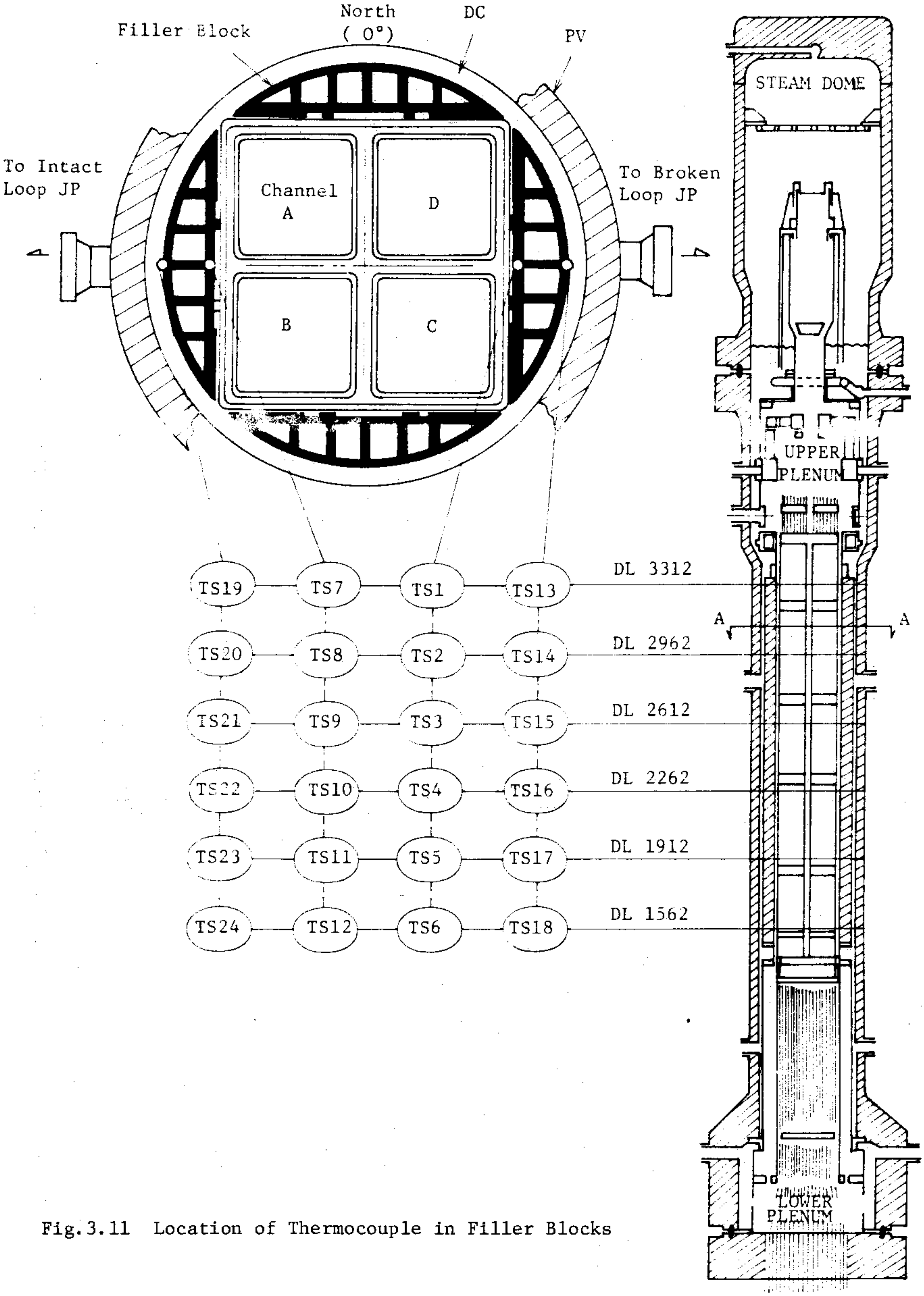

Fig.3.11 Location of Thermocouple in Filler Blocks

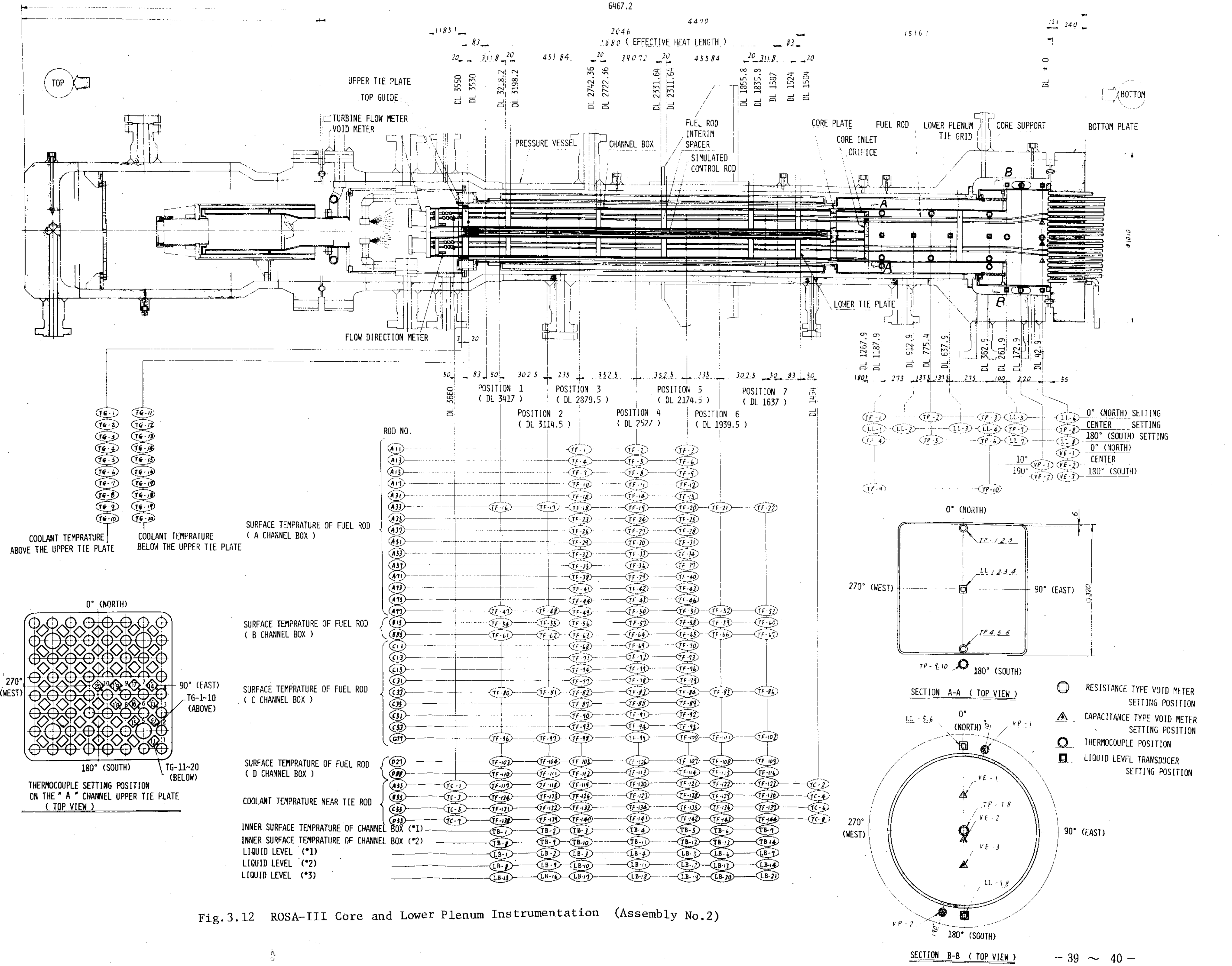

Fig.3.12 ROSA-III Core and Lower Plenum Instrumentation (Assembly No.2)

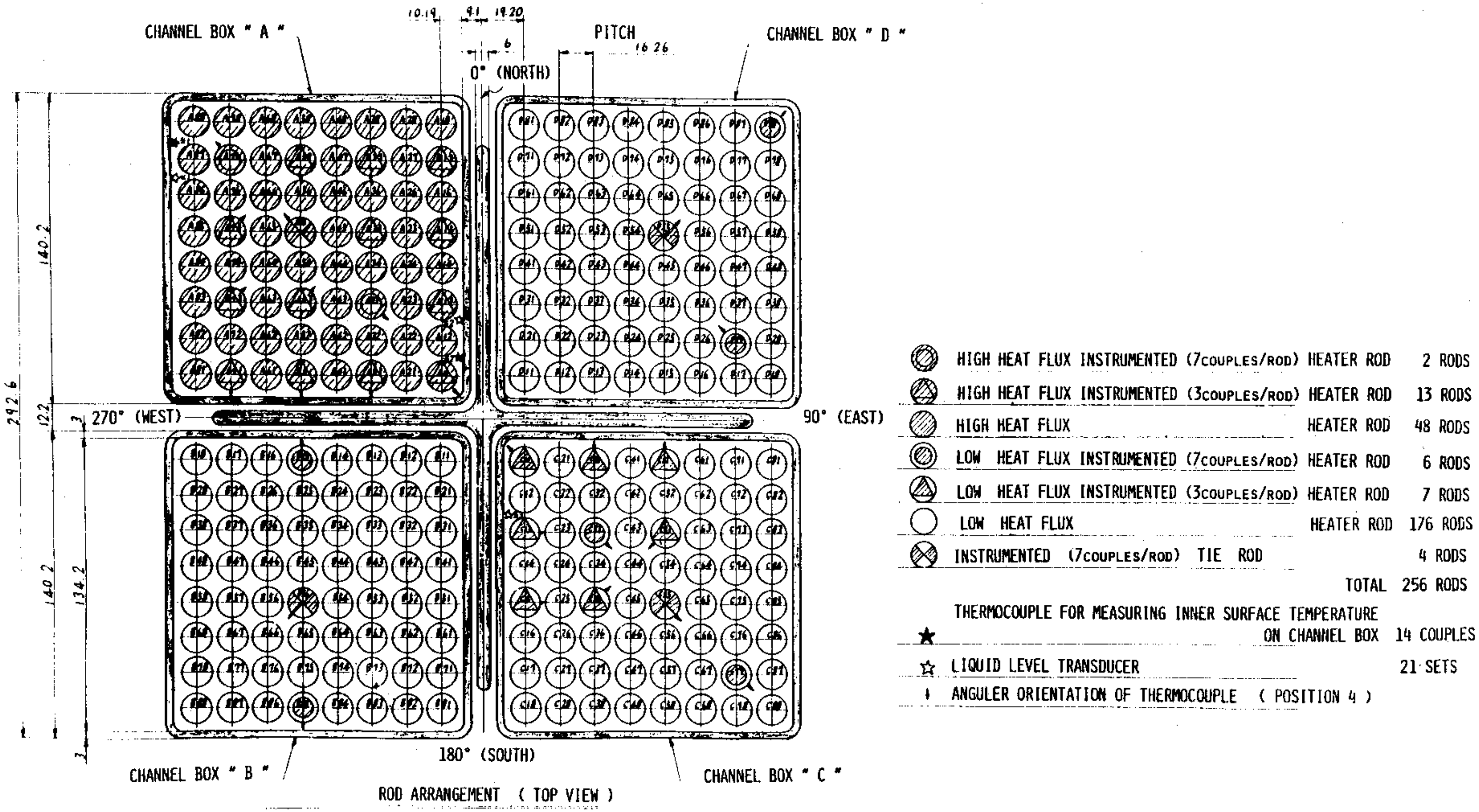

Fig.3.13 ROSA-III Core Map

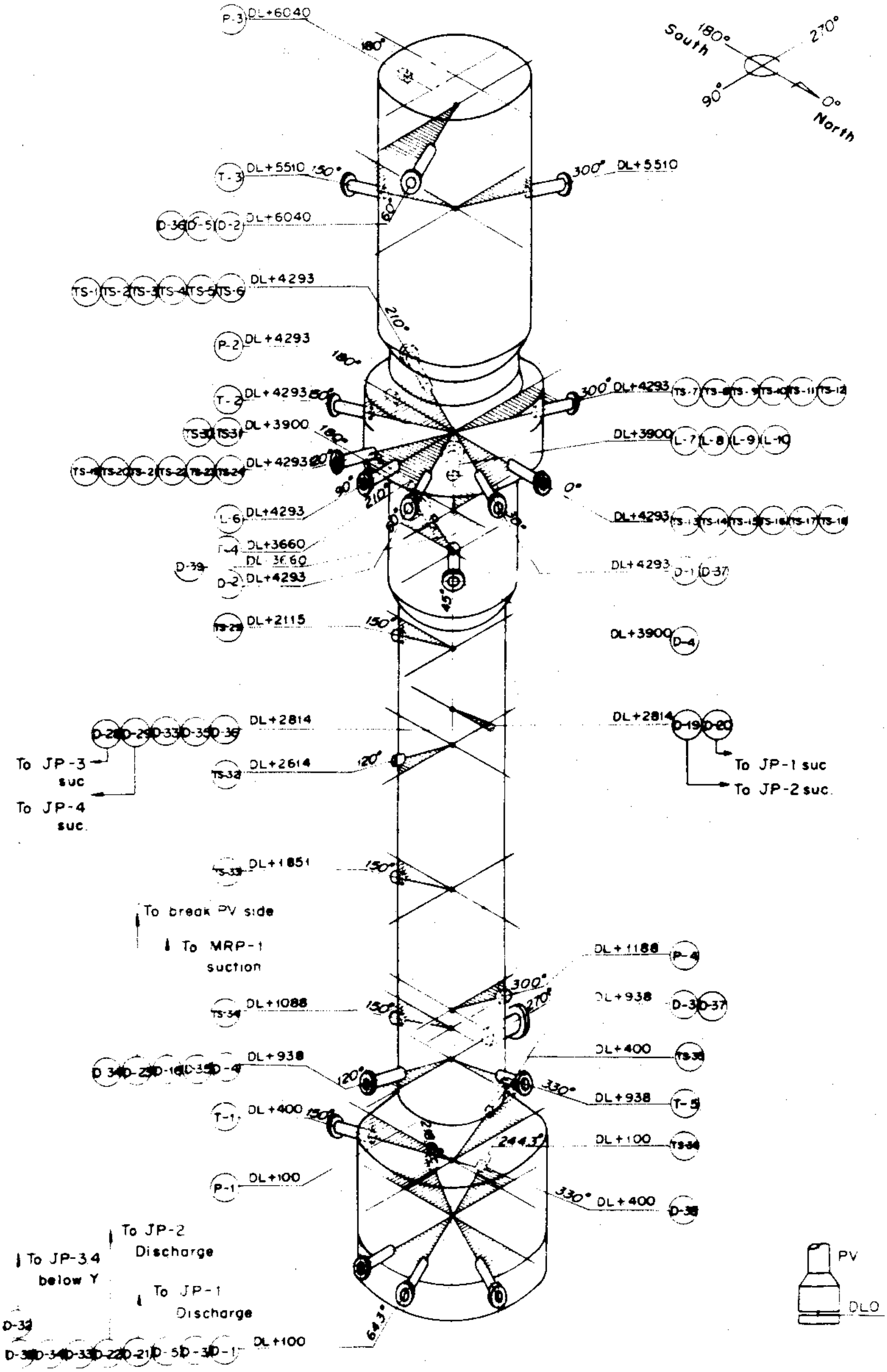

Fig.3.14 Lead Out Nozzles for Measurement in the Pressure Vessel

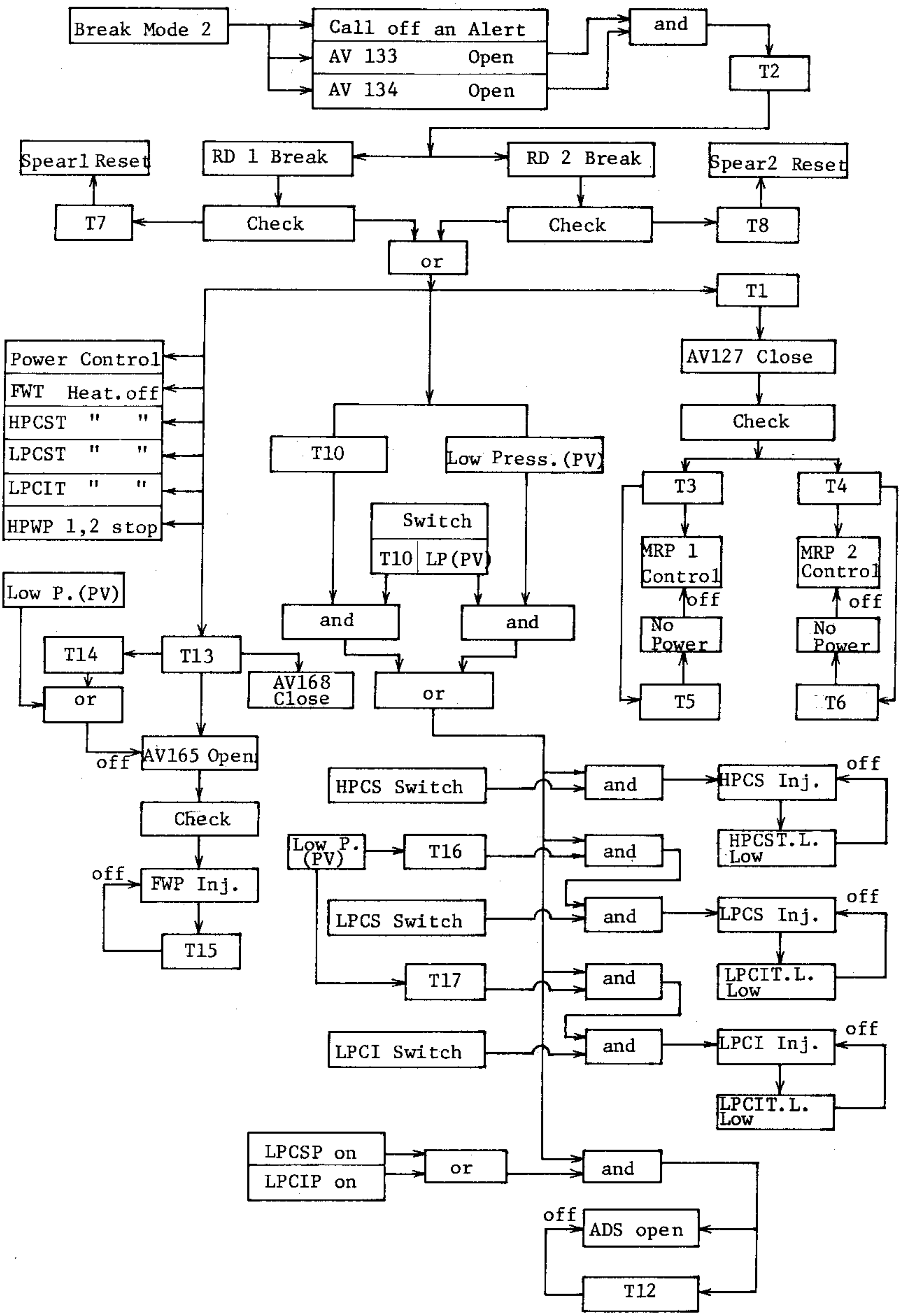

Fig.4.1 Break Mode 2 for RUN 706 in the ROSA-III Program

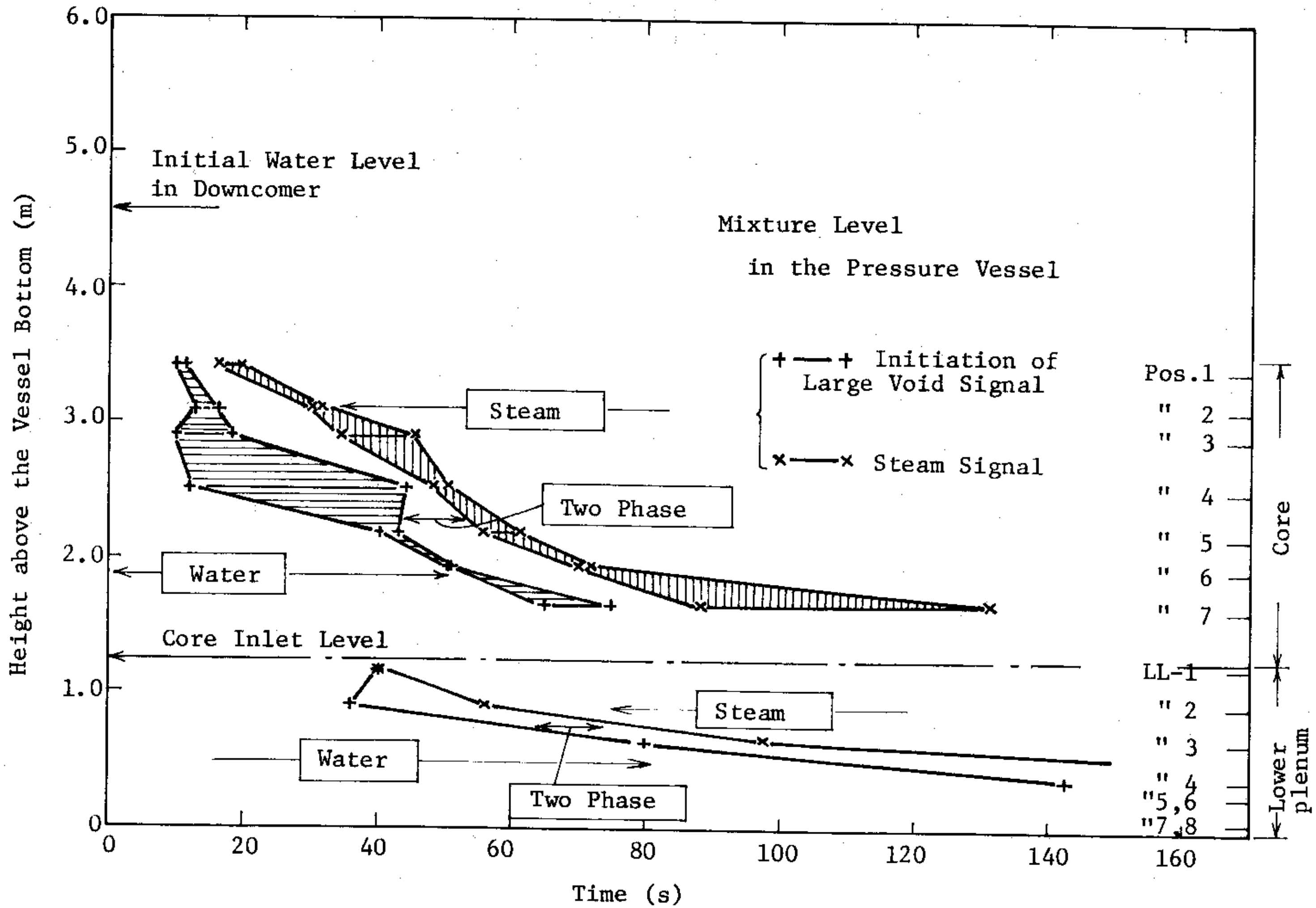

Fig.5.1 Transients of Mixture Level in the Core and the Lower Plenum Reduced from Level Meters

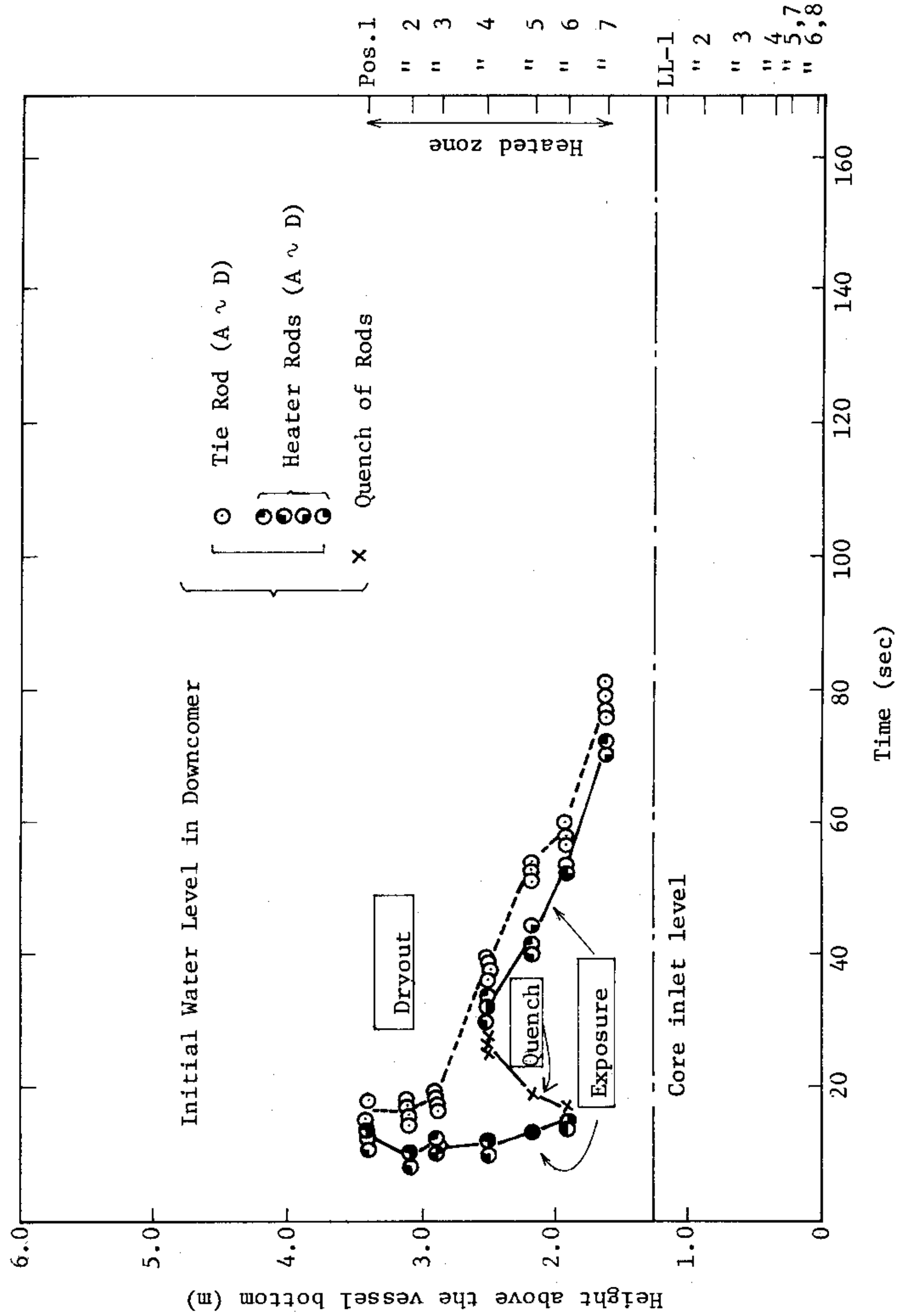

Fig.5.2 Transients of Exposure and Quench Phenomena in the Core Reduced from Rod Temperatures

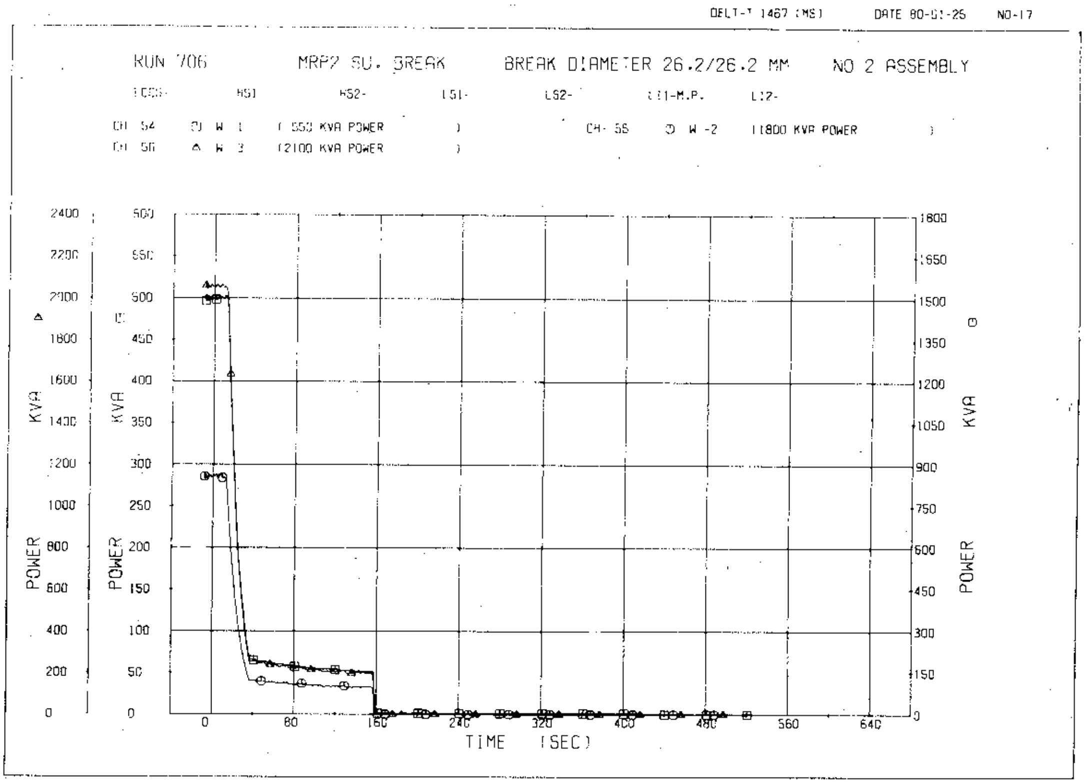

Fig.5.3 Power Transients of 550 kW, 1800 kW and 2100 kW Power Supply

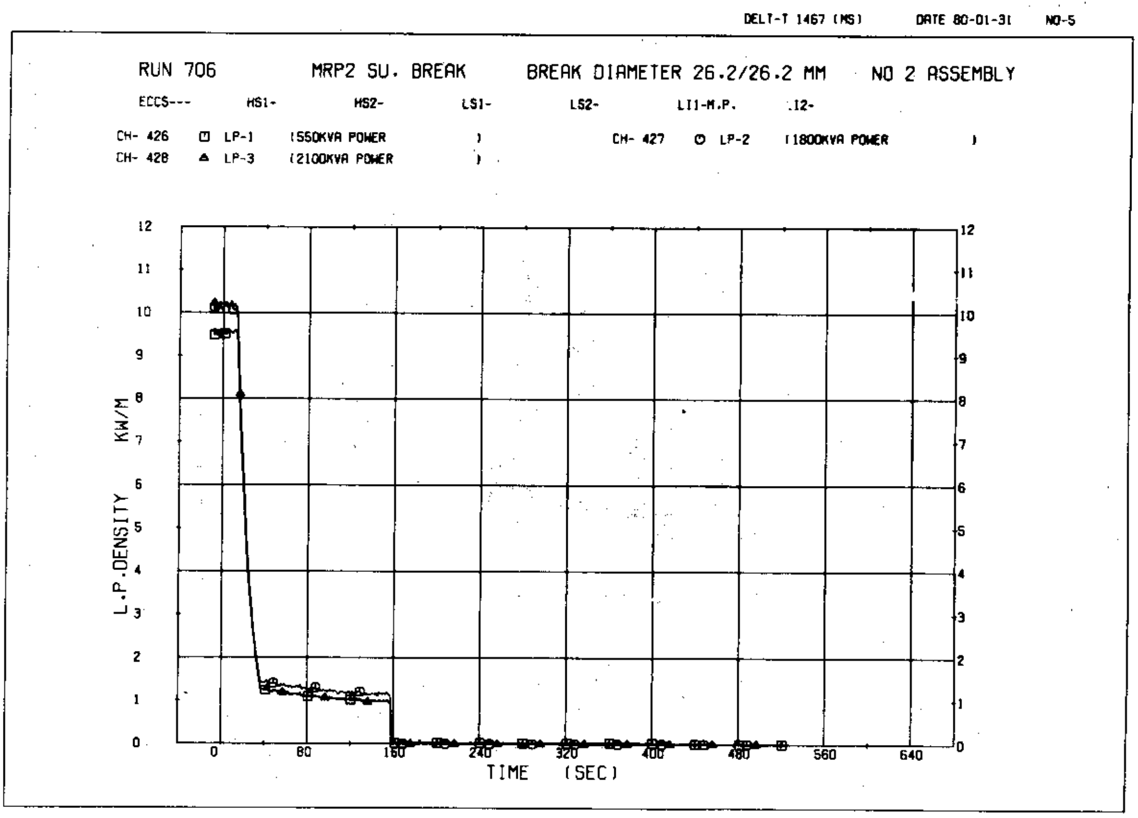

Fig.5.4 Linear Power Density of 550 kW, 1800 kW and 2100 kW Power Supply

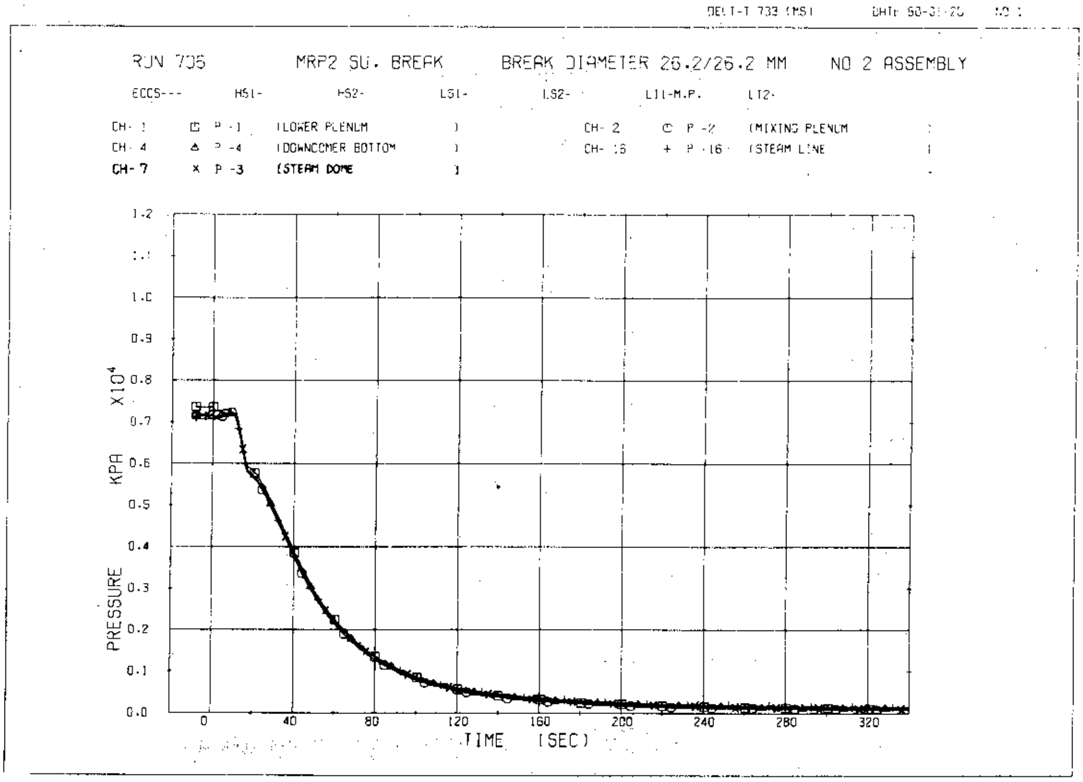

Fig.5.5 Pressure in the Pressure Vessel

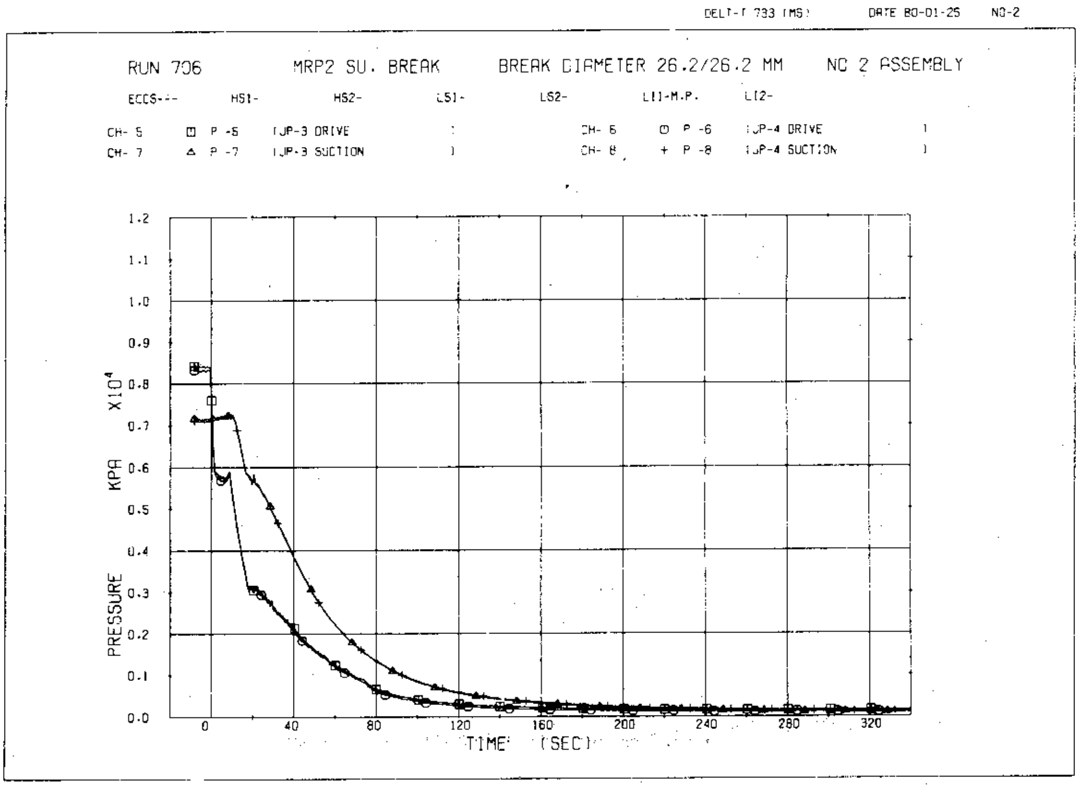

Fig.5.6 Pressure in the Jet Pumps

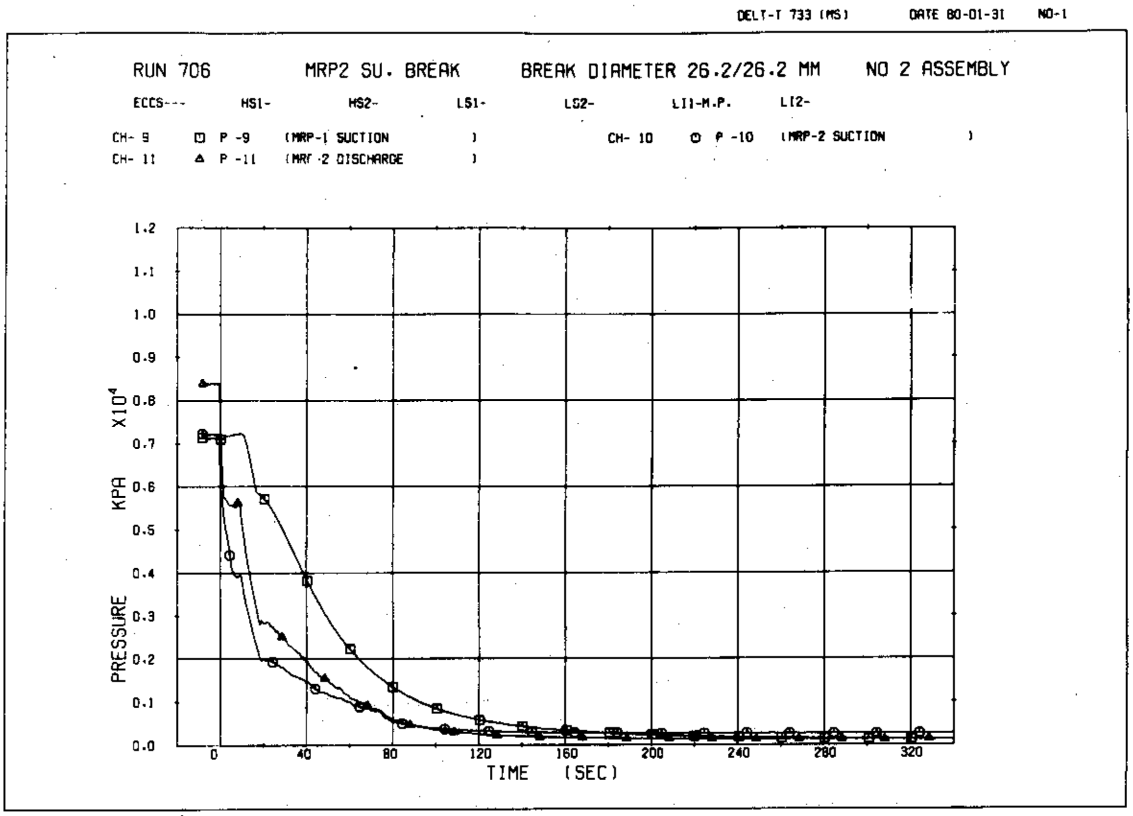

Fig.5.7 Pressure at the Recirculation Pumps

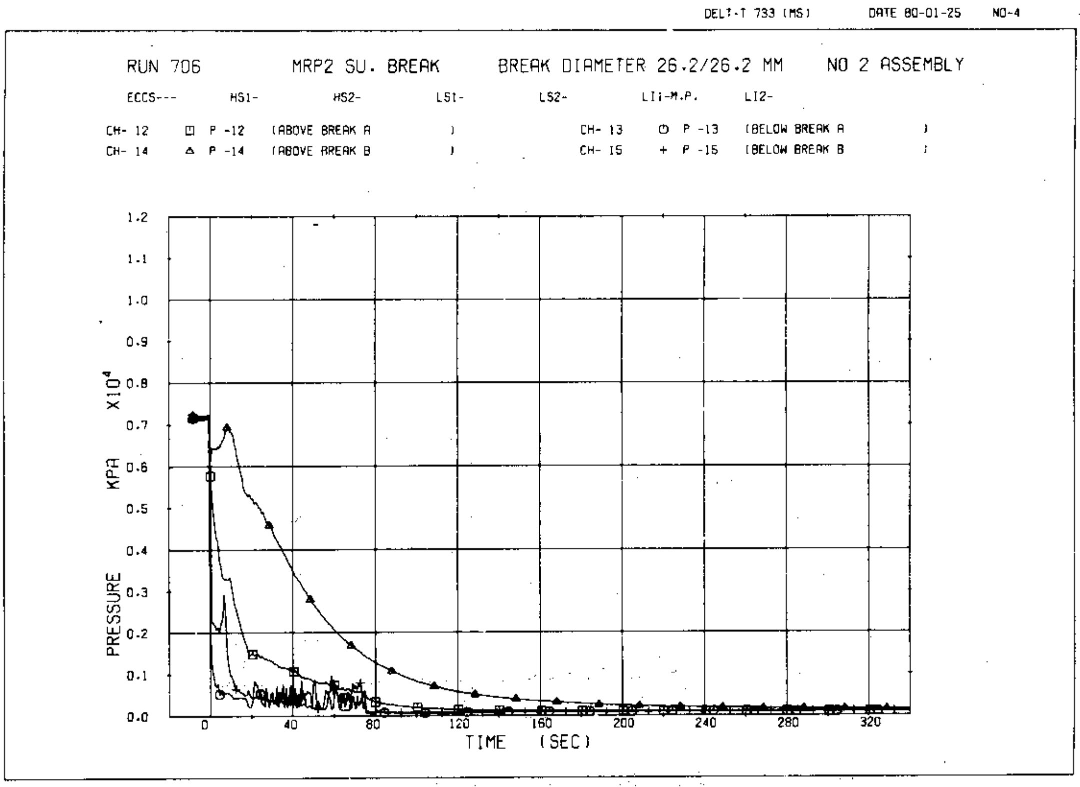

Fig.5.8 Pressure at the Break Units A and B

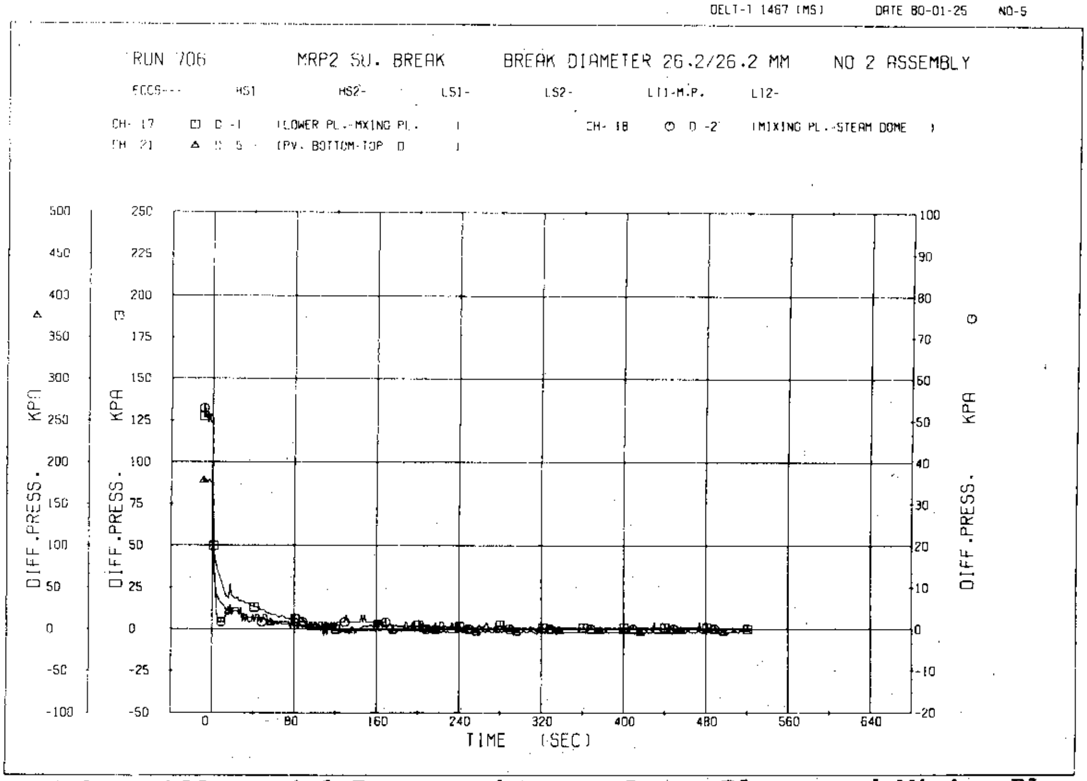

Fig. 5.9 Differential Pressure between Lower Plenum and Mixing Plenum, Mixing Plenum and Steam Dome, and Top and Bottom of Pressure Vessel

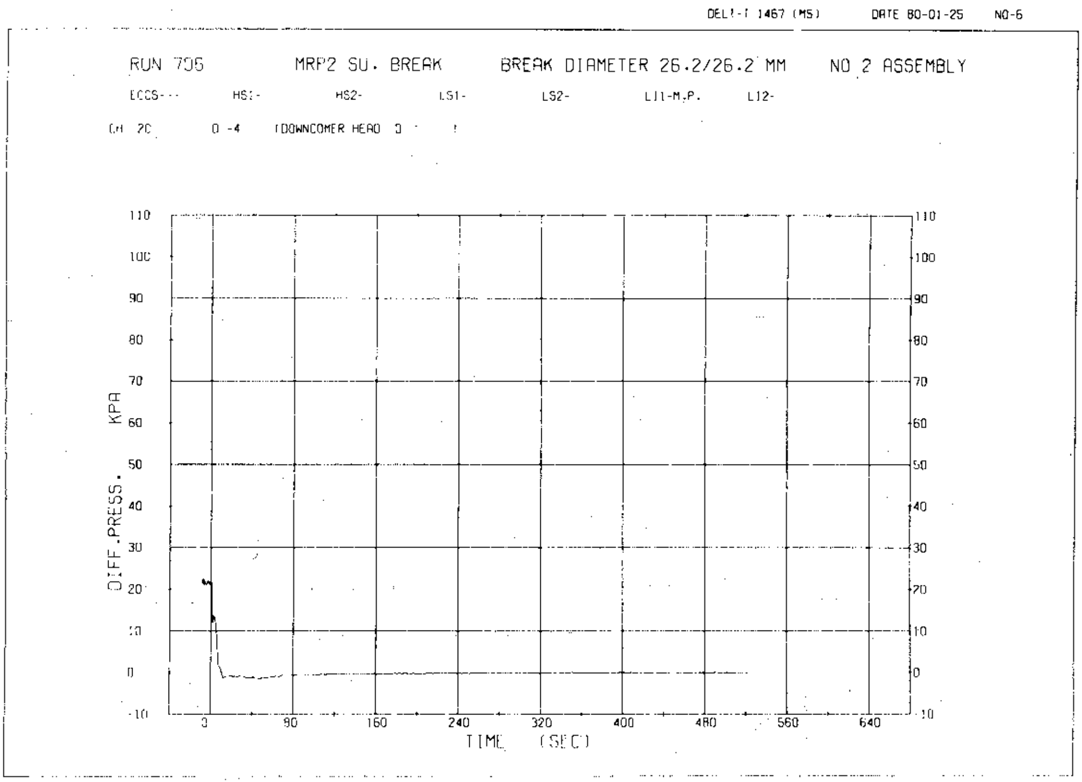

Fig. 5.10 Differential Pressure in Downcomer (Downcomer Head)

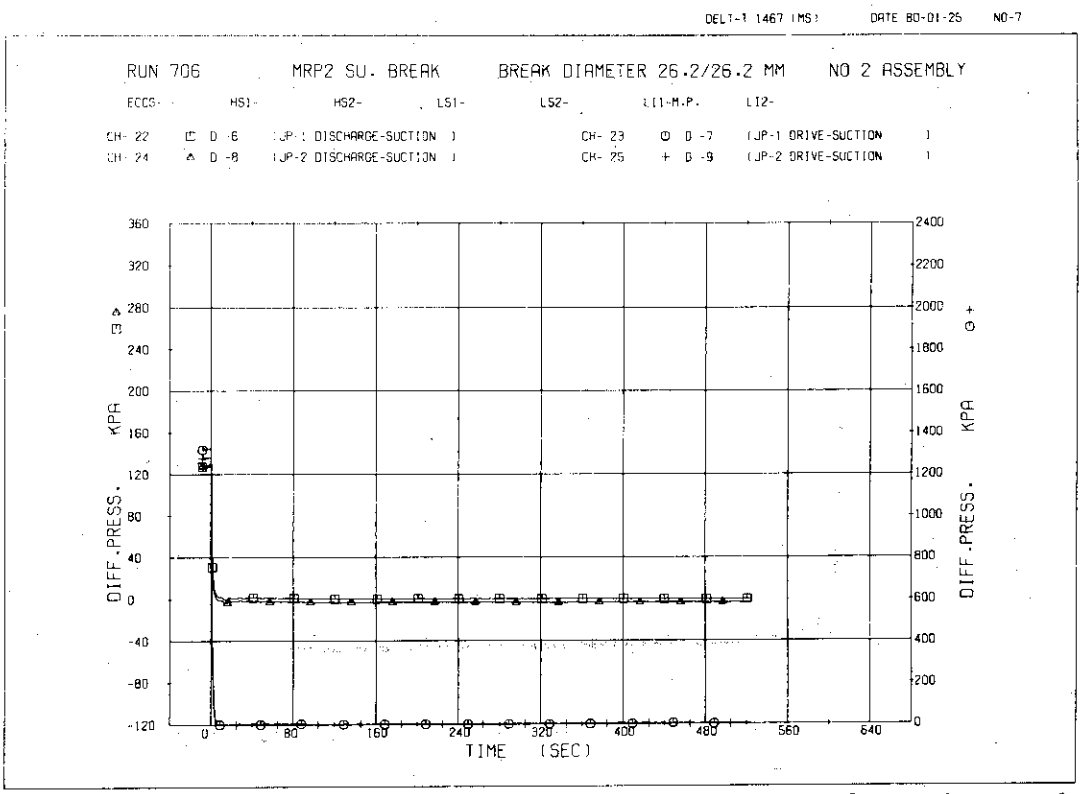

Fig.5.11 Differential Pressure between Discharge and Suction, and between Drive and Suction of the Jet Pumps of Intact Loop

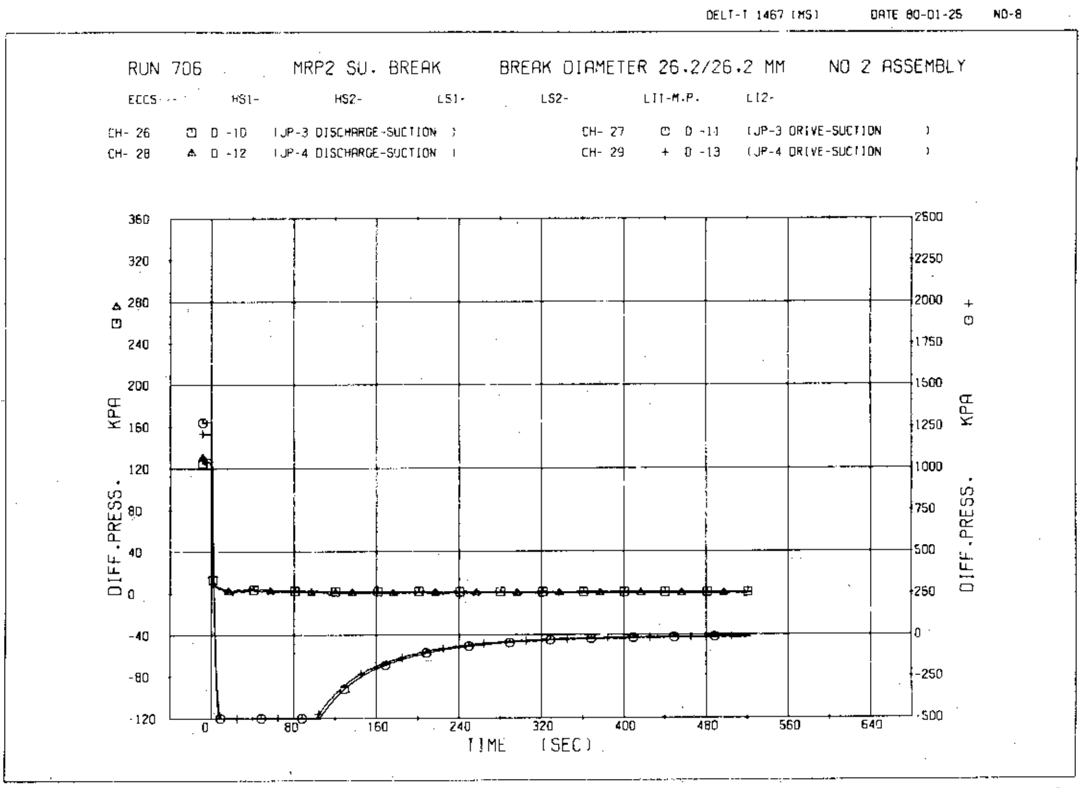

Fig.5.12 Differential Pressure between Discharge and Suction, and between Drive and Suction of the Jet Pumps of Blowdown Loop

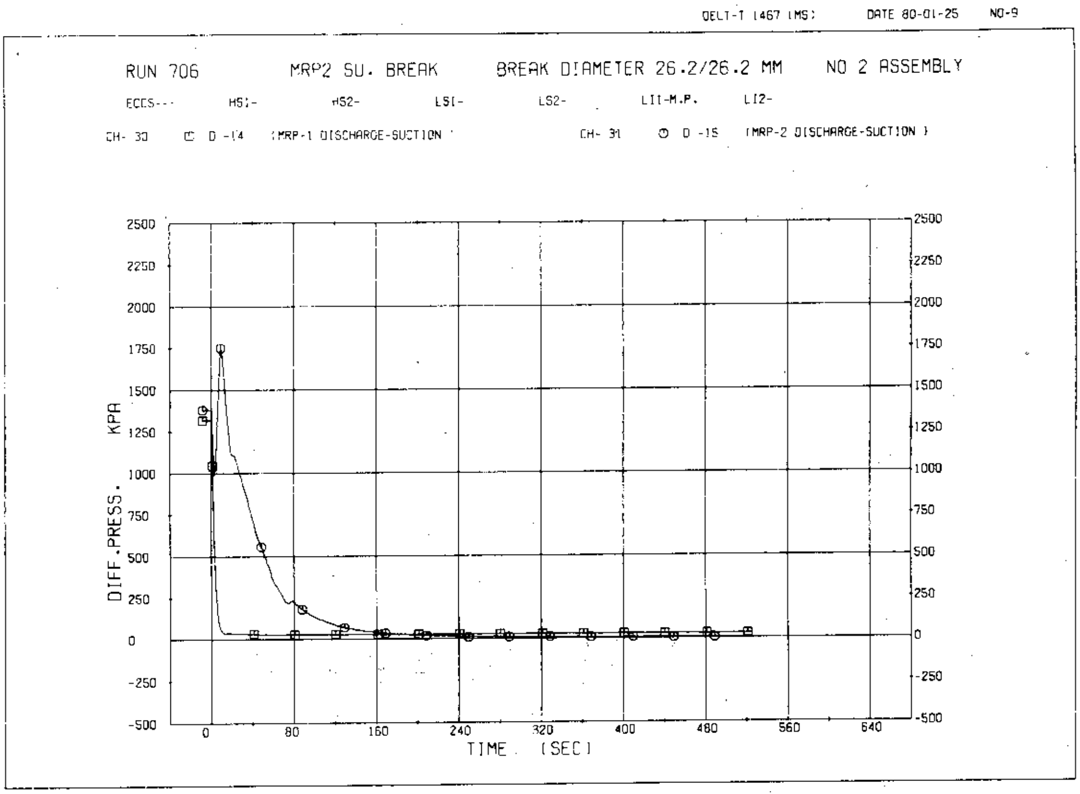

Fig.5.13 Differential Pressure across the Recirculation Pumps

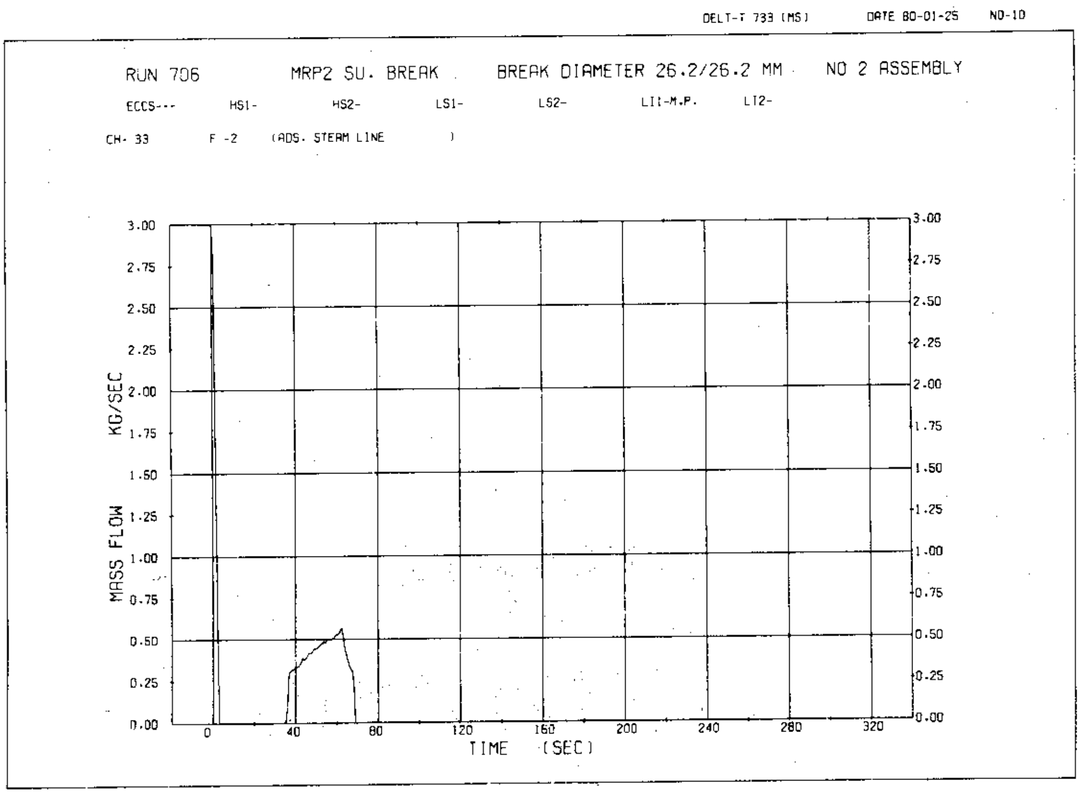

Fig.5.14 Flow Rate in the Steam Line and ADS Line

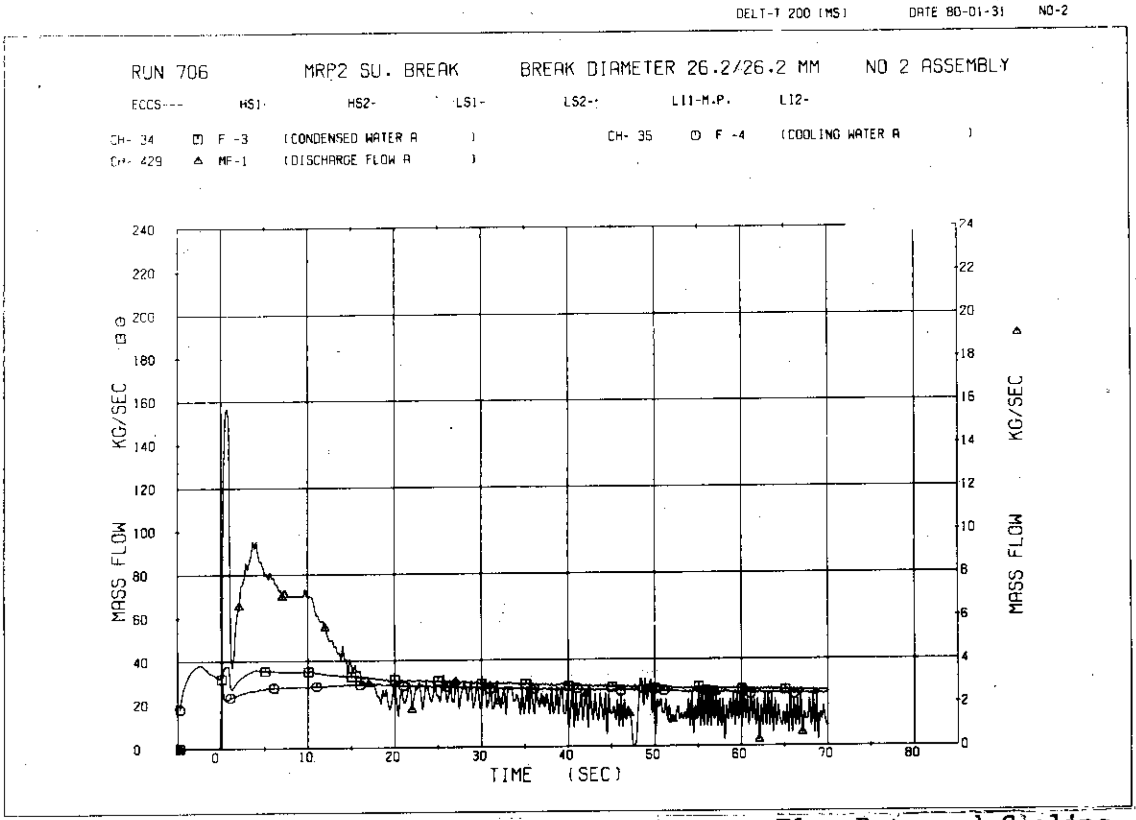

Fig. 5.15 Discharge Flow Rate, Condensed Water Flow Rate and Cooling Water Flow Rate at Break A

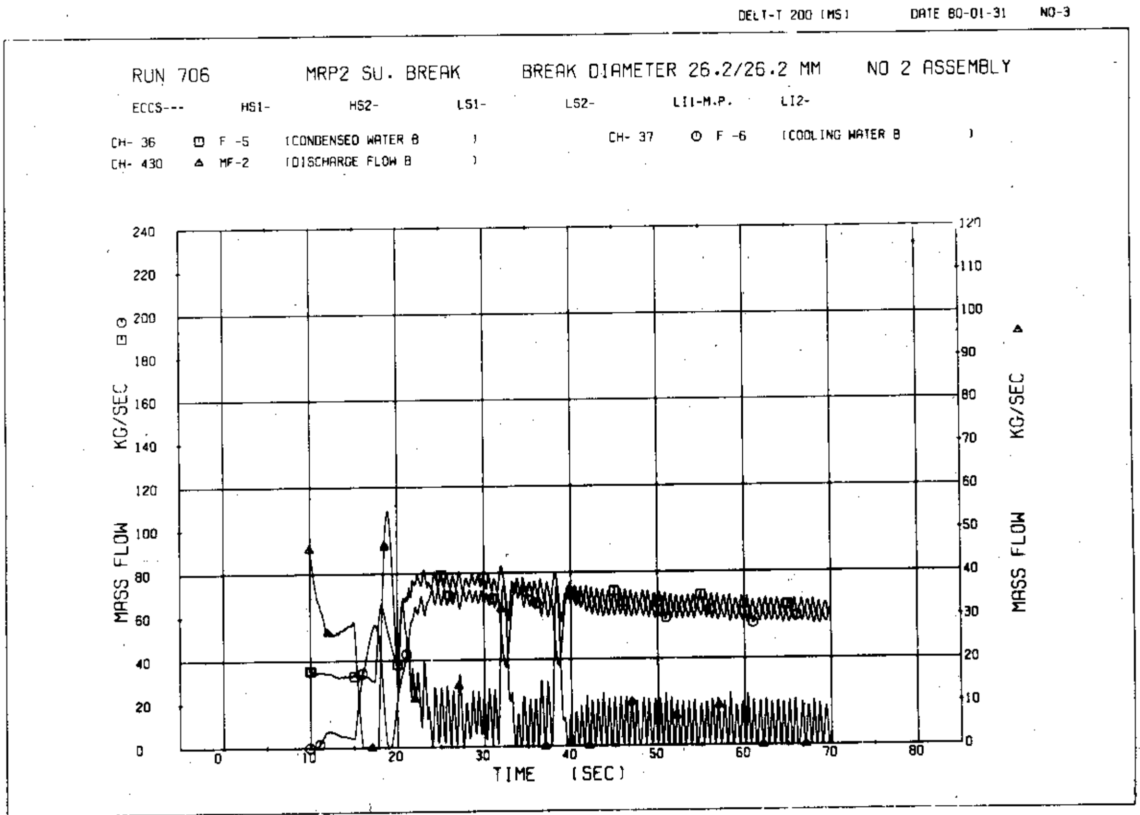

Fig. 5.16 Discharge Flow Rate, Condensed Water Flow Rate and Cooling Water Flow Rate at Break B

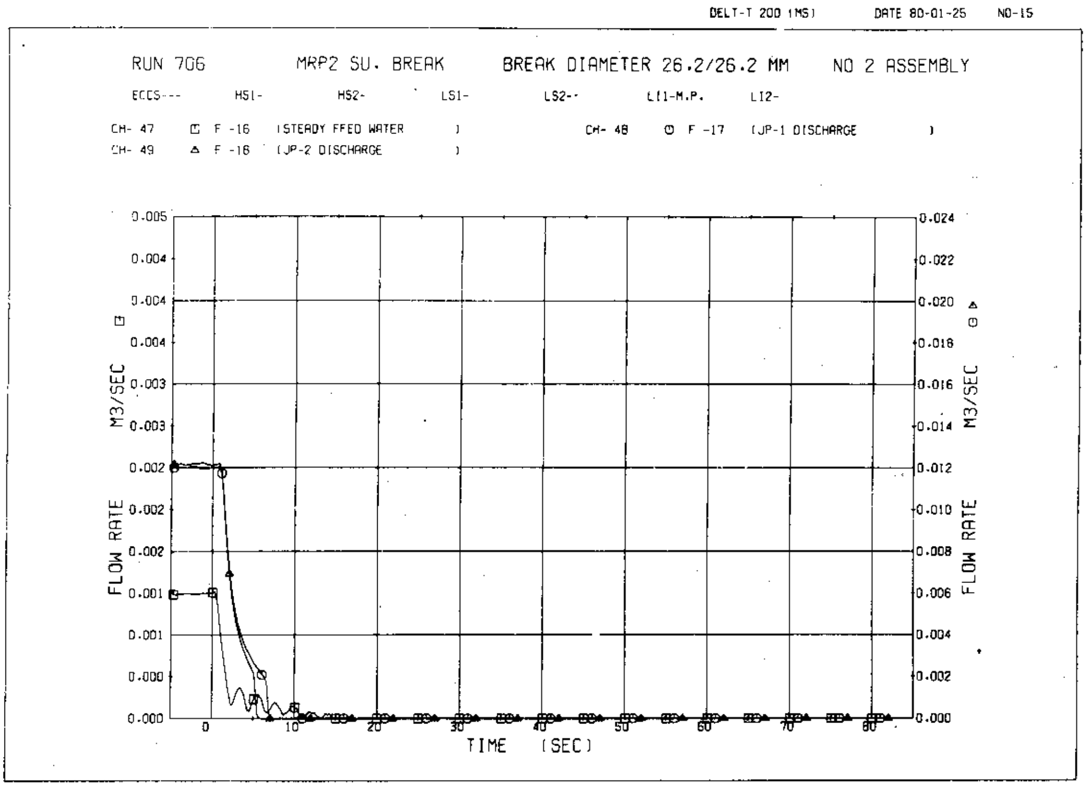

Fig.5.17 Flow Rates of Steady State Feed Water and Discharge Flows at Intact Loop Jet Pumps

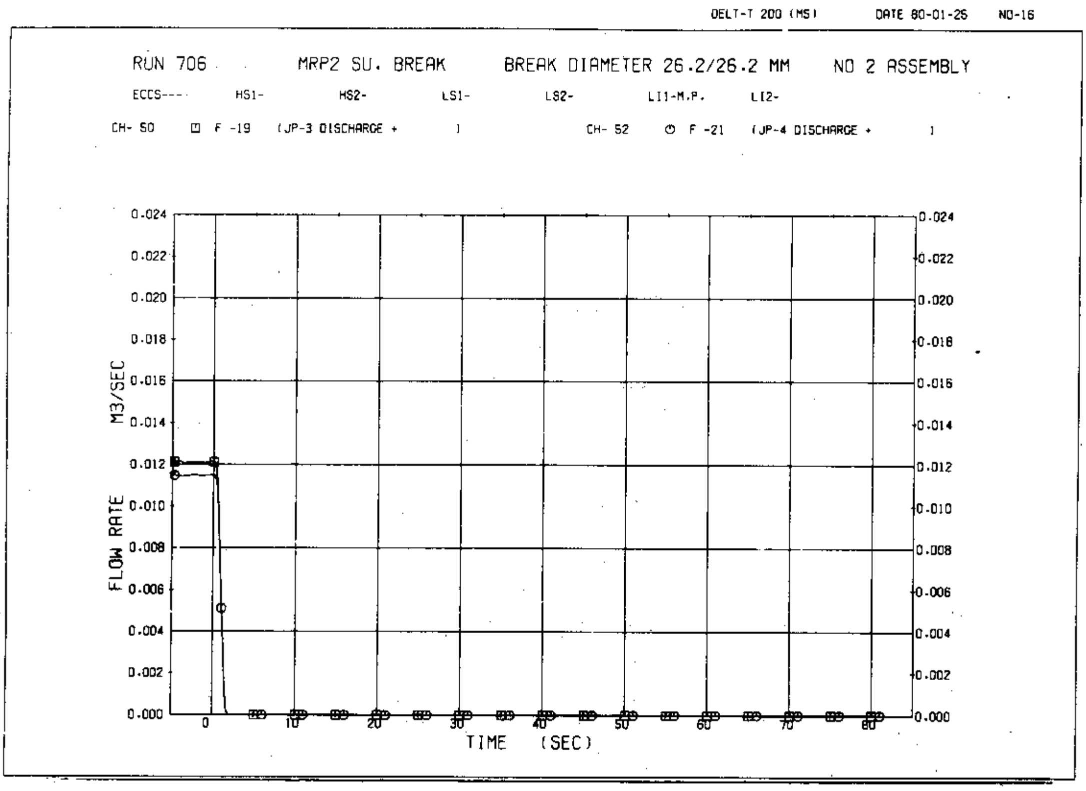

Fig.5.18 Discharge Flow Rates at Blowdown Loop Jet Pumps

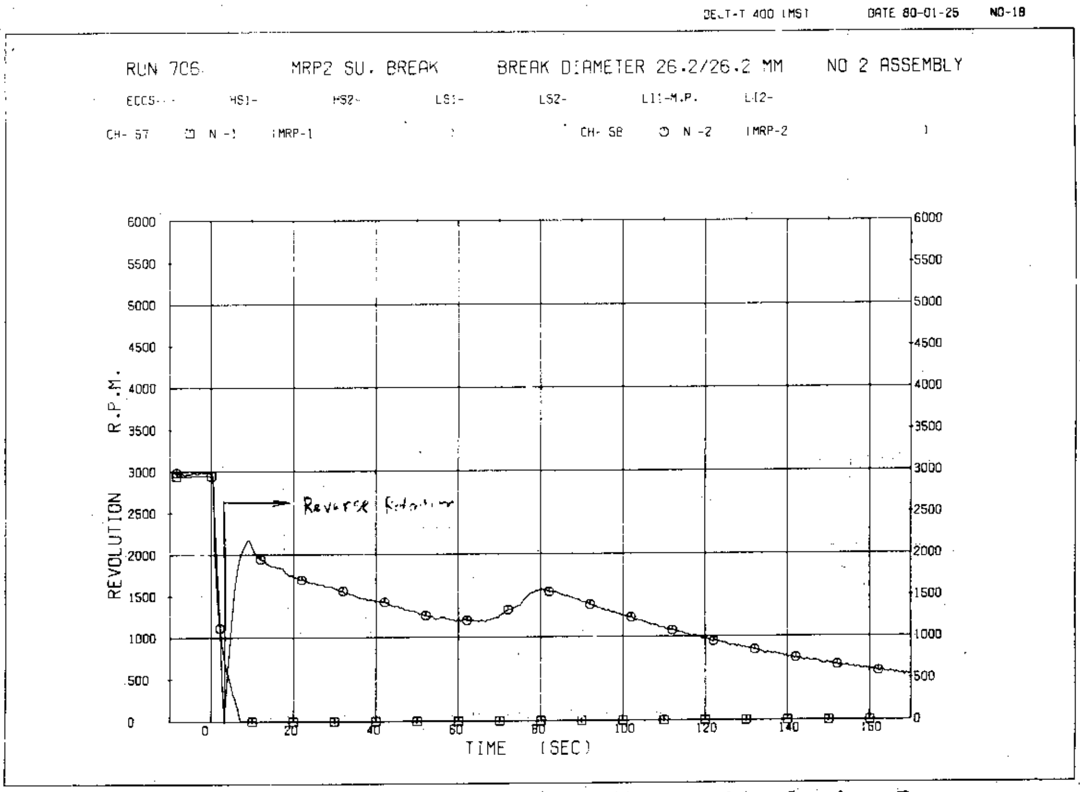

Fig.5.19 Revolution Speeds of the Recirculation Pumps

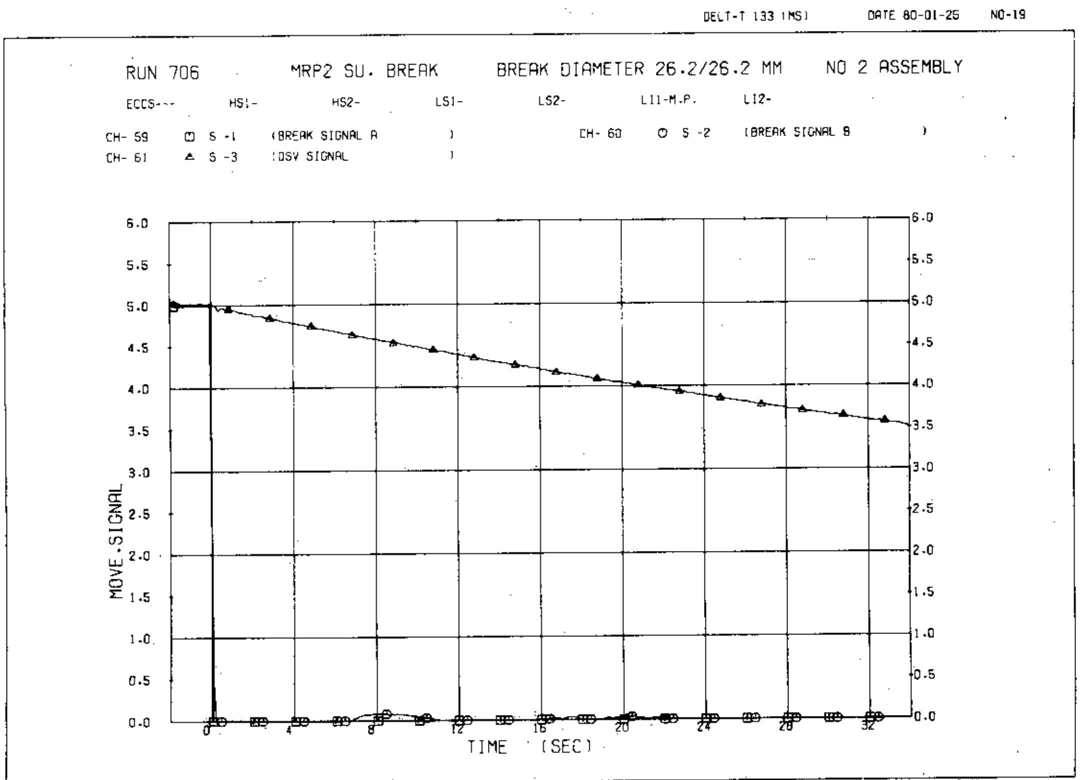

Fig.5.20 Two Break Signals and QSV Closure Signal

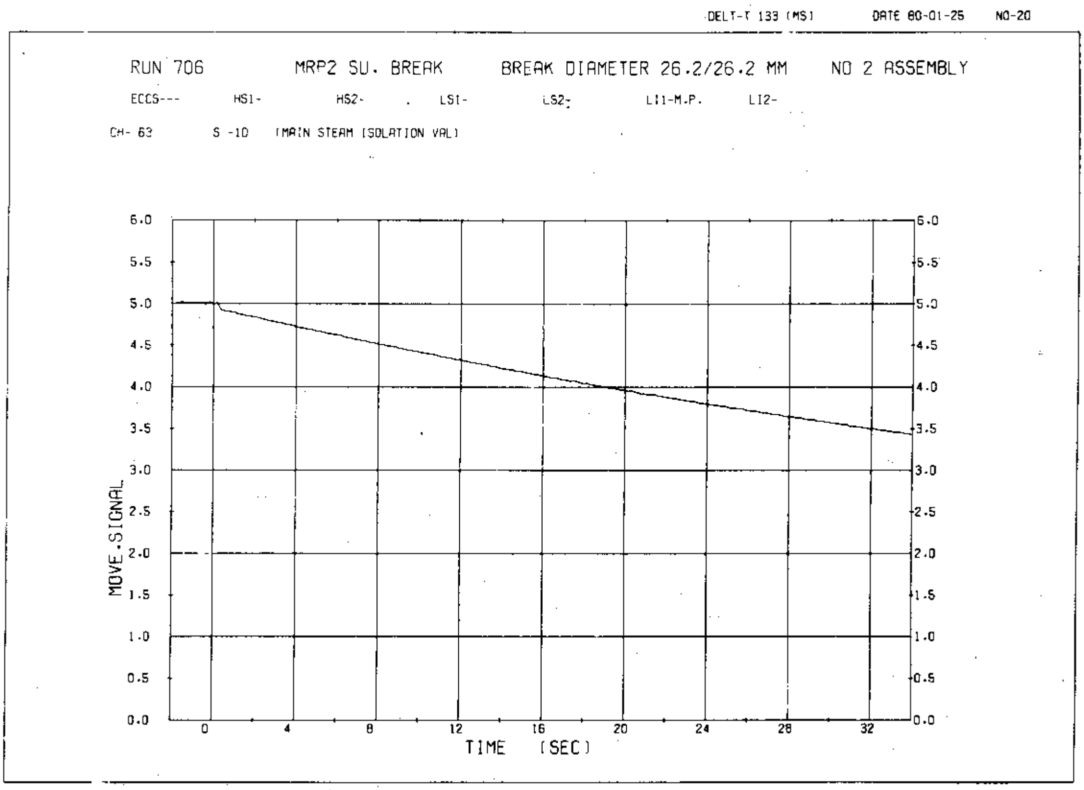

Fig.5.21 Closure Signal of Steady State Steam Line

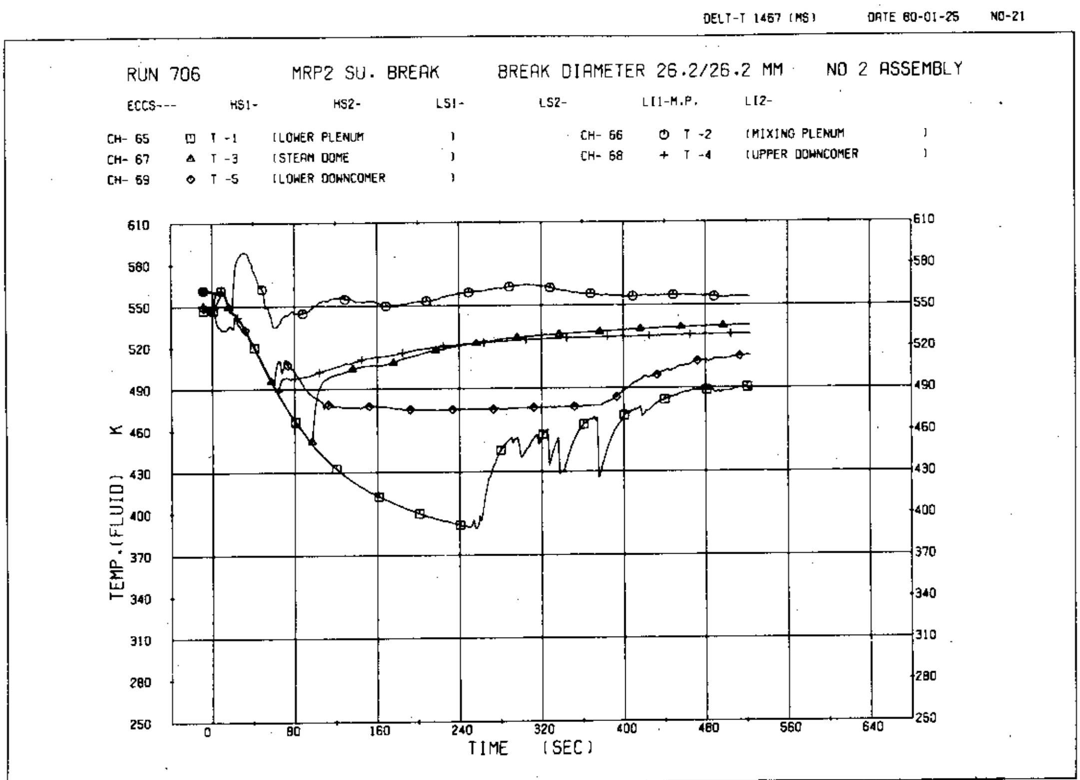

Fig.5.22 Fluid Temperatures in the Pressure Vessel

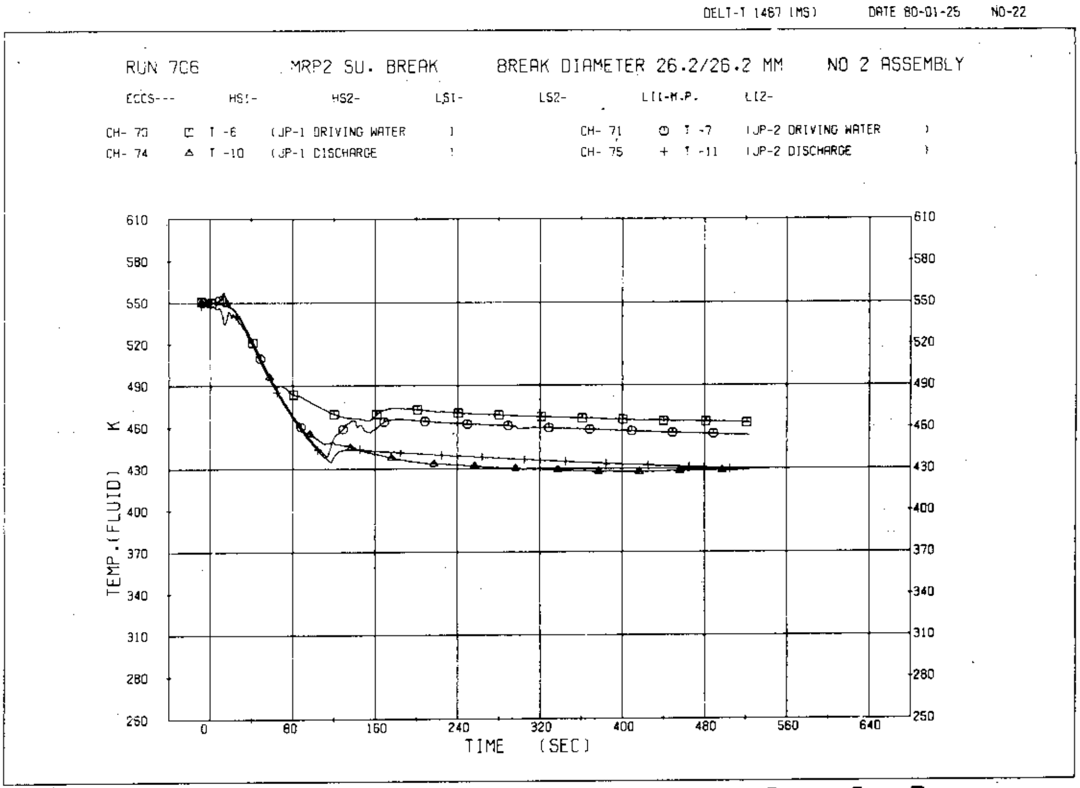

Fig.5.23 Fluid Temperatures in the Intact Loop Jet Pumps

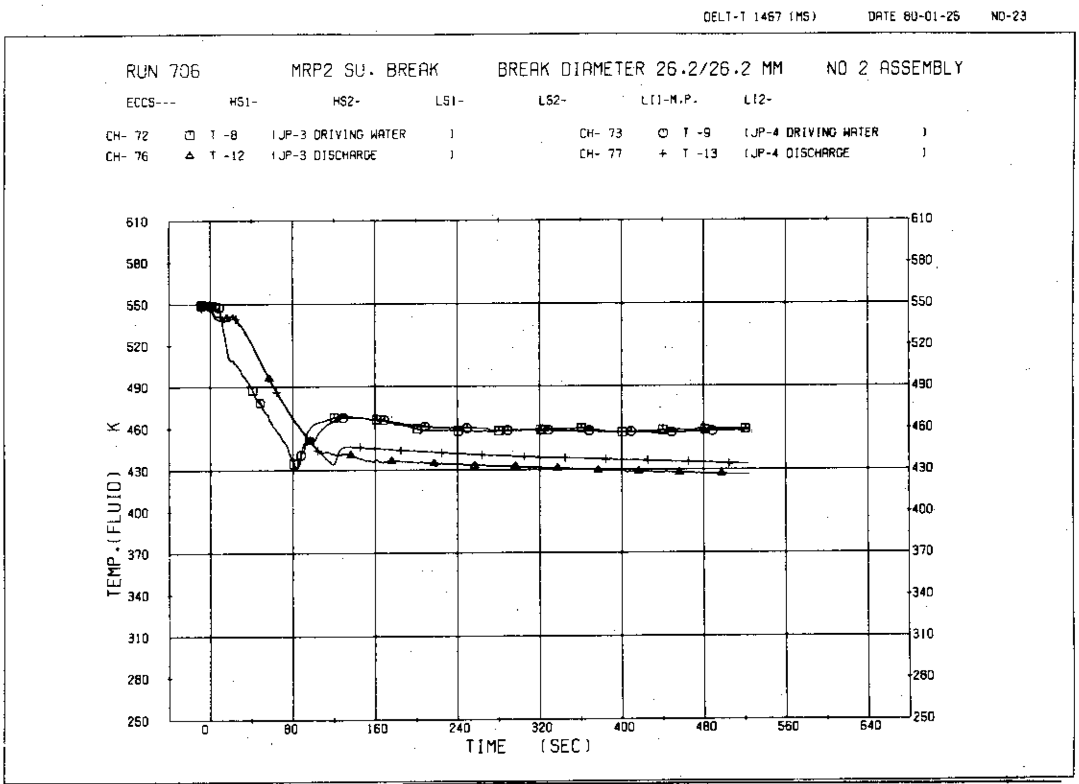

Fig.5.24 Fluid Temperatures in the Blowdown Loop Jet Pumps

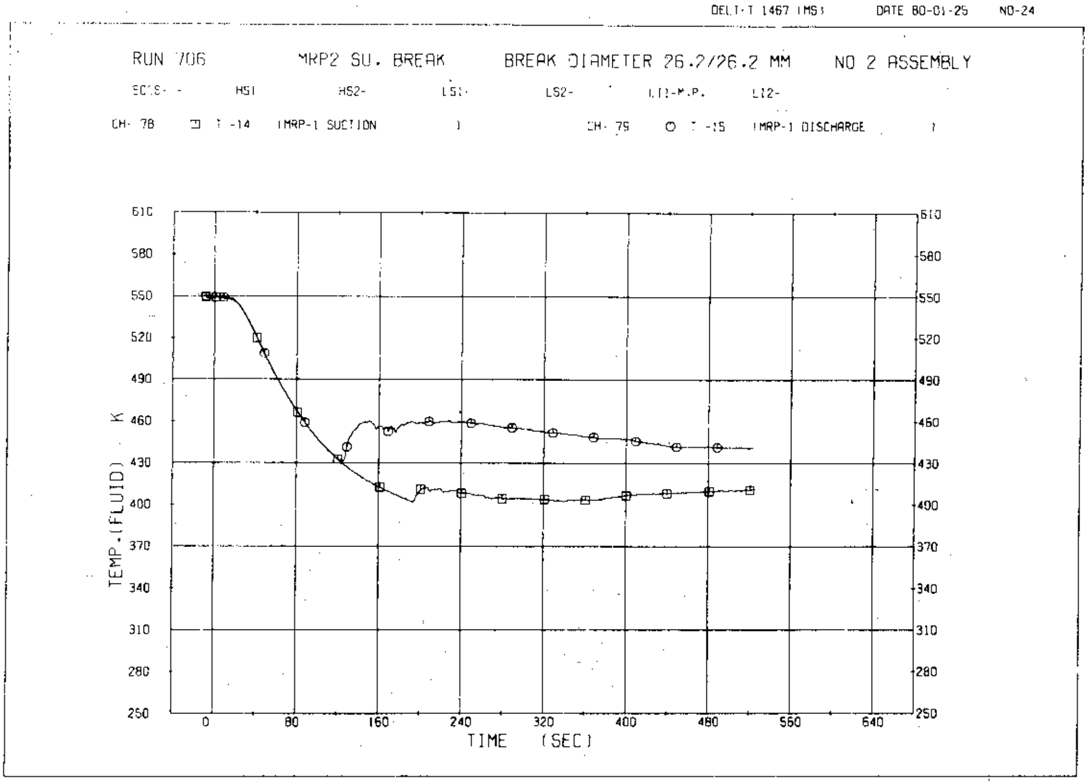

Fig. 5.25 Fluid Temperatures at the Intact Loop Recirculation Pump

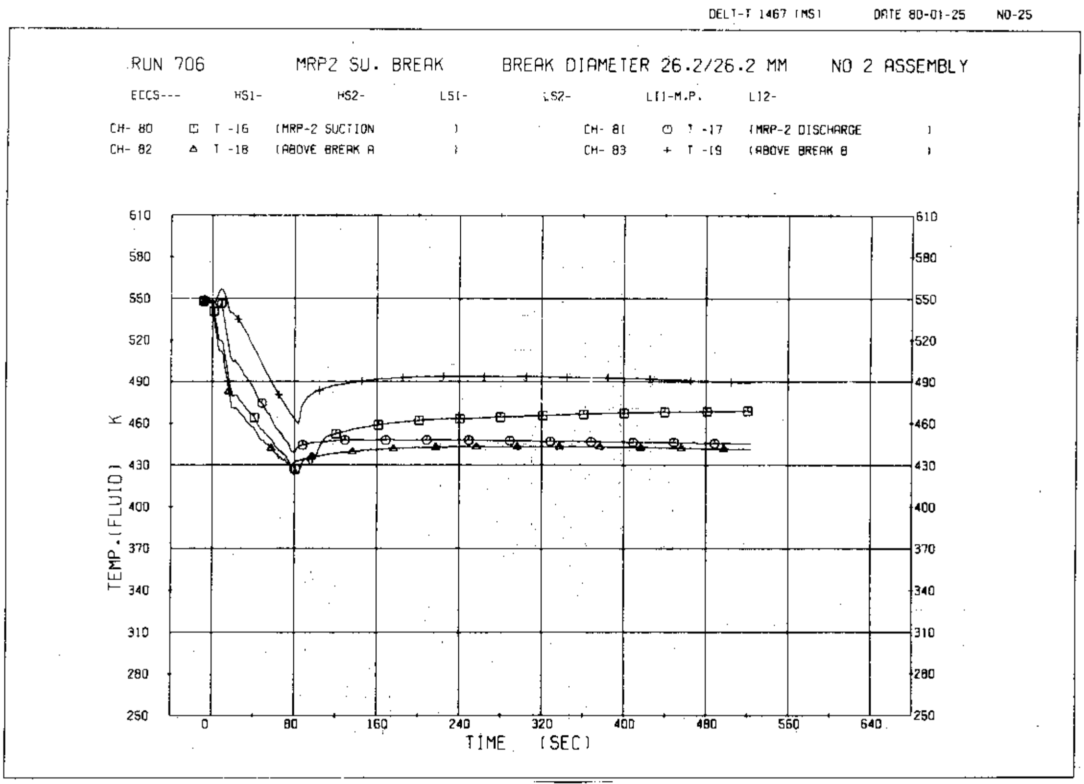

Fig. 5.26 Fluid Temperatures at the Blowdown Loop Recirculation Pump and above the Break Units A and B

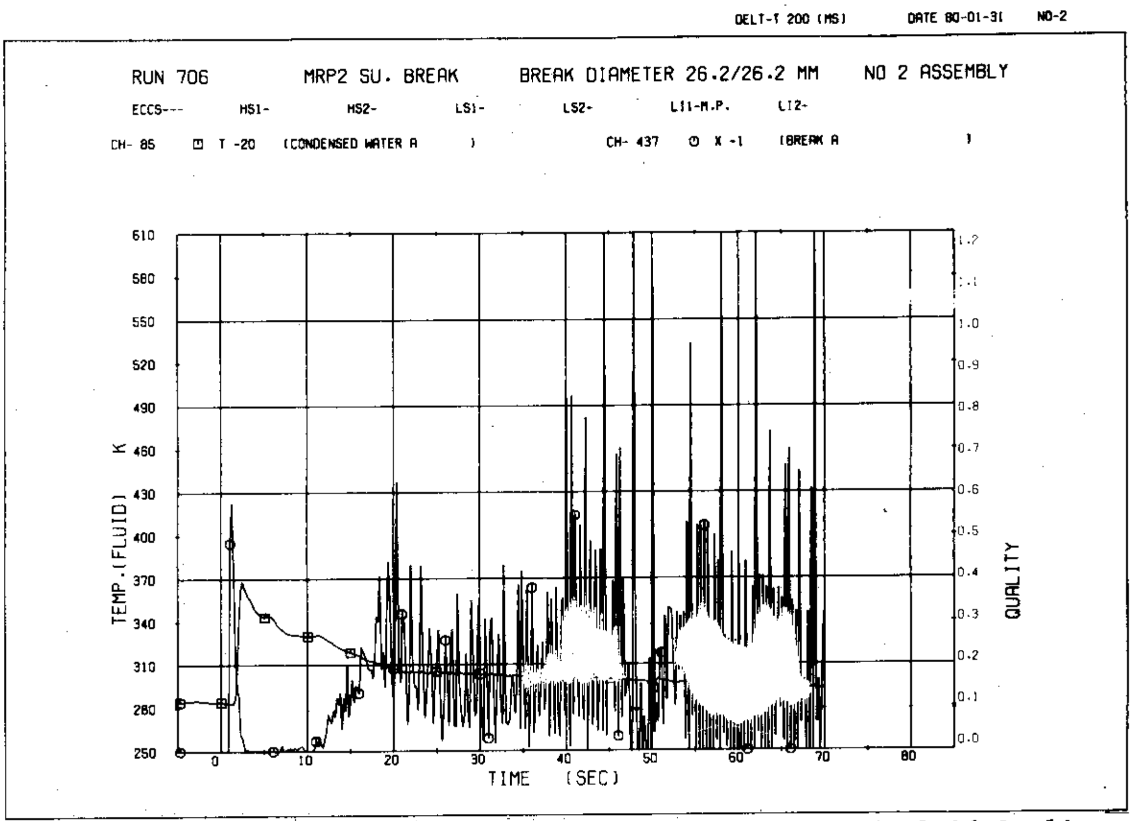

Fig.5.27 Fluid Temperature in the Condensed Water and Fluid Quality above the Break Unit A

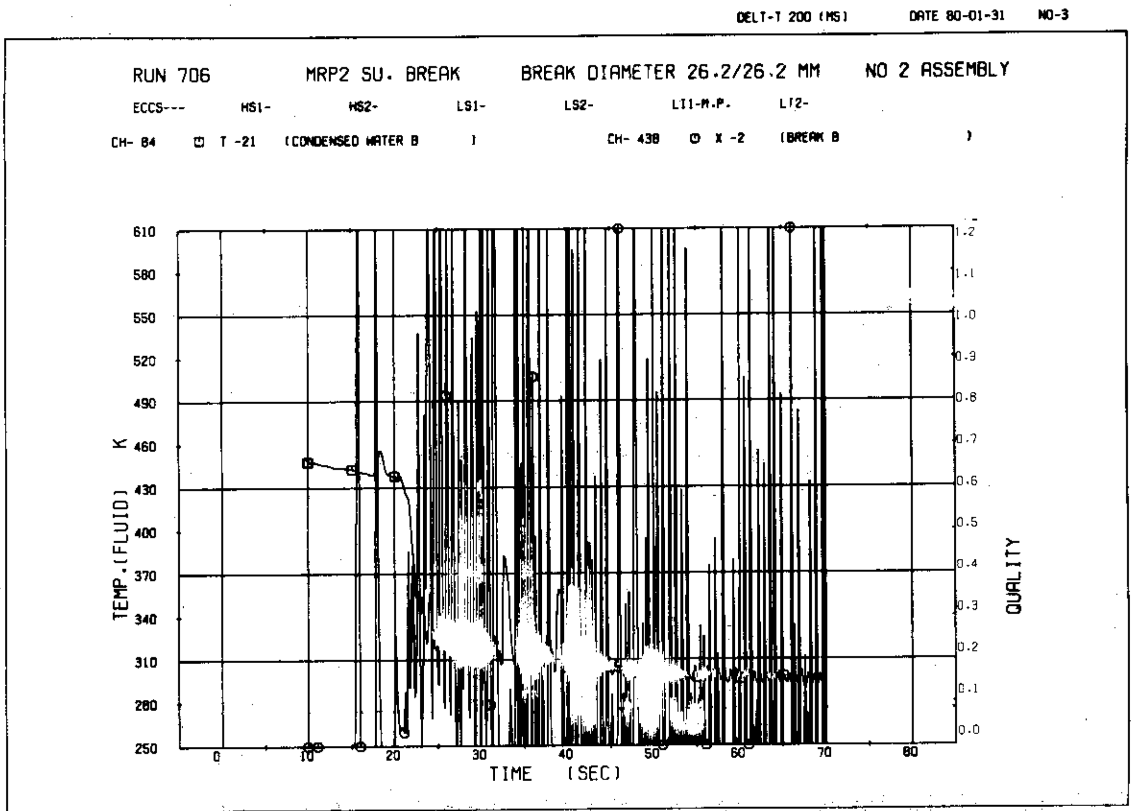

Fig.5.28 Fluid Temperature in the Condensed Water and Fluid Quality above the Break Unit B

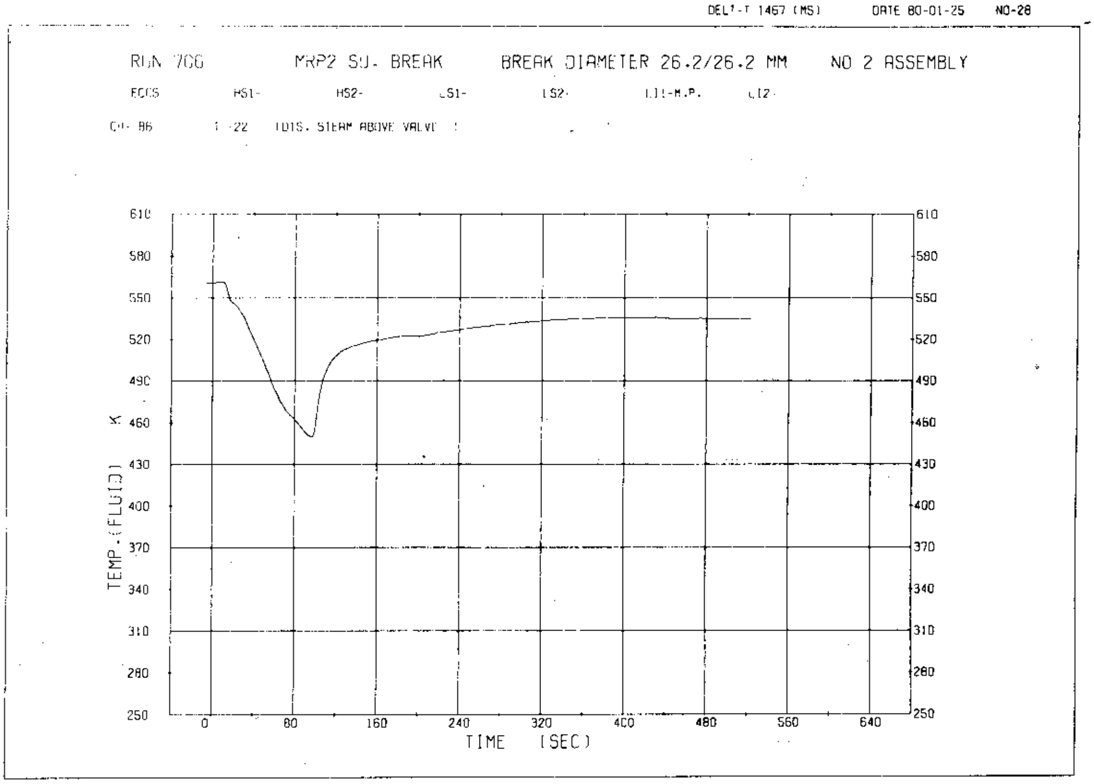

Fig.5.29 Fluid Temperature at the Upstream of Steady State Steam Line

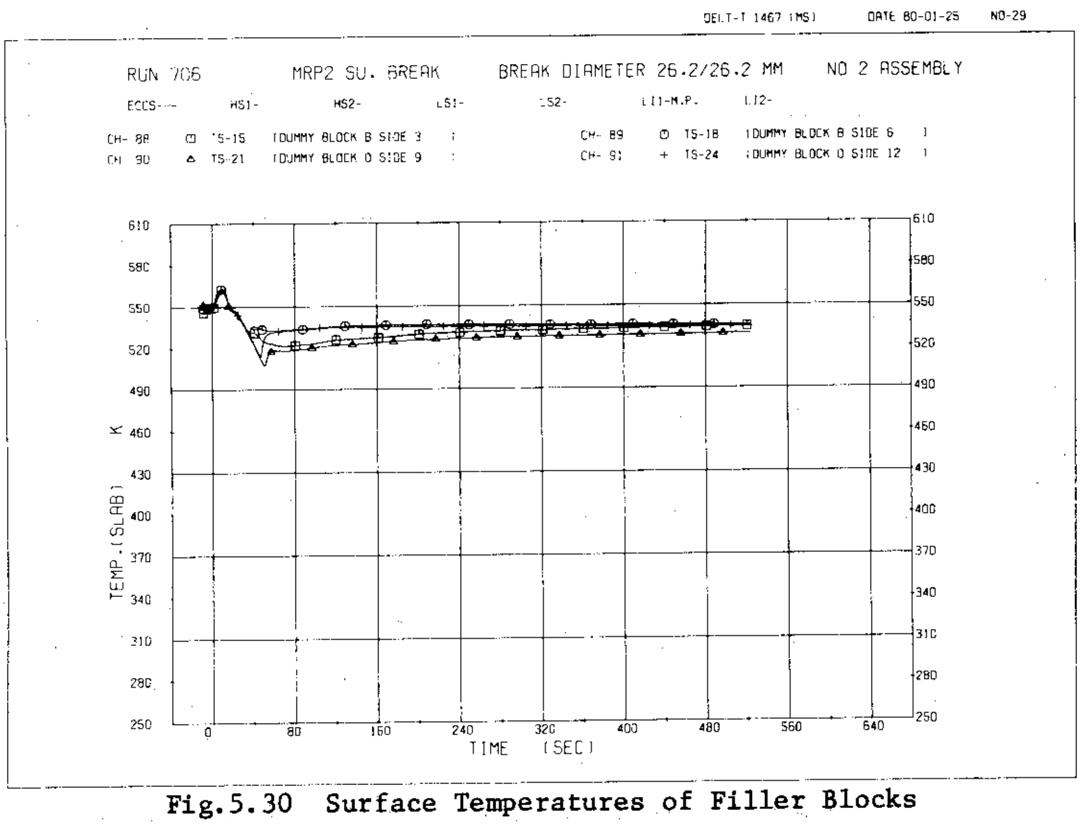

Fig.5.30 Surface Temperatures of Filler Blocks

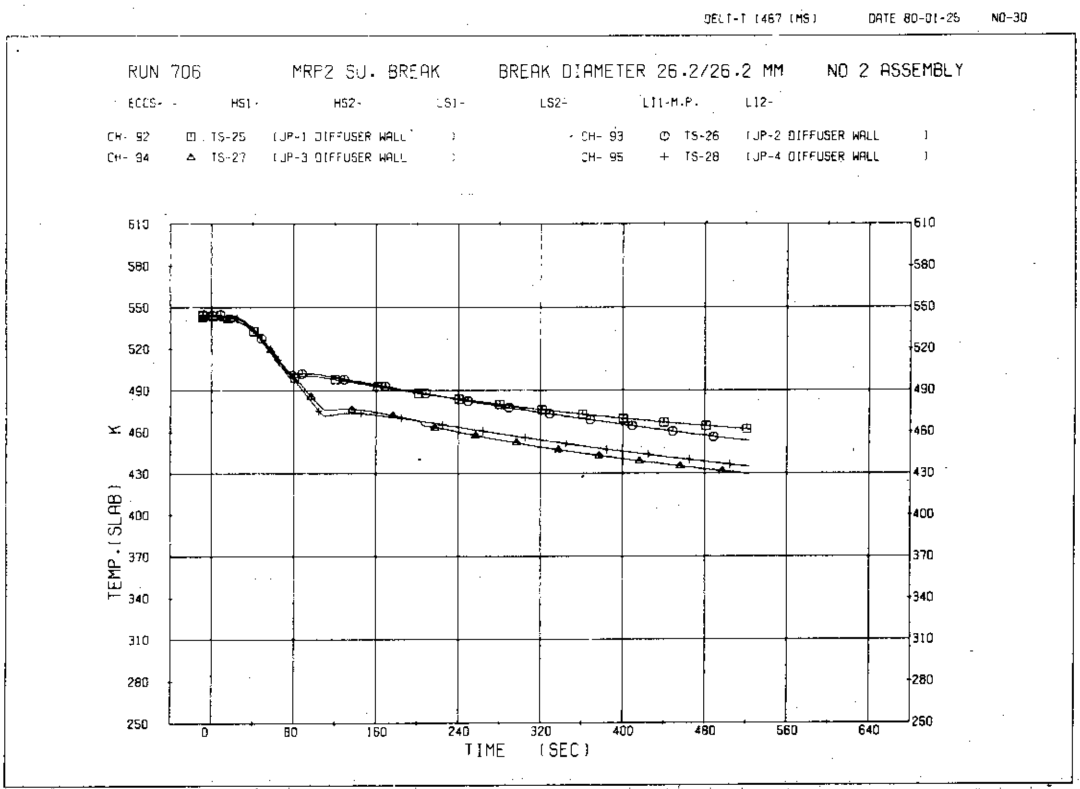

Fig.5.31 Surface Temperatures at the Inner Walls of Jet Pumps

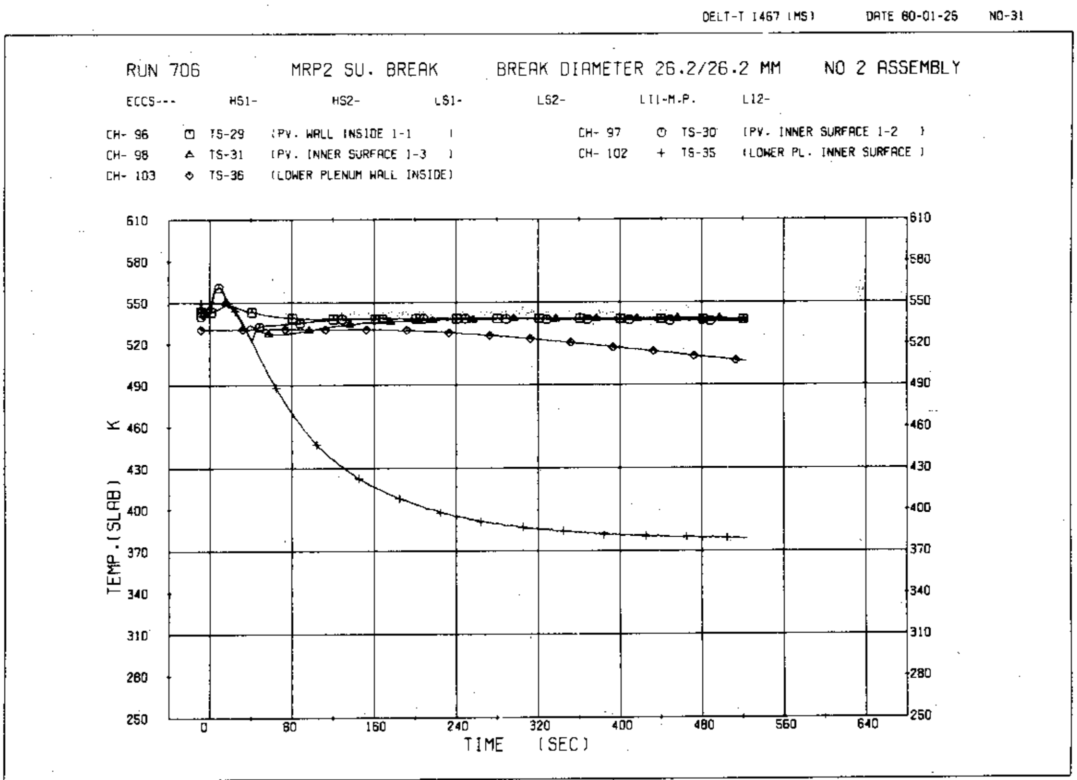

Fig.5.32 Inner Surface Temperatures of the Pressure Vessel

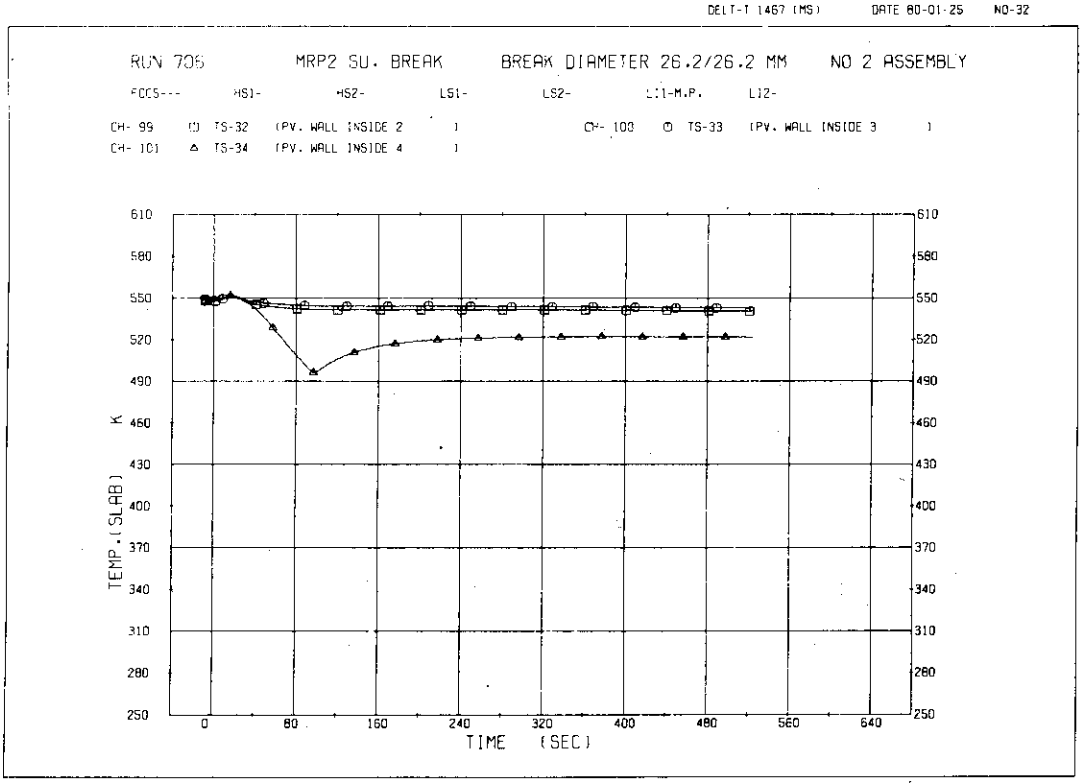

Fig.5.33 Metal Temperatures of the Pressure Vessel

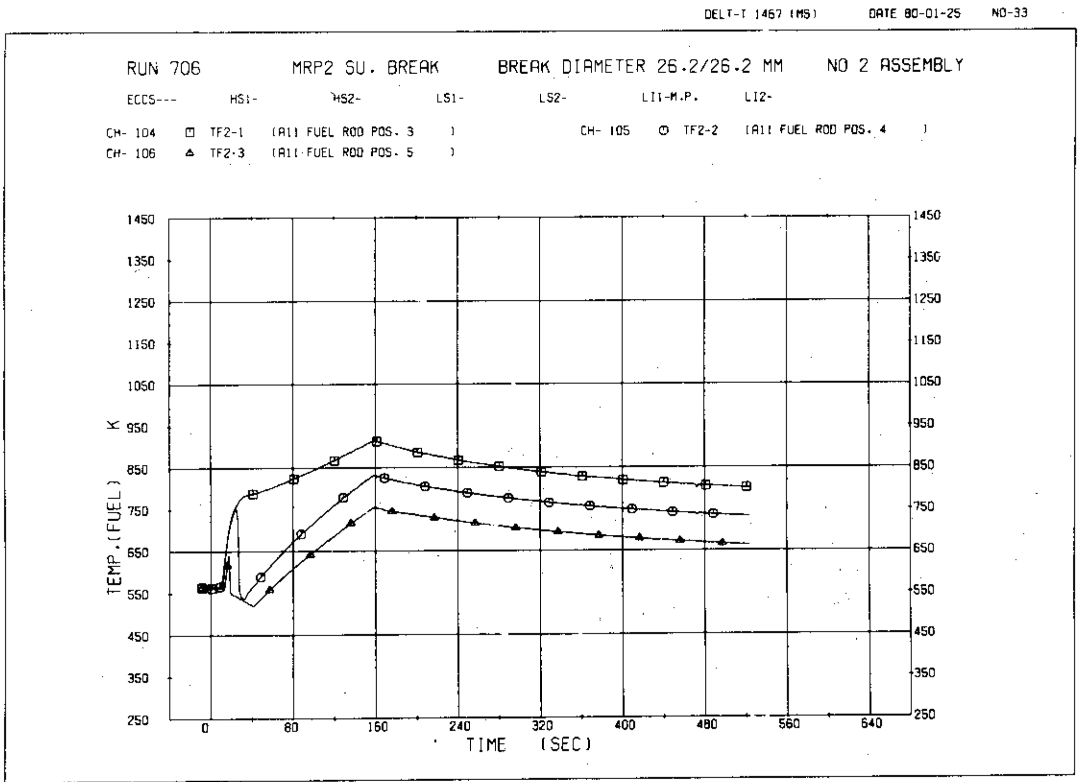

Fig.5.34 Surface Temperatures of the Fuel Rod A11 (The same as those of A13, A15, A17, A35, A37, A51, A53, A57, A71, A75)

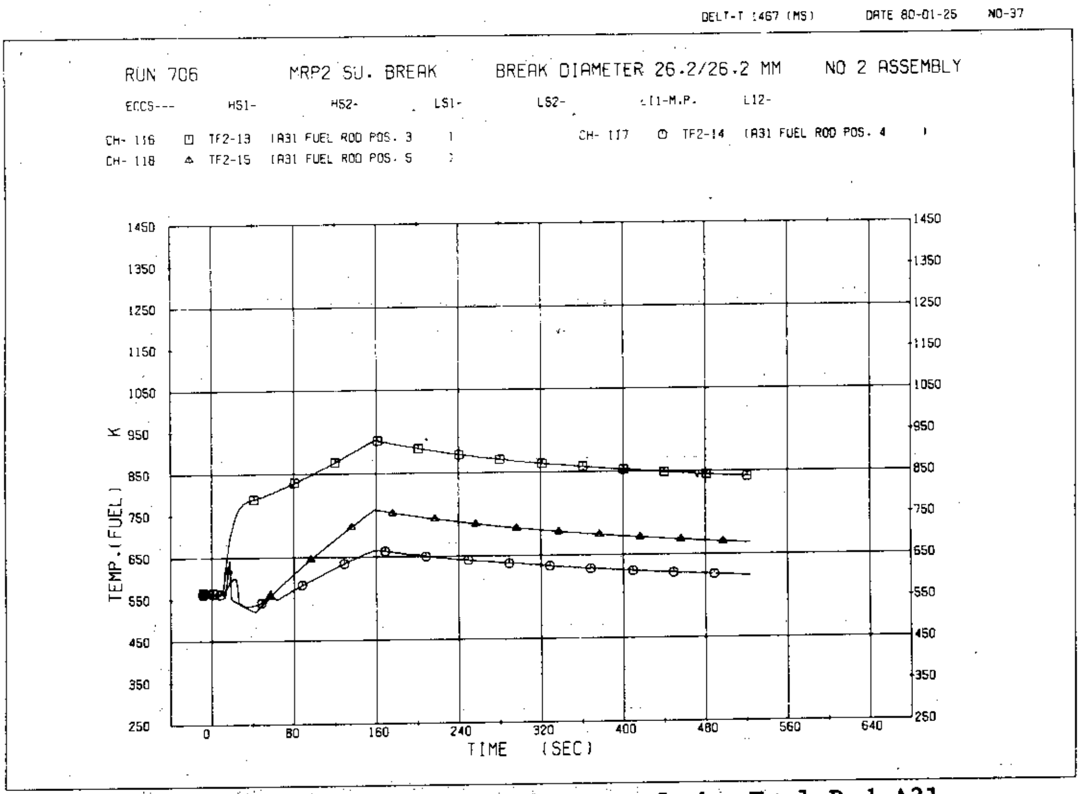

Fig.5.35 Surface Temperatures of the Fuel Rod A31

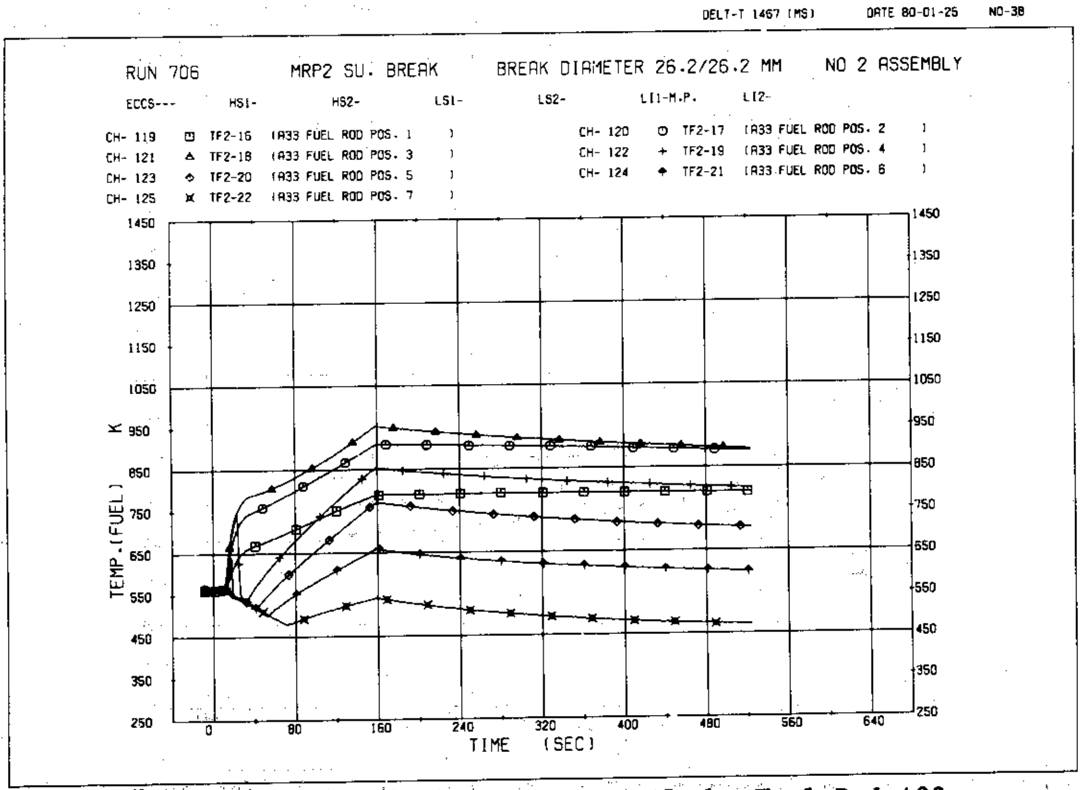

Fig.5.36 Surface Temperatures of the Fuel Rod A33

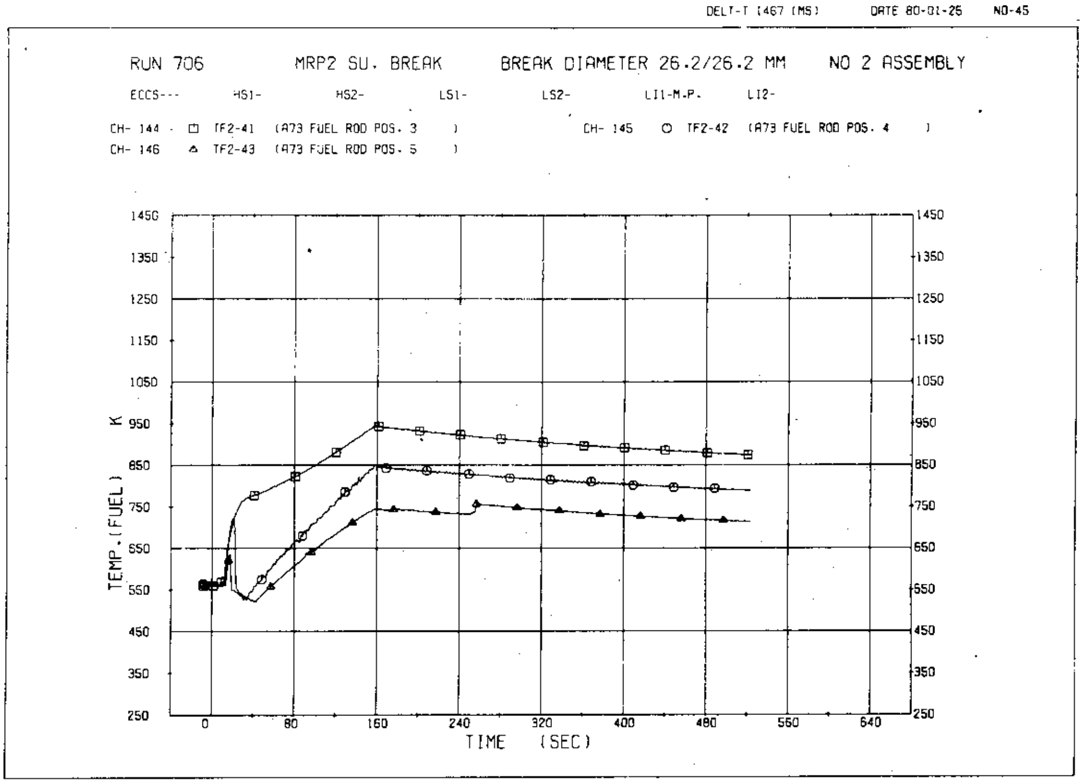

Fig.5.37 Surface Temperatures of the Fuel Rod A73

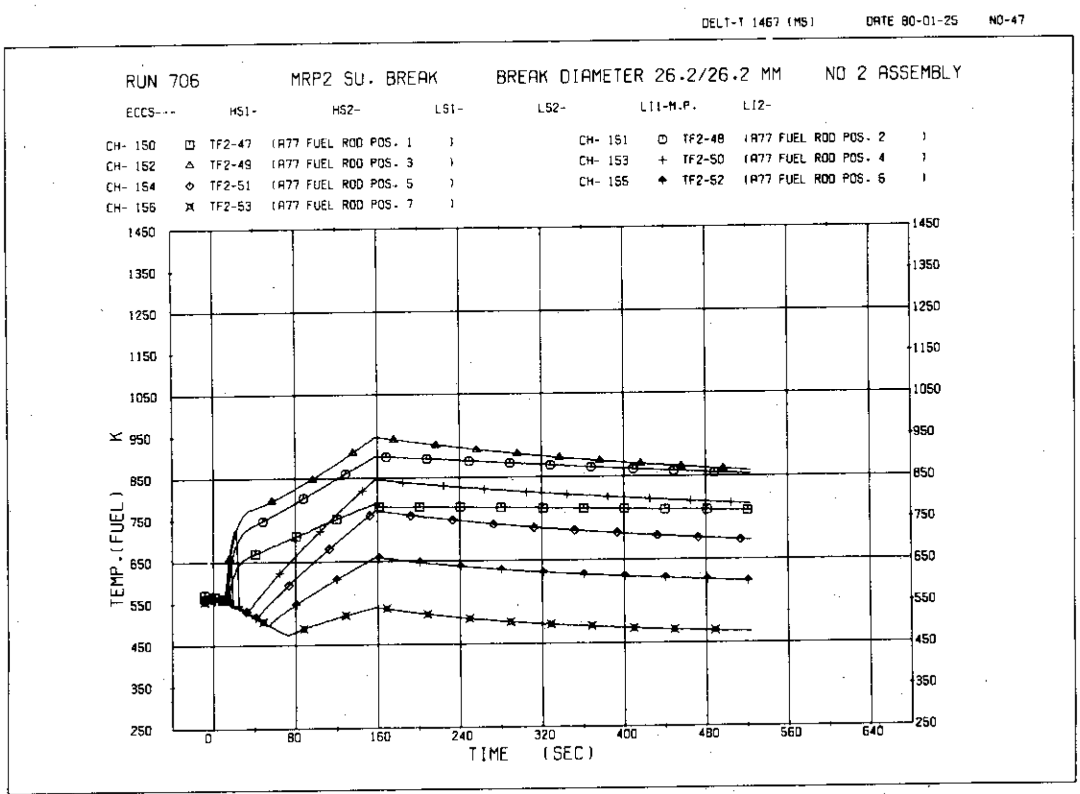

Fig.5.38 Surface Temperatures of the Fuel Rod A77

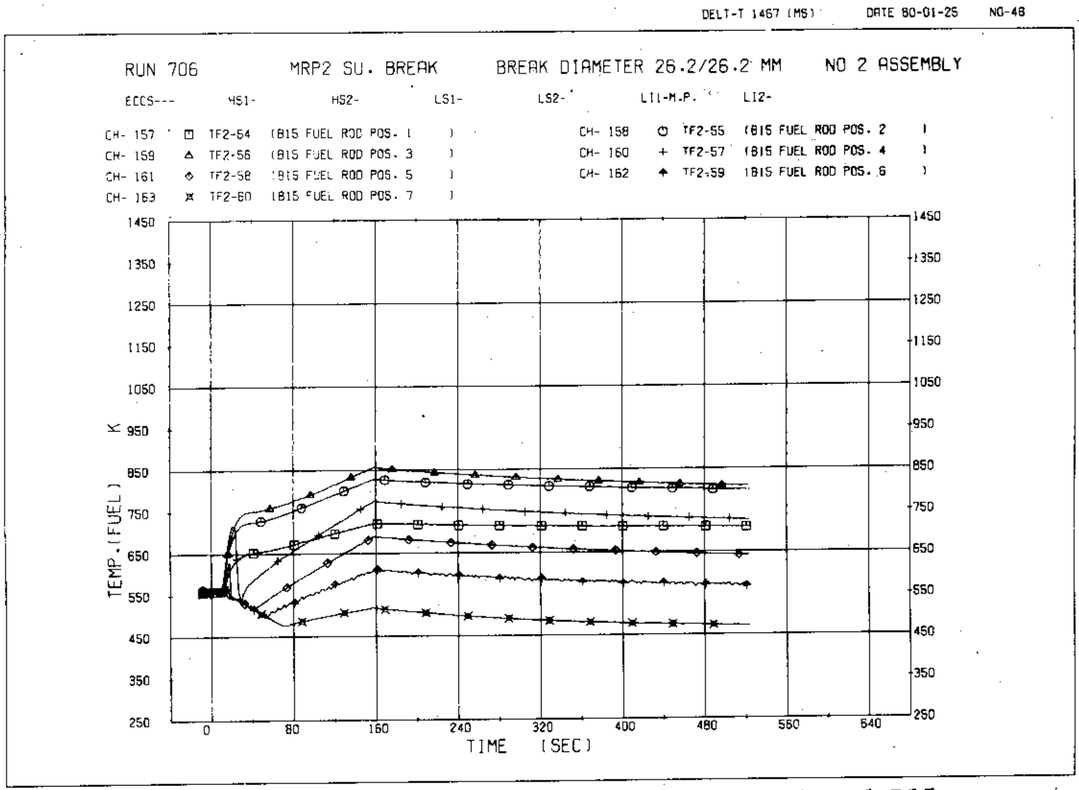

Fig.5.39 Surface Temperatures of the Fuel Rod B15

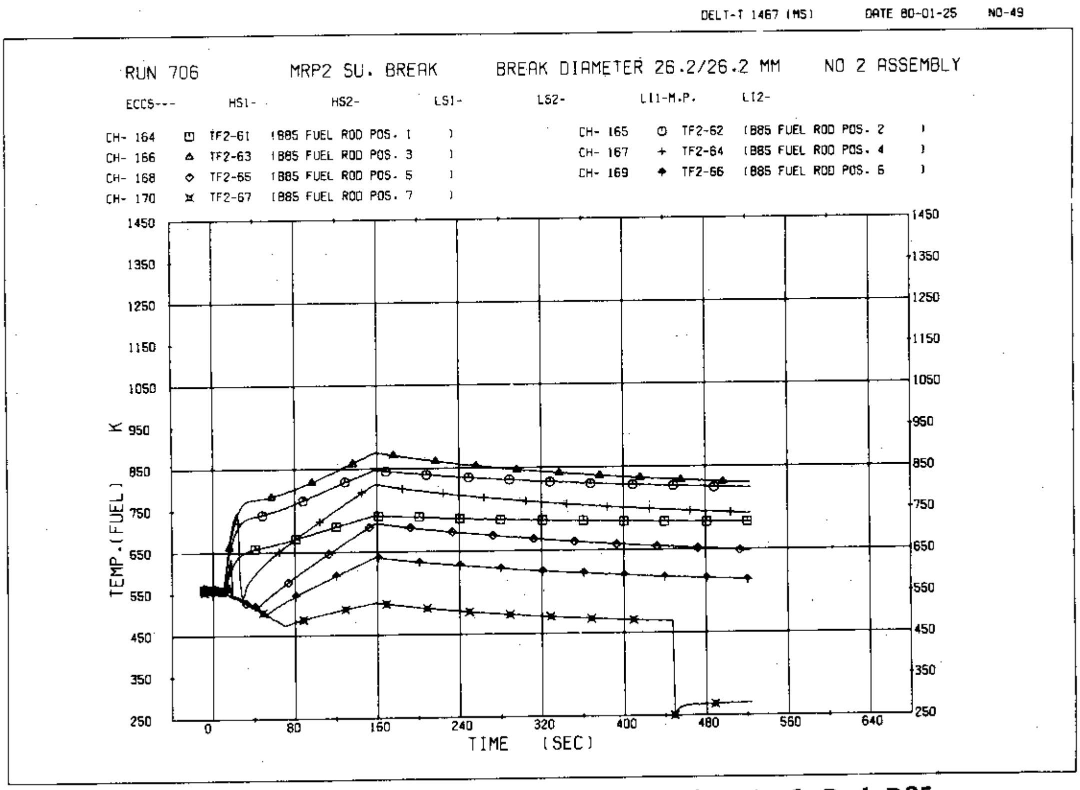

Fig.5.40 Surface Temperatures of the Fuel Rod B85

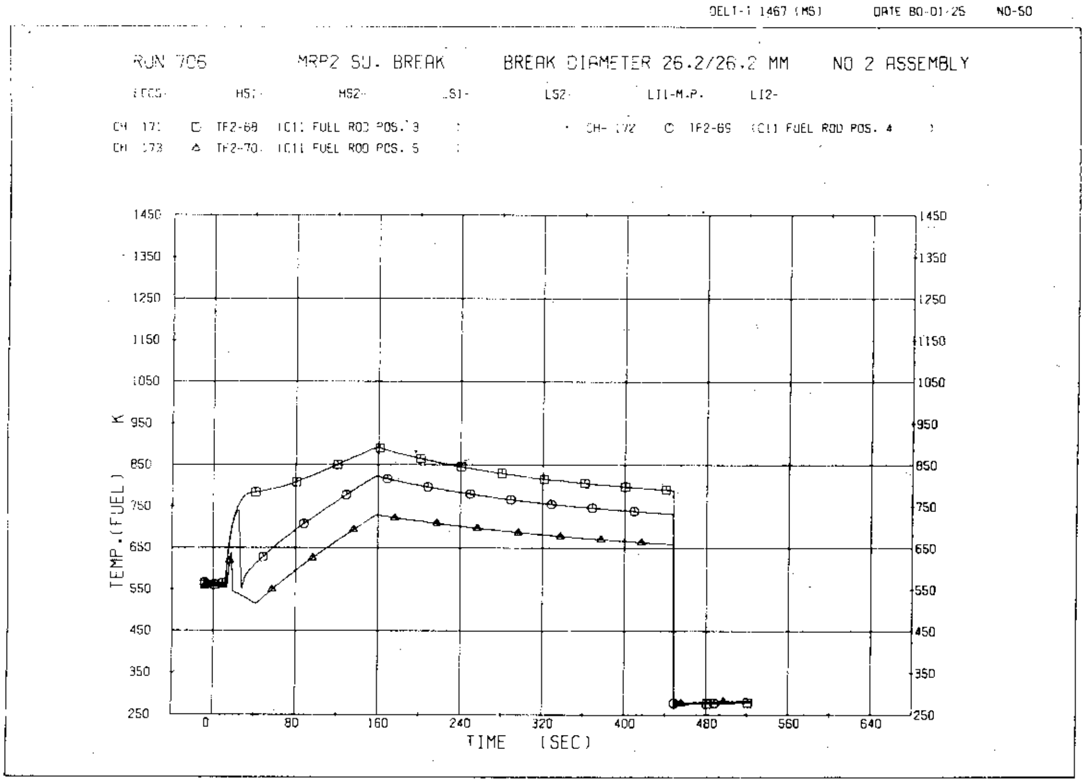

Fig.5.41 Surface Temperatures of the Fuel Rod C11 (The same as those of C13, C15, C31, C35, C51, C53)

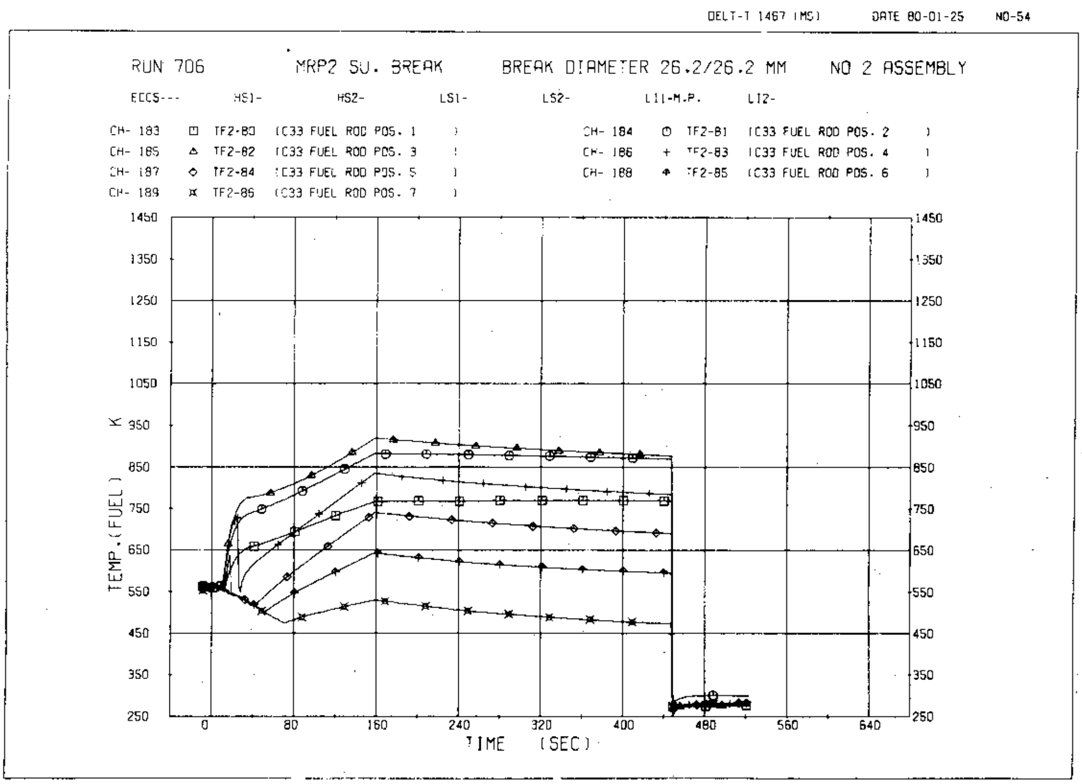

Fig.5.42 Surface Temperatures of the Fuel Rod C33

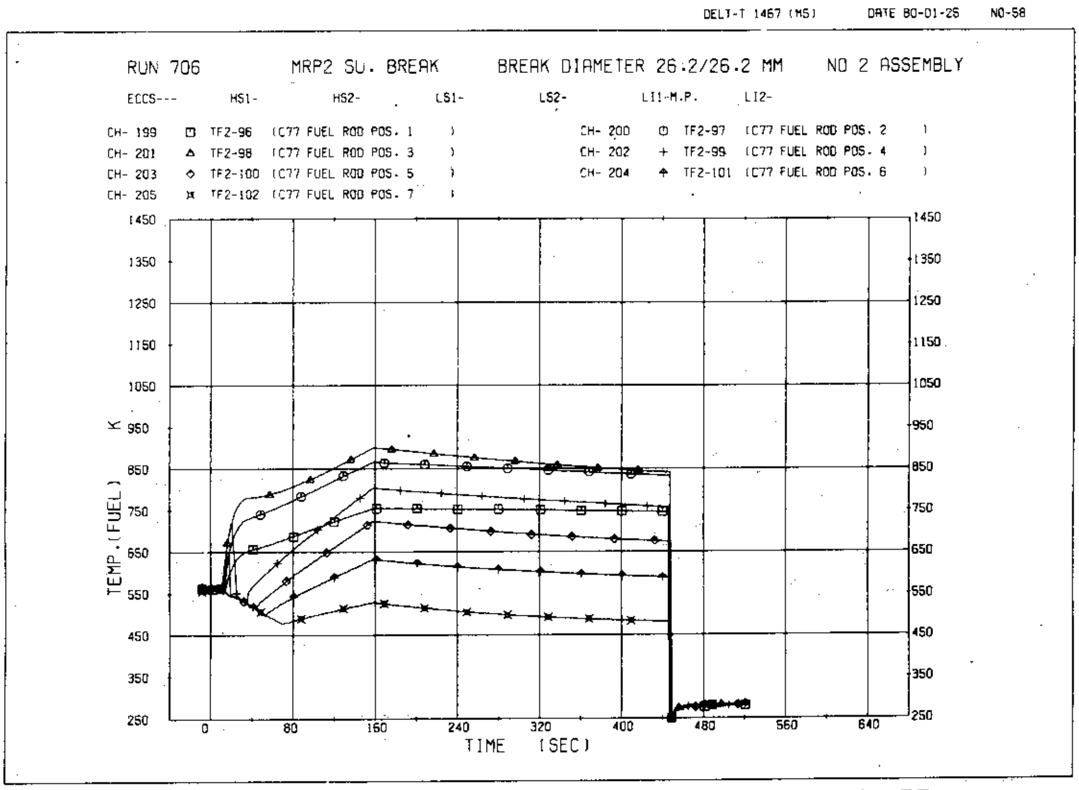

Fig.5.43 Surface Temperatures of the Fuel Rod C77

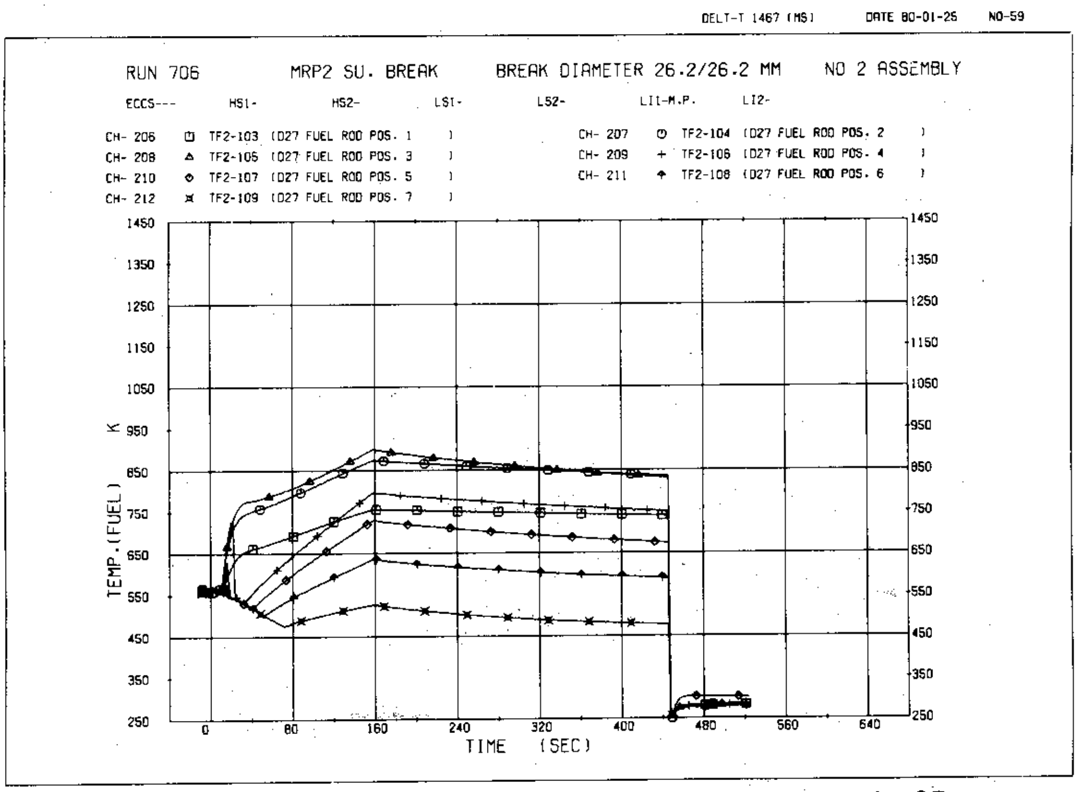

Fig.5.44 Surface Temperatures of the Fuel Rod D27

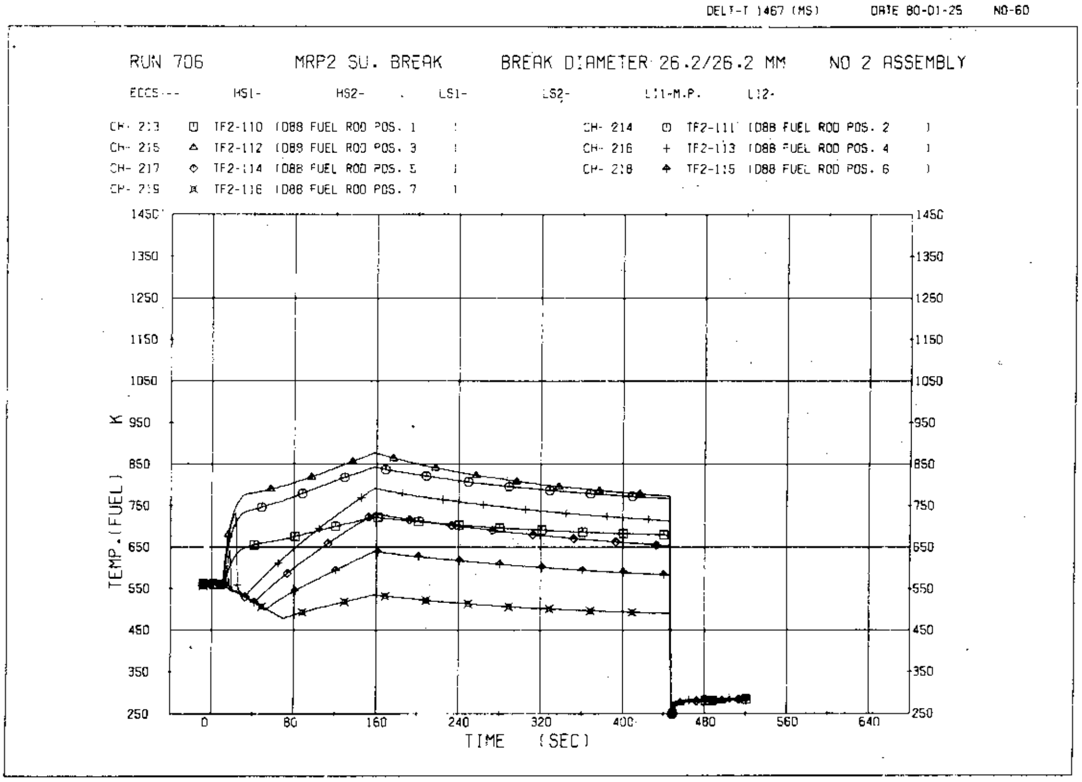

Fig. 5.45 Surface Temperatures of the Fuel Rod D88

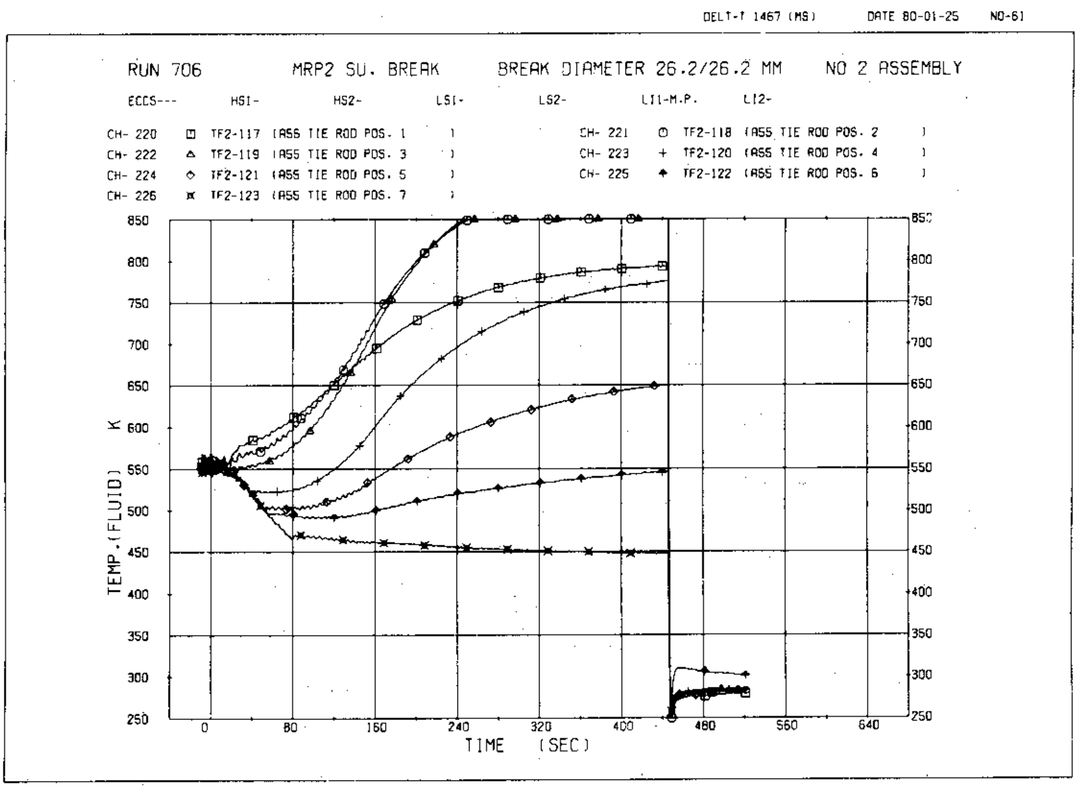

Fig. 5.46 Fluid Temperatures around the Tie Rod A55

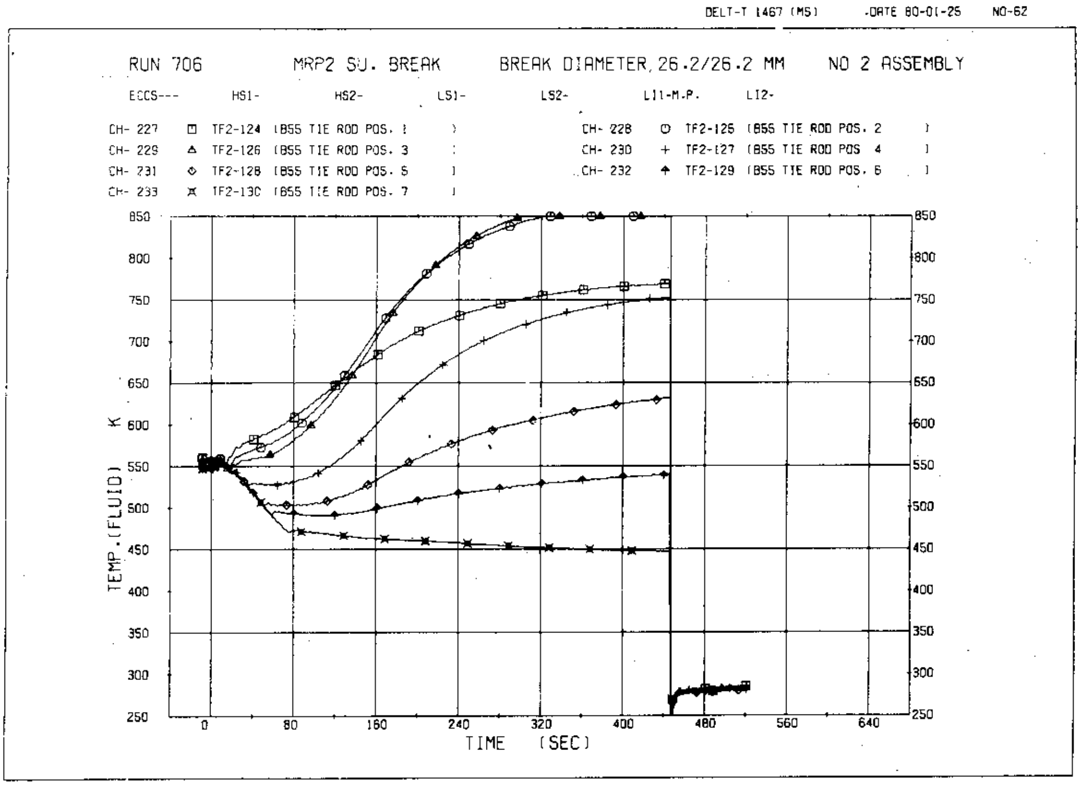

Fig.5.47 Fluid Temperatures around the Tie Rod B55

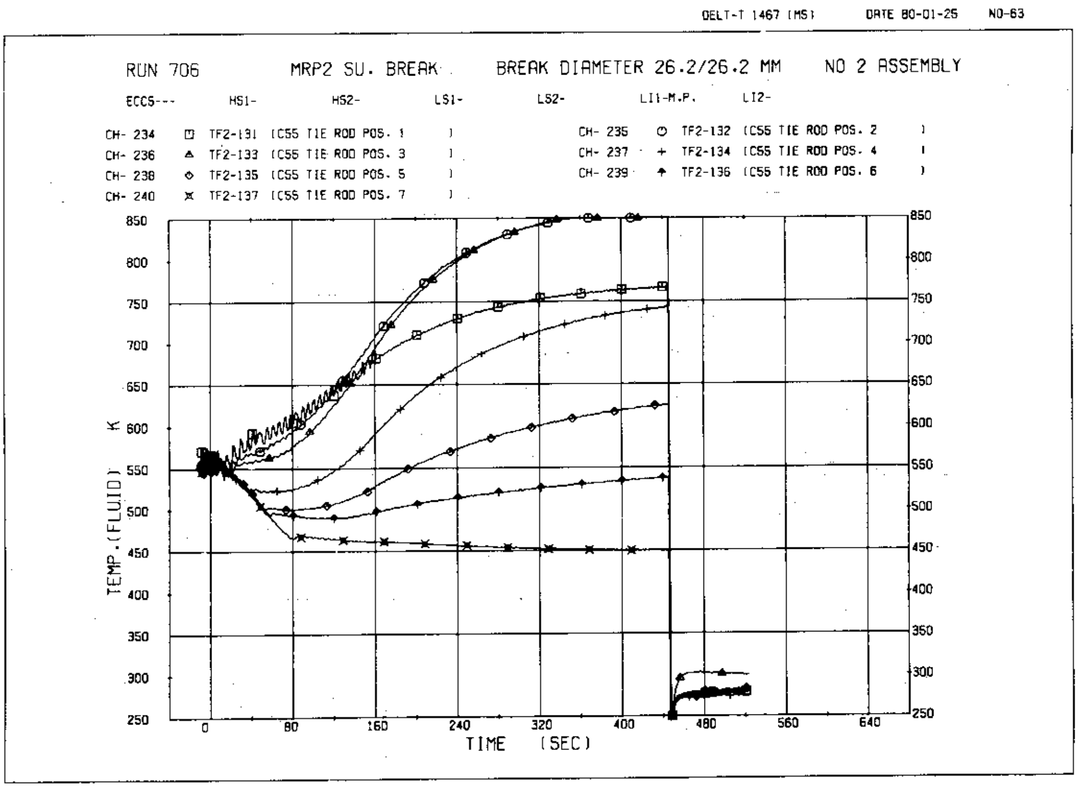

Fig.5.48 Fluid Temperatures around the Tie Rod C55

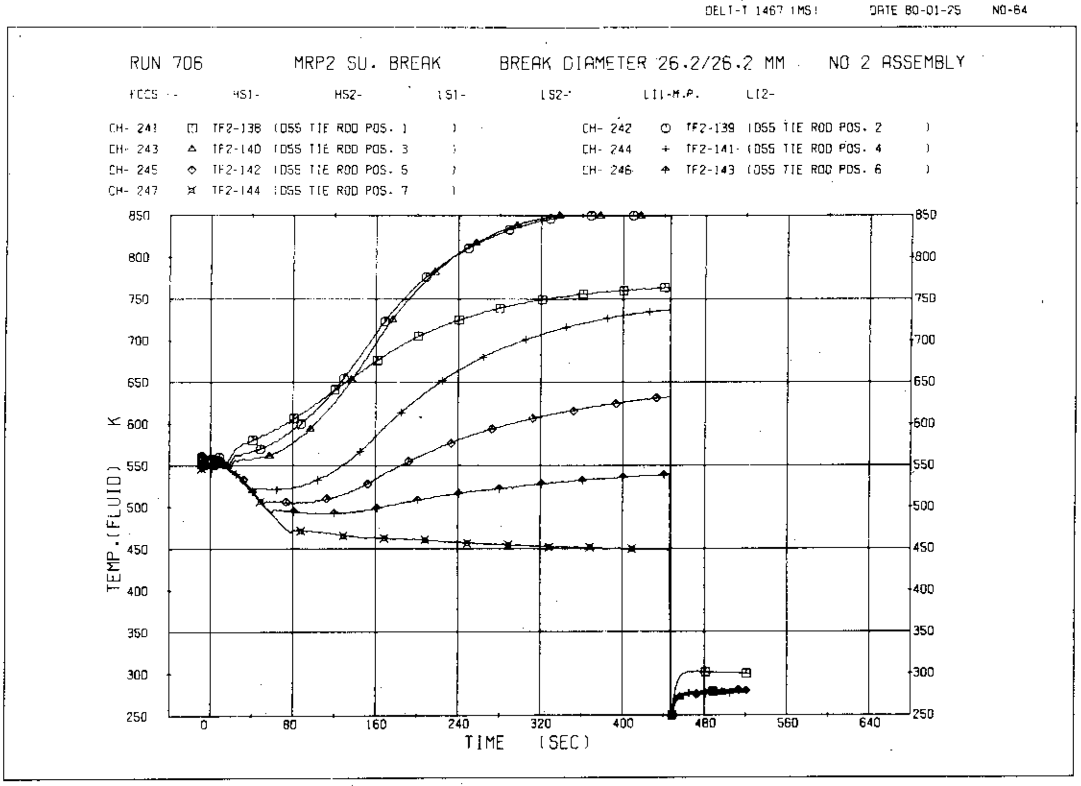

Fig.5.49 Fluid Temperatures around the Tie Rod D55

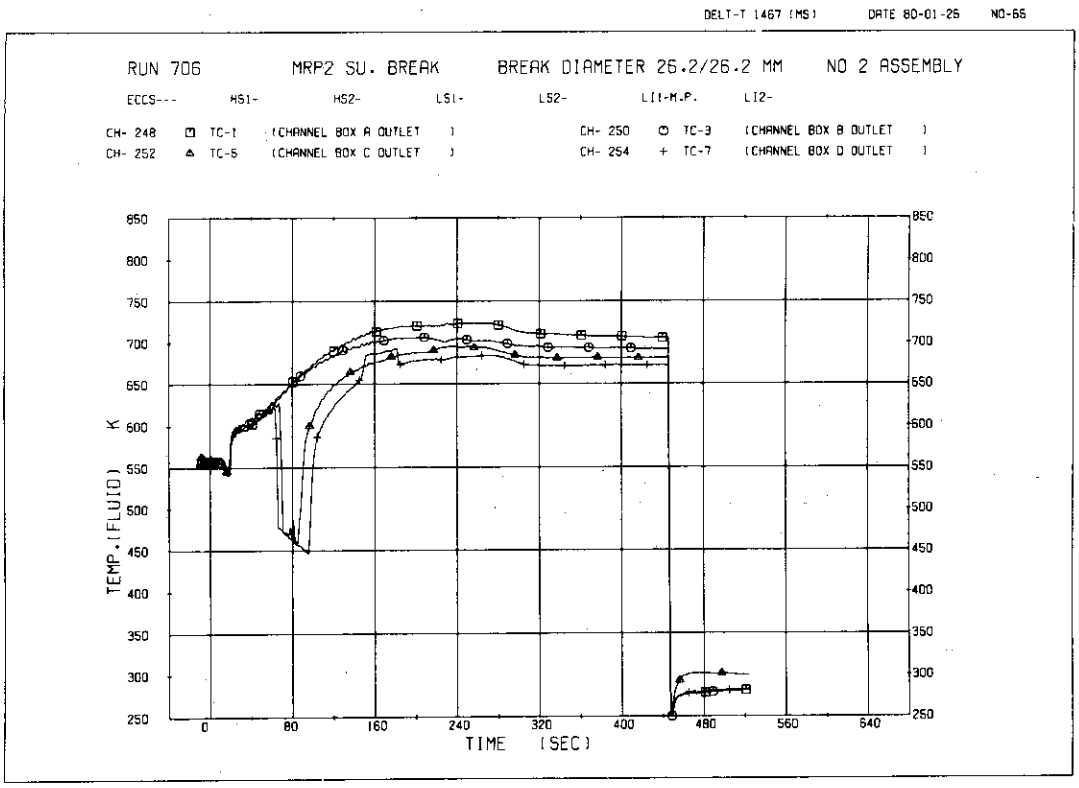

Fig.5.50 Fluid Temperatures at the Outlet of Each Channel Box A,B,C,D

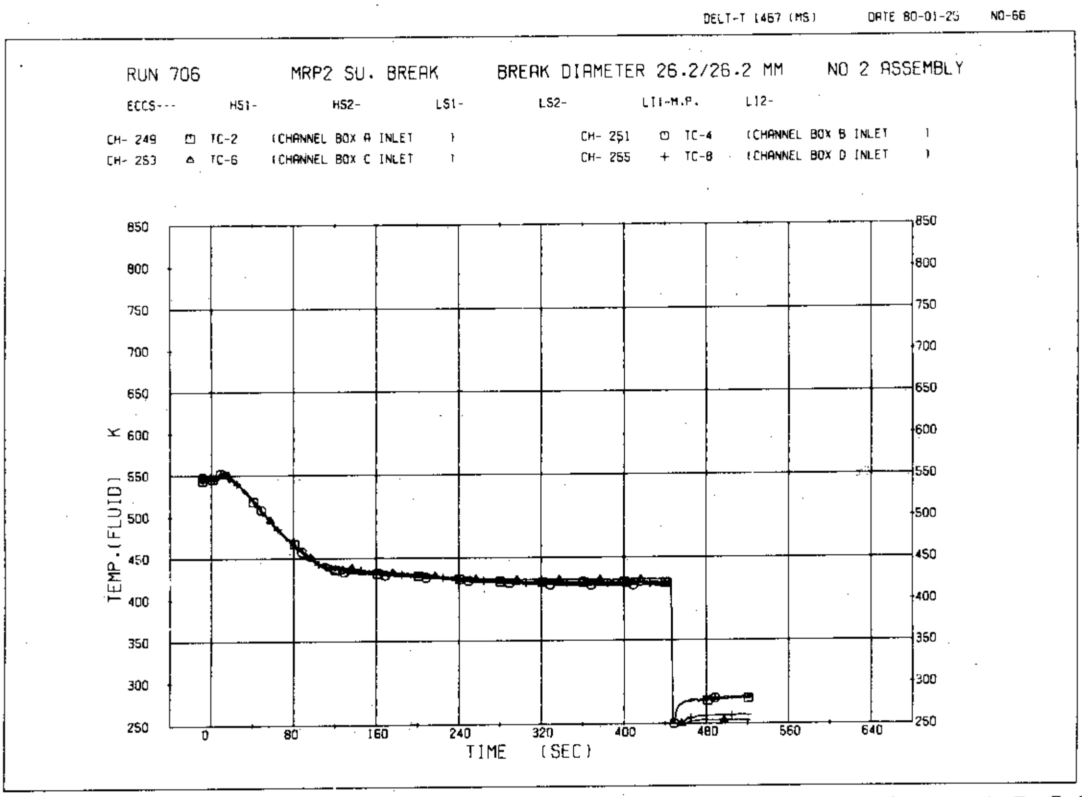

Fig.5.51 Fluid Temperatures at the Inlet of Each Channel Box A,B,C,D

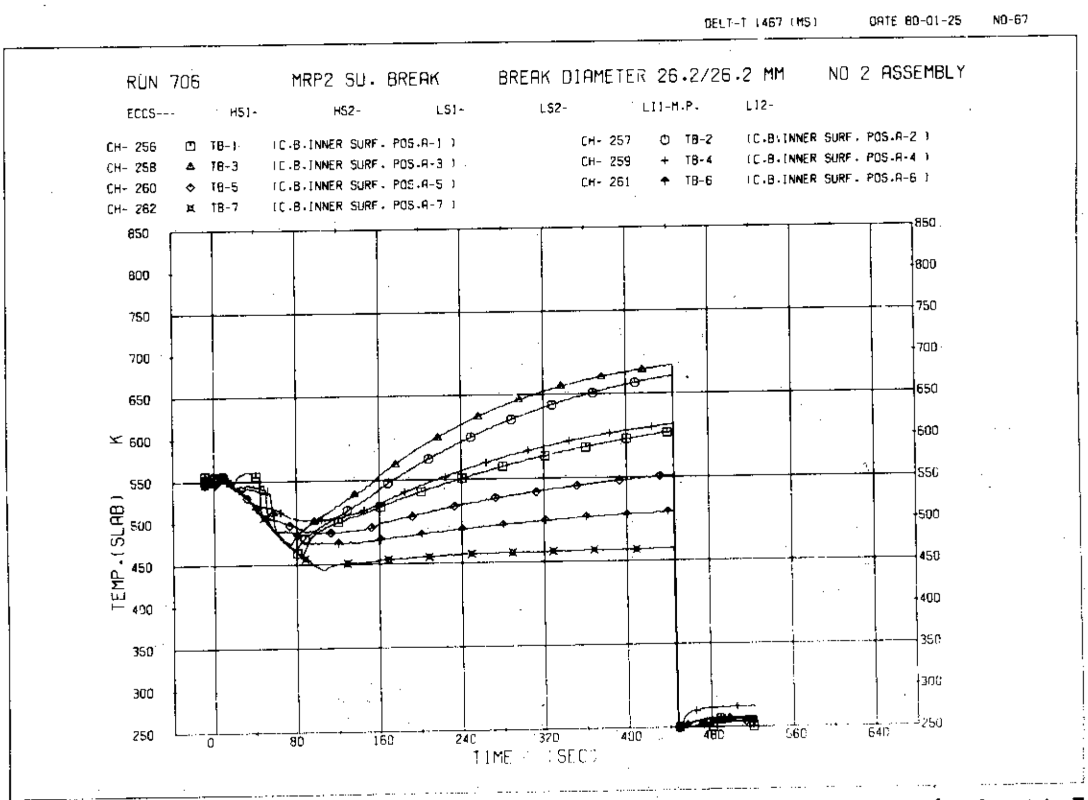

Fig.5.52 Inner Surface Temperatures of the Channel Box A (A-1 ∿ A-7)

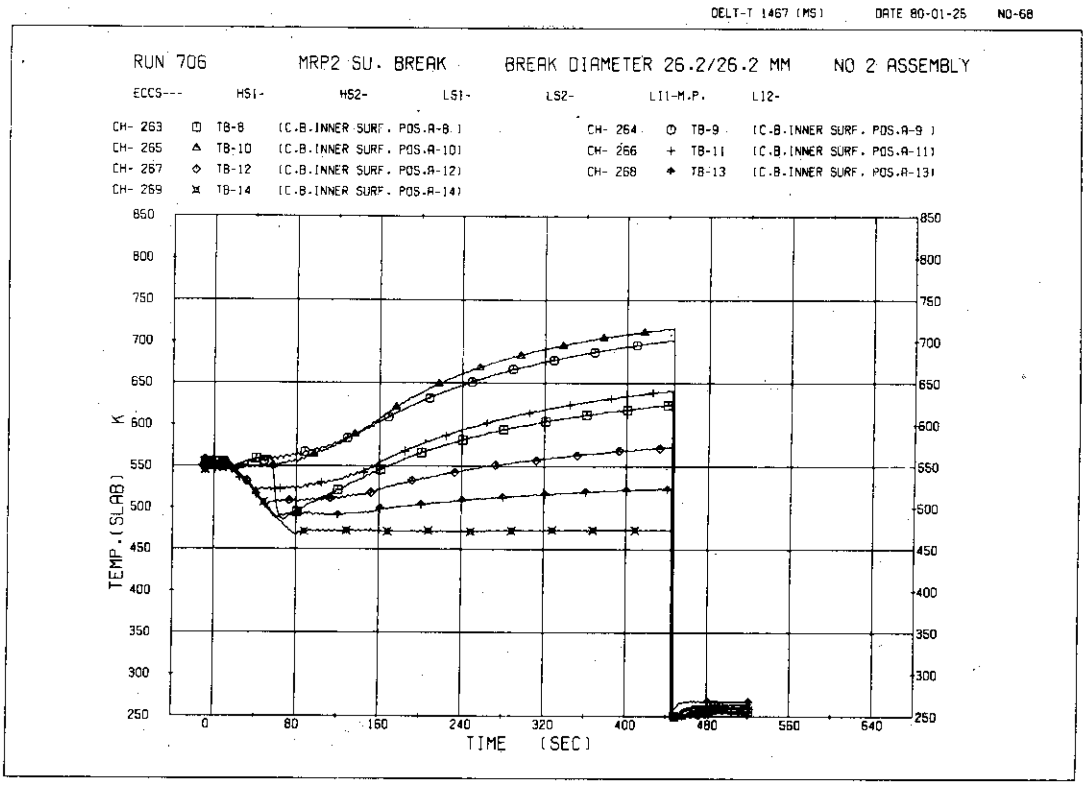

Fig.5.53 Inner Surface Temperatures of the Channel Box A (A-8 ∿ A-14)

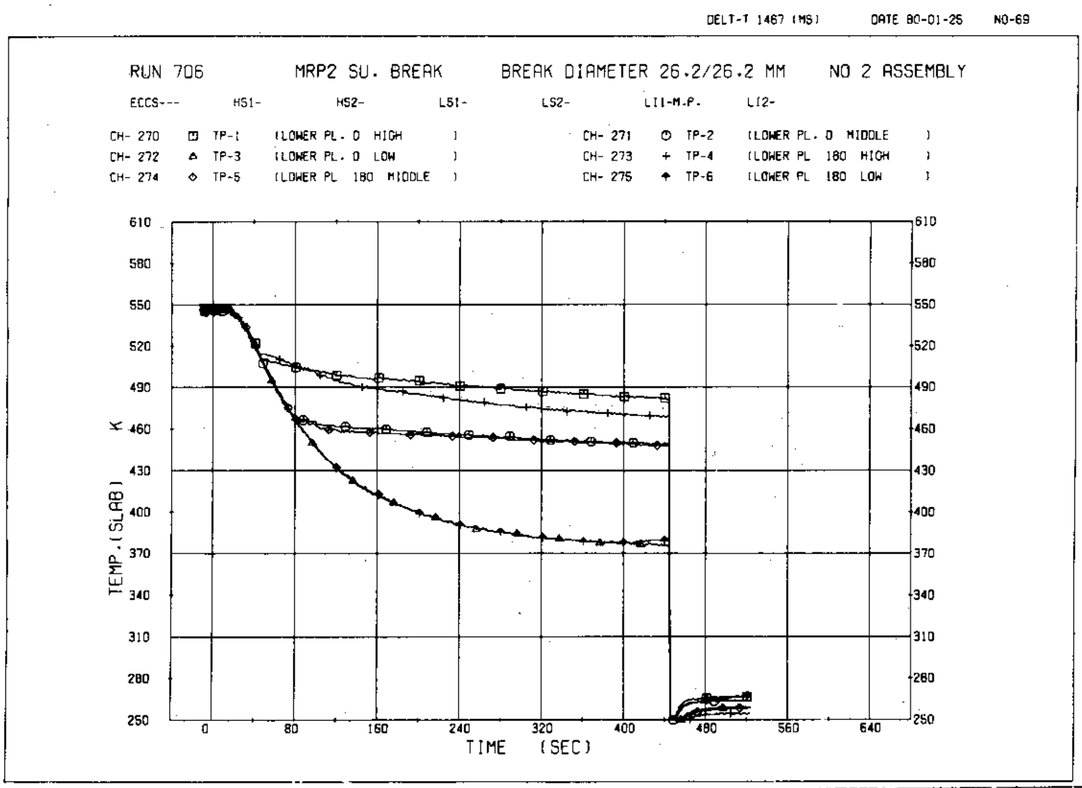

Fig.5.54 Inner Surface Temperatures at the Core Support in the Lower Plenum

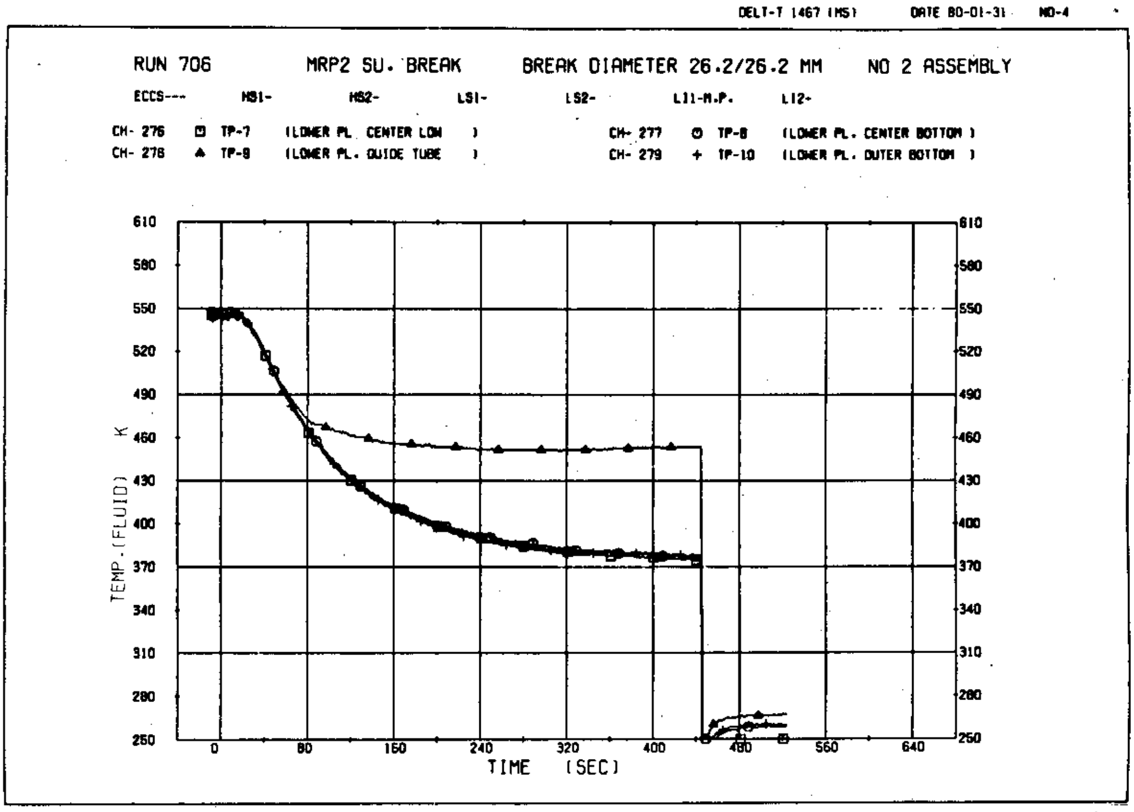

Fig.5.55 Fluid Temperatures in the Lower Plenum and in the Guide Tube

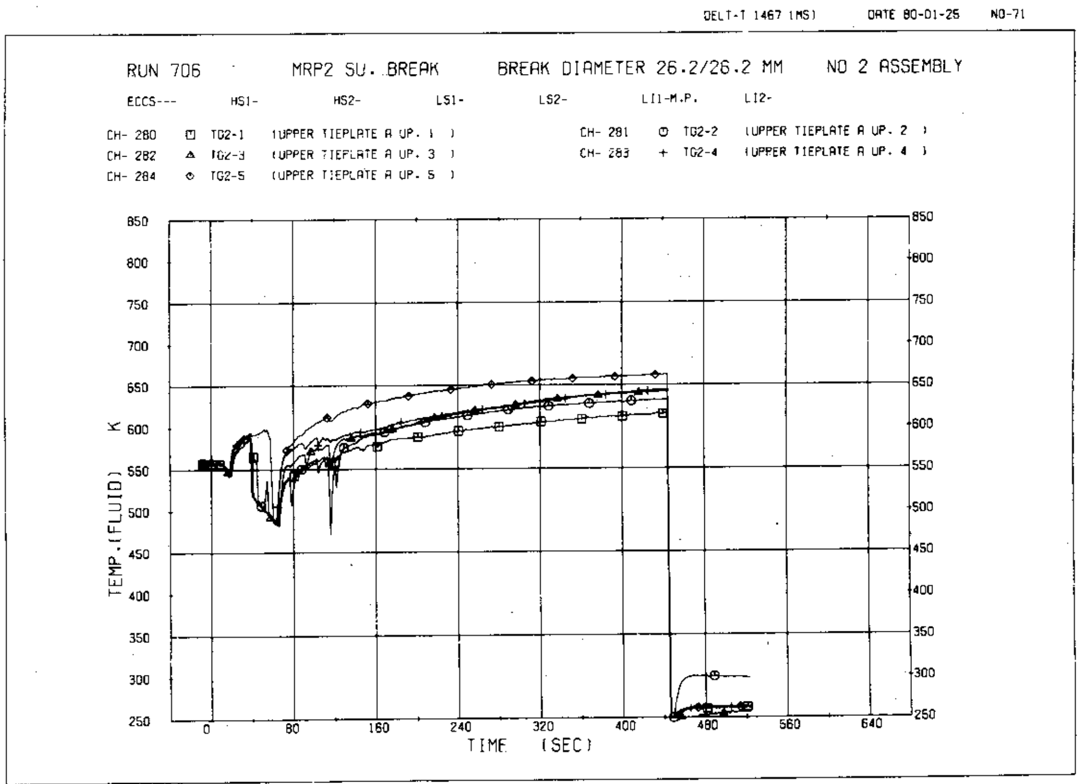

Fig.5.56 Fluid Temperatures at the Upper Side of Upper Tie-Plate in Channel A (1 ∿ 5)

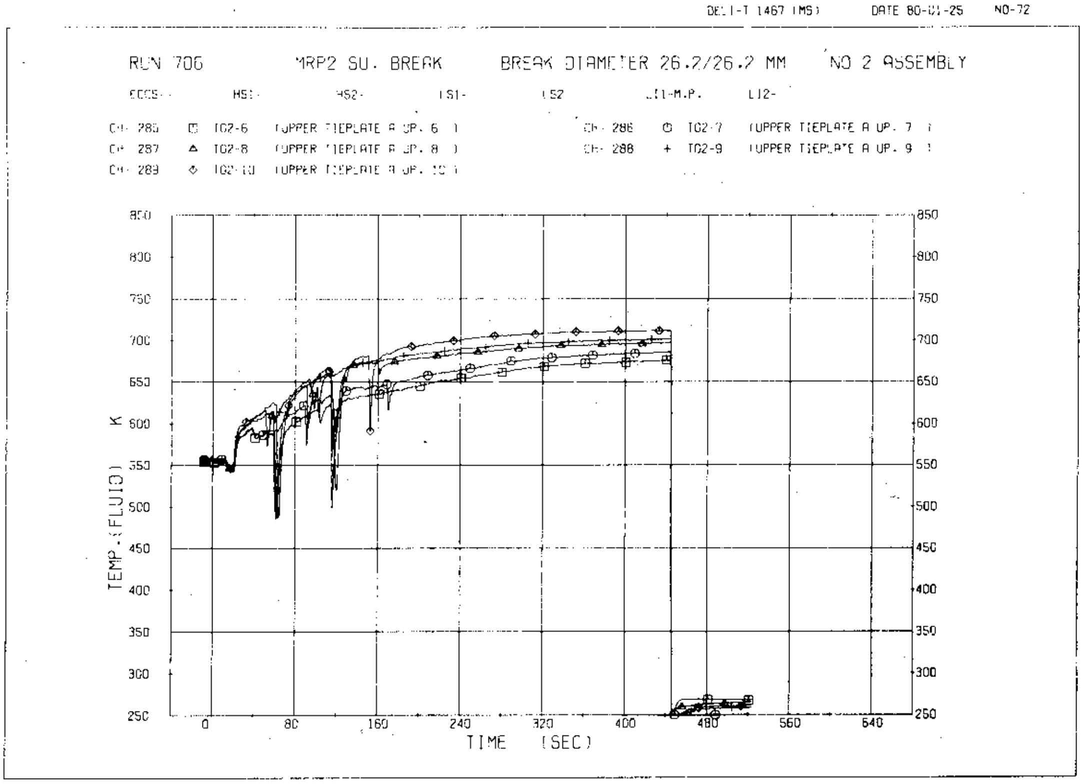

Fig.5.57 Fluid Temperatures at the Upper Side of Upper Tie-Plate in Channel A (6 ∿ 10)

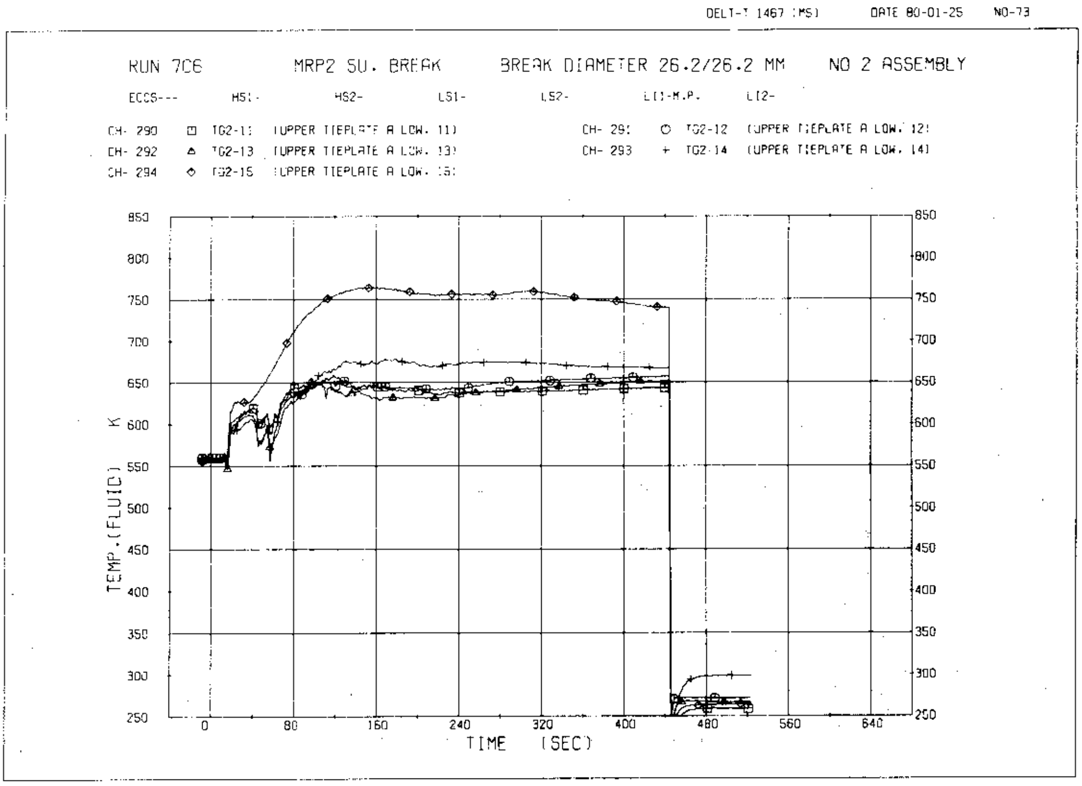

Fig.5.58 Fluid Temperatures at the Lower Side of Upper Tie-Plate in Channel A (11 ∿ 15)

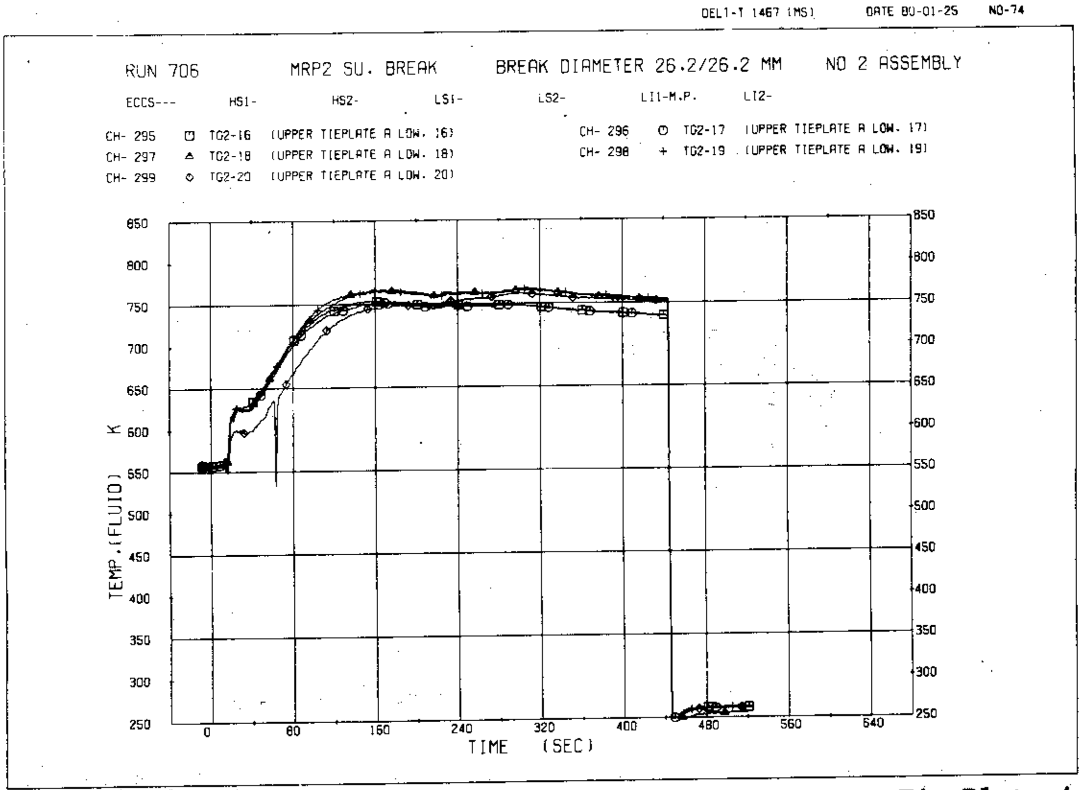

Fig.5.59 Fluid Temperatures at the Lower Side of Upper Tie-Plate in Channel A (16 ∿ 20)

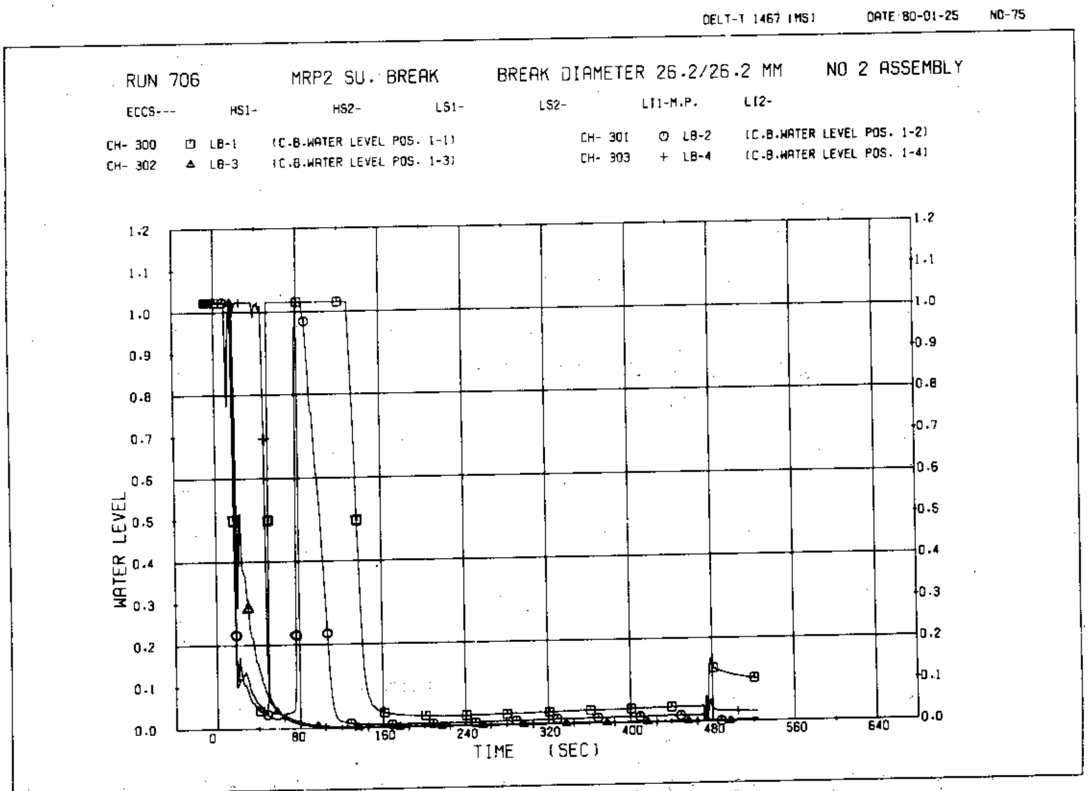

Fig.5.60 ON-OFF Signals of the Level Meters in Channel A (Pos.1-1 ∿ 1-4)

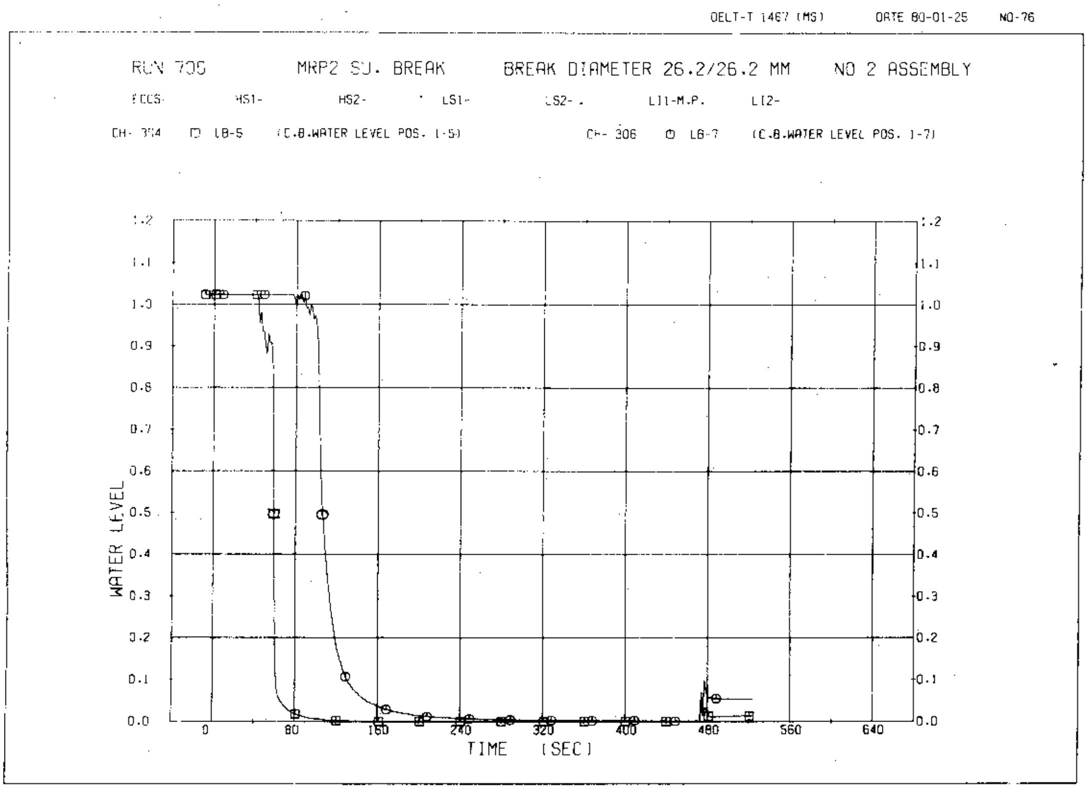

Fig.5.61 ON-OFF Signals of the Level Meters in Channel A (Pos.1-5 ∿ 1-7)

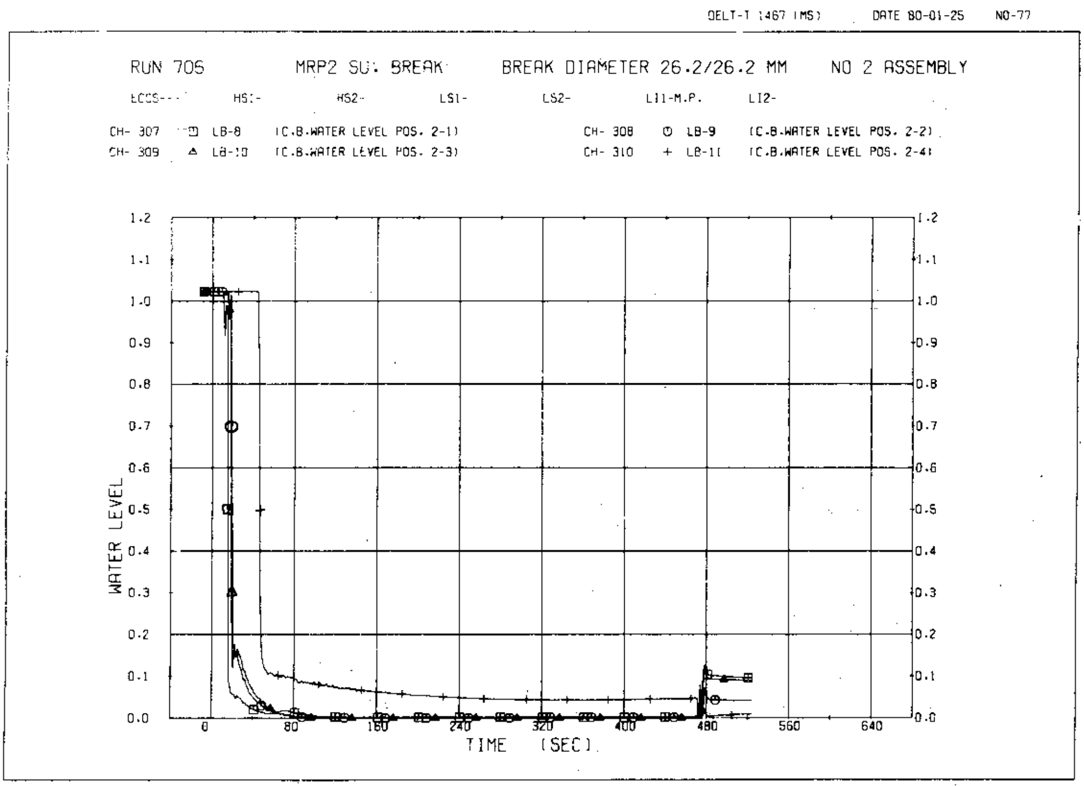

Fig.5.62 ON-OFF Signals of the Level Meters in Channel A (Pos.2-1 ∿ 2-4)

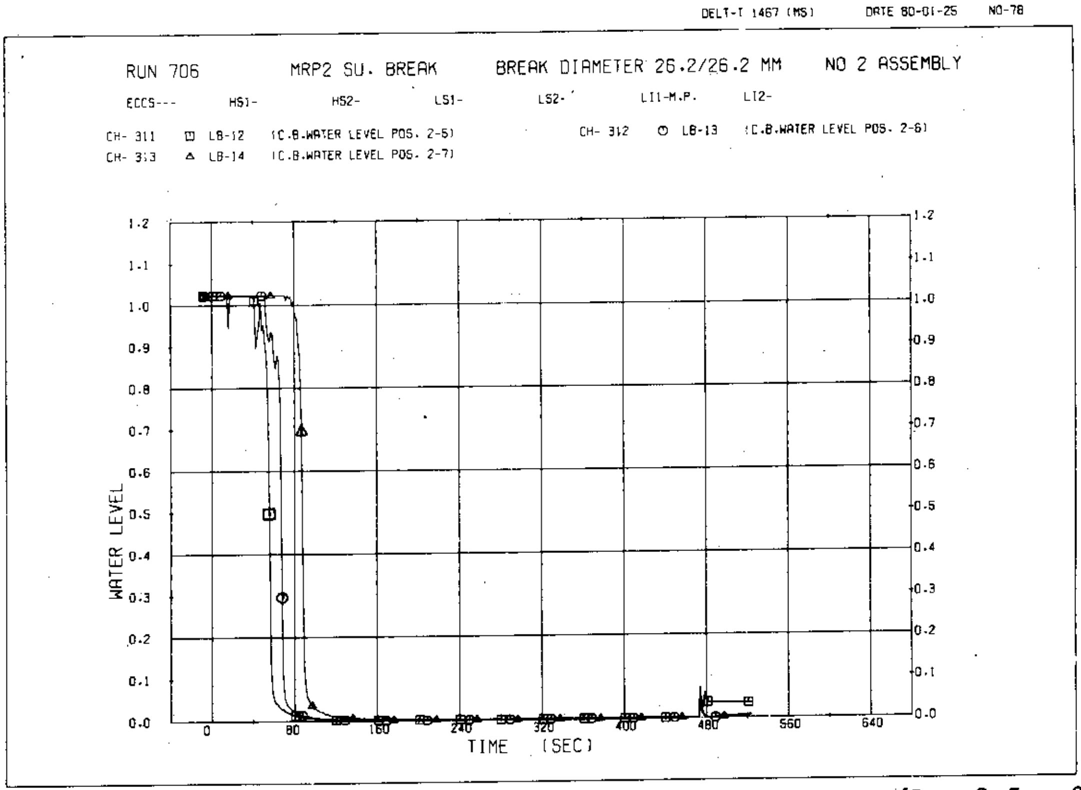

Fig.5.63 ON-OFF Signals of the Level Meters in Channel A (Pos.2-5 ∿ 2-7)

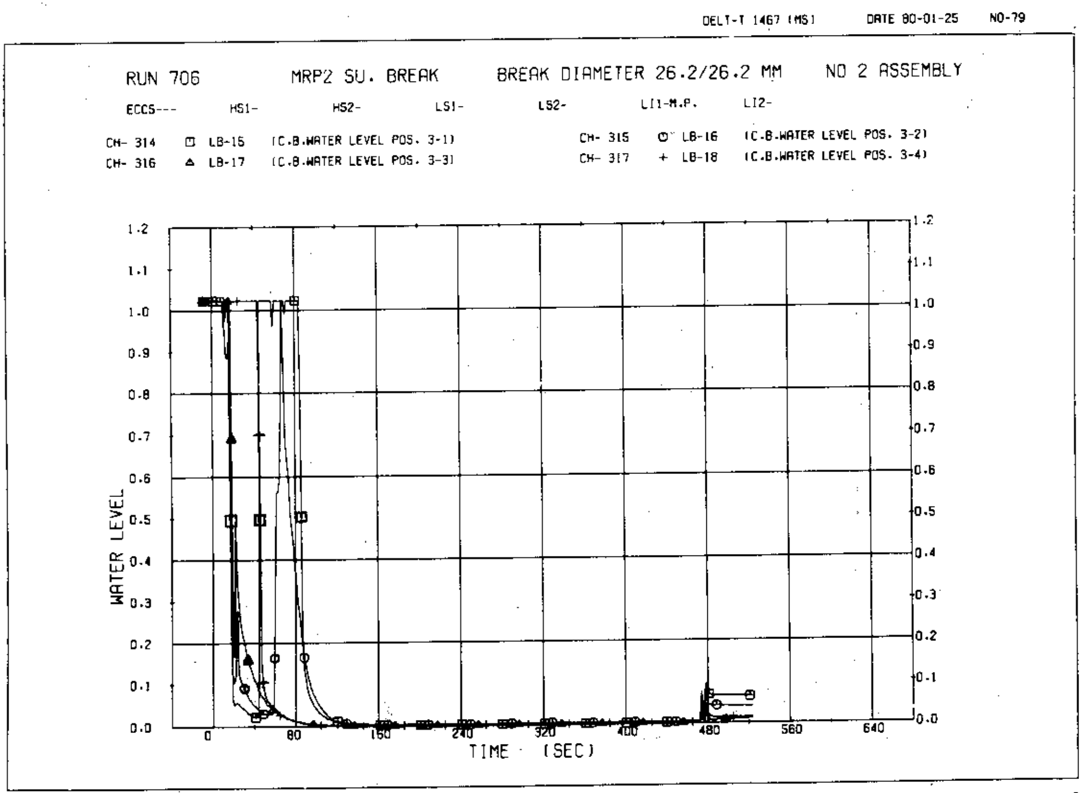

Fig.5.64 ON-OFF Signals of the Level Meter in Channel C (Pos.3-1 ∿ 3-4)

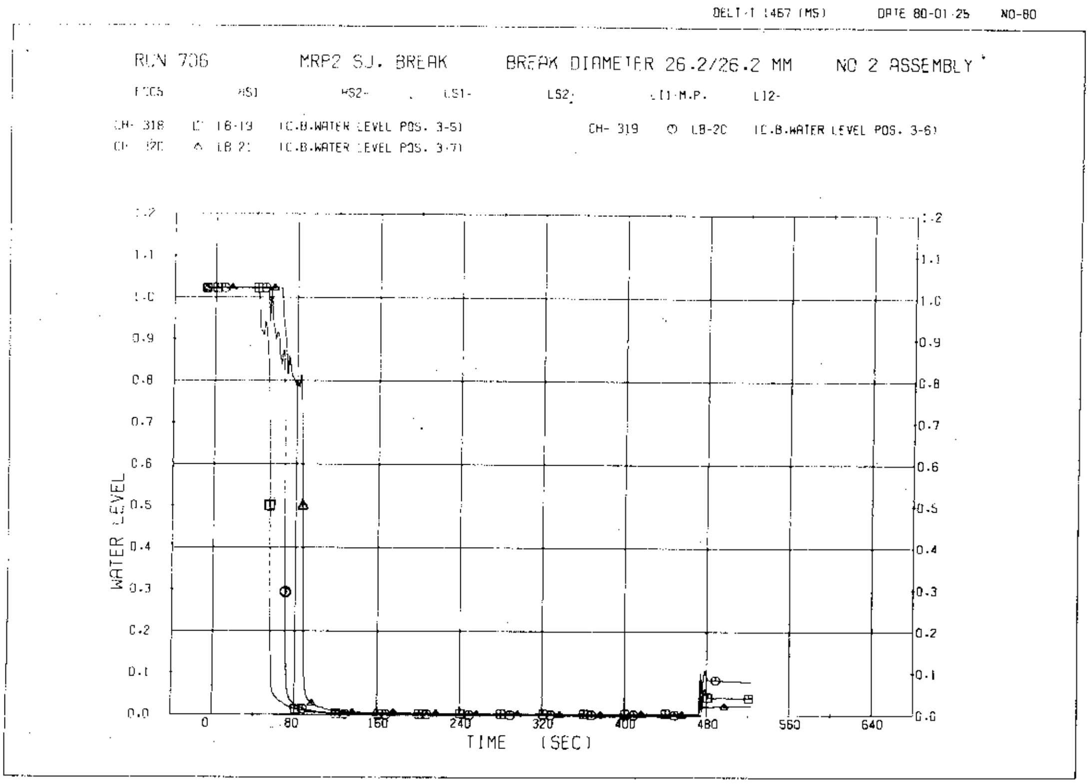

Fig.5.65 ON-OFF Signals of the Level Meter in Channel C (Pos.3-5 ∿ 3-7)

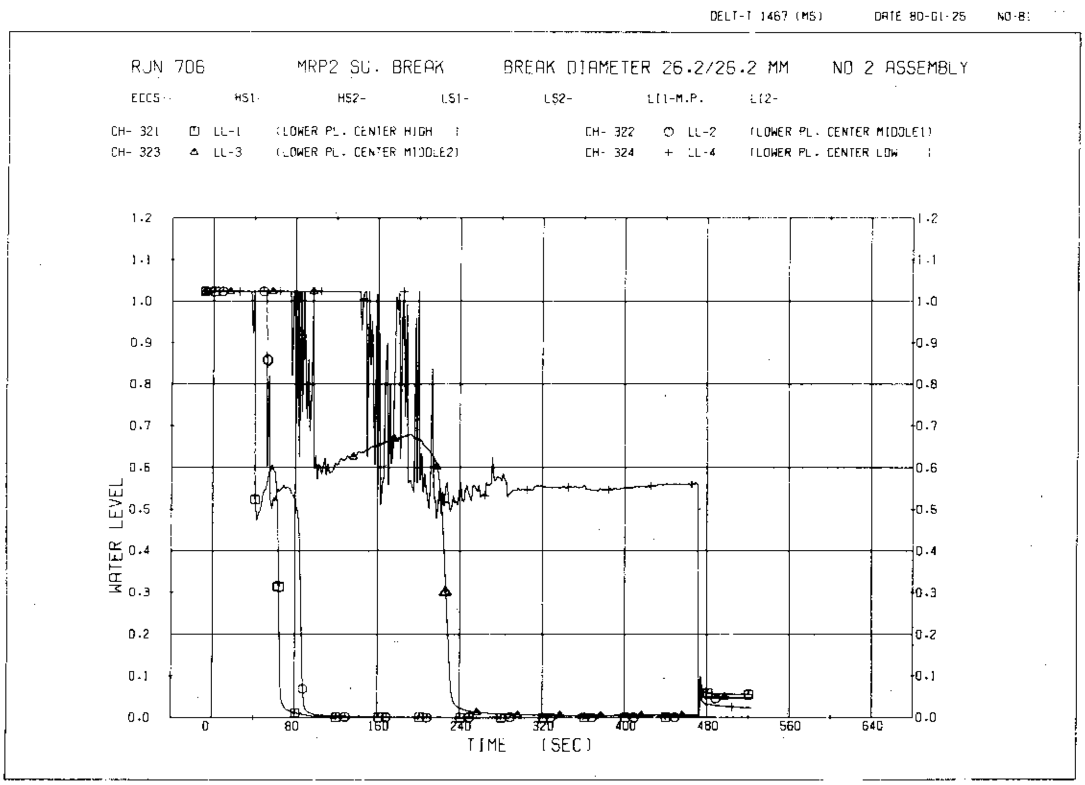

Fig.5.66 ON-OFF Signals of the Level Meter in the Lower Plenum (LL-1 ∿ LL-4)

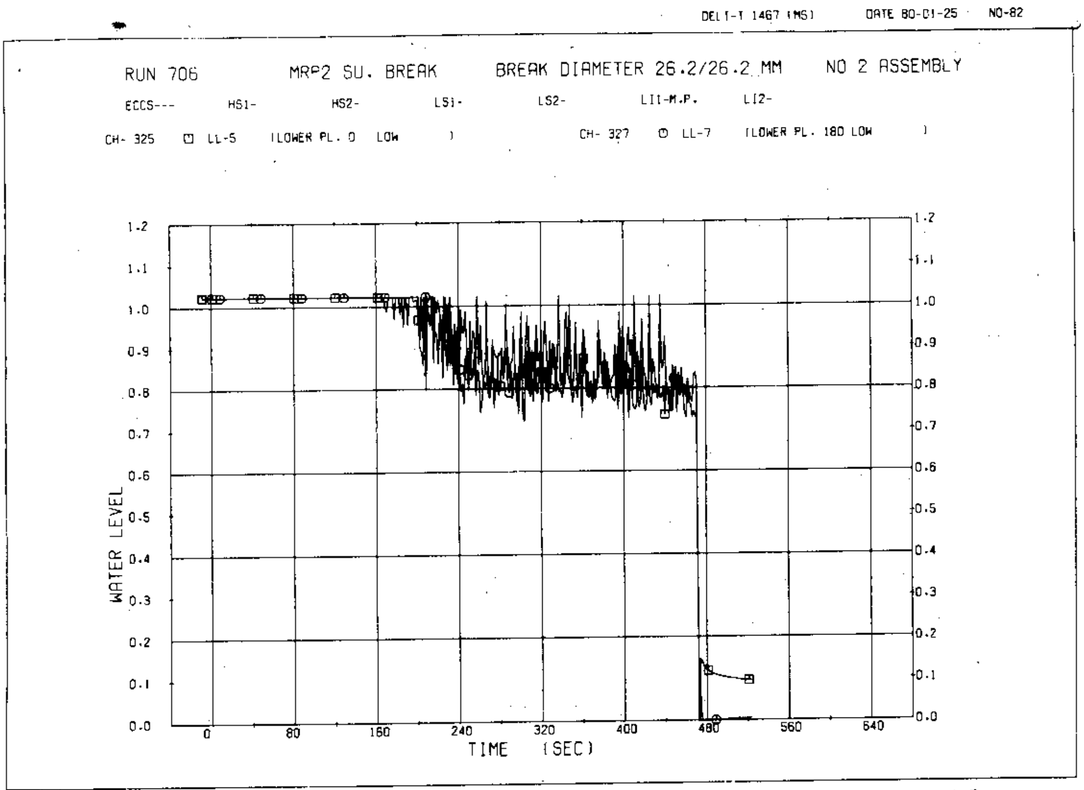

Fig.5.67 ON-OFF Signals of the Level Meter in the Lower Plenum (LL-5 ∿ LL-8)